KINETICS AND MECHANISMS OF THE OXIDATION OF NICOTINIC ACID, L-CYSTEIC ACID, L-ASPARTIC ACID AND L-TRYPTOPHAN BY PERMANGANATE ION IN AQUEOUS ACIDIC MEDIUM

BY

ANWETING, IDONGESIT BASSEY
B.Sc (HONS) CHEMISTRY (UNIUYO) 2006
(M.Sc/SCIE/05043/2009-2010)

A THESIS SUBMITTED TO THE SCHOOL OF POSTGRDUATE STUDIES, AHMADU BELLO UNIVERSITY, ZARIA, NIGERIA, IN PARTIAL FULFILMENT OF THE REQUIREMENTS FOR THE AWARD OF MASTER OF SCIENCE DEGREE IN INORGANIC CHEMISTRY

DEPARTMENT OF CHEMISTRY, FACULTY OF SCIENCE, AHMADU BELLO UNIVERSITY, ZARIA, NIGERIA

DECEMBER, 2012

DECLARATION

I, Anweting, Idongesit Bassey hereby declare that the work in this Thesis titled "Kinetics and Mechanisms of the Oxidation of Nicotinic Acid, L-Cysteic Acid, L-Aspartic Acid and L-Tryptophan by Permanganate Ion in Aqueous Acidic Medium" was performed by me in the Department of Chemistry under the supervision of Prof. J.F. Iyun and Dr. S.O. Idris. The information derived from literature have been duly acknowledged and a list of references provided. No part of this work has been presented for another degree or diploma at any institution.

Anweting, Idongesit Bassey **Signature ……** **Date…….**

CERTIFICATION

This thesis titled "Kinetics and Mechanisms of the Oxidation of Nicotinic Acid, L-Cysteic Acid, L-Aspartic Acid and L-Tryptophan by Permanganate Ion in Aqueous Acidic Medium" by Anweting, Idongesit Bassey, meets the regulations governing the award of the Degree of Master of Science in Inorganic Chemistry of Ahmadu Bello University, and is approved for its contribution to knowledge and literary presentation.

Prof. J.F. Iyun Chairman, Supervisory Committee	_____ Signature	_____ Date
Dr. S. O.Idris Member, Supervisory Committee	_____ Signature	_____ Date
Prof. V.O.Ajibola Head of Department	_____ Signature	_____ Date
Prof. A. A. Joshua Dean, School of Postgraduate Studies	_____ Signature	_____ Date

DEDICATION

This thesis is dedicated to Almighty God and to the blessed memory of my late beloved parents, may their souls rest in peace.

ACKNOWLEDGMENT

I sincerely wish to express my profound gratitude to the Almighty God, the giver of life, for His sustainable and enabling grace upon my life throughout the duration of my study in Ahmadu Bello University, Zaria.

My thanks go to Prof. J.F. Iyun and Dr. S.O. Idris, my able supervisors who had painstakingly and meticulously guided me from the inception to the completion of this work. In fact, their inputs regarding the success of this work in the area of contribution, corrections, encouragement and advice, cannot be over emphasized. I wish to reciprocate their gesture by saying that I am grateful. The Head of Chemistry Department, Ahmadu Bello University, Zaria, Prof. V.O.Ajibola and all the staff of the Department, are also worth thanking for the encouragement, support, motivation and understanding they displayed when this work was on- going. I also wish to thank all M.Sc students of the Department for their encouragement and care.

Pastor Julius Olajire, my spiritual mentor and all the members of Charismatic Renewal Ministries, Glory Centre Zaria deserve special thanks for their prayers, support, care and encouragement during the duration of this work. I also wish to thank my cousin, Mr. Francis Anweting, for all the help and support he rendered to enable me successfully complete this project.

My good friends Etekaboy, Roland, Etim, Edoho, Idorenyin, Kenneth, Inemesit, Frank and Njinga deserve special thanks.

“To God be all the glory”

ABSTRACT

The kinetics and mechanisms of oxidation of nicotinic acid, L – cysteic acid, L – aspartic acid and L– tryptophan have been investigated in aqueous acidic medium at 28.0±1.0°C, I = 0.5 mol dm^{-3} (Na_2SO_4), $[H^+]$ = 0.1mol dm^{-3} (H_2SO_4) for nicotinic acid and L – tryptophan, for L – cysteic acid, the reaction was studied at 27.0±1.0°C, I = 0.5 mol dm^{-3} (Na_2SO_4), $[H^+]$ = 0.1mol dm^{-3} (H_2SO_4). For L – aspartic acid, the reaction was studied at 29.0±1.0°C, I = 1.0 mol dm^{-3} (Na_2SO_4) and $[H^+]$ = 0.2mol dm^{-3} (H_2SO_4). The stoichiometry is 1:1 (oxidant: reductant) for MnO_4^- – nicotinic acid and L – tryptophan systems, and 2:5 (oxidant: reductant) for MnO_4^- – L – cysteic acid and L – aspartic acid systems. The rate of reaction is first order with respect to all the reductants and oxidant and second orders overall in all the systems investigated. The rate of reaction showed dependence on acid concentrations. The reactions conform to the following rate laws:

$$-\frac{d}{dt}[MnO_4^-] = k_2[MnO_4^-][\text{nicotinic acid}]$$

where k_2 = (1.72 ± 0.015) × 10^{-1} $dm^3mol^{-1}s^{-1}$ at 28.0±1.0°C, I = 0.5 mol dm^{-3} and $[H^+]$ = 0.1mol dm^{-3},

$$-\frac{d}{dt}[MnO_4^-] = k_2[MnO_4^-][\text{L – cysteic acid}]$$

where k_2 = (5.49 ± 0.07) × $10^{-1}$$dm^3mol^{-1}s^{-1}$at 27.0±1.0°C, I = 0.5 mol dm^{-3} and $[H^+]$ = 0.1mol dm^{-3} ,

$$-\frac{d}{dt}[MnO_4^-] = k_2[MnO_4^-][\text{L – aspartic acid}]$$

where k_2 =(3.50 ± 0.06) ×10^{-2} $dm^3mol^{-1}s^{-1}$ at 29.0±1.0°C, I = 1.0 mol dm^{-3} and $[H^+]$ = 0.2mol dm^{-3},

$$-\frac{d}{dt}[MnO_4^-] = k_2[MnO_4^-][\text{L – tryptophan}]$$

where k_2= (8.75 ± 0.14) × 10^{-2} $dm^3mol^{-1}s^{-1}$,at 28.0±1.0°C, I = 0.5 mol dm^{-3} and $[H^+]$ = 0.1mol dm^{-3} .

The rate of reaction displayed negative salt effect for MnO_4^- – nicotinic acid, L –cysteic acid and L – tryptophan systems, whereas positive salt effect was displayed for MnO_4^-–L– aspartic acid system. The reactions were sensitive to changes in the dielectric constant of the medium for the reactions involving nicotinic acid, L – aspartic acid and L – tryptophan. Added anions and cations were found to catalysed the reactions for all the systems. The

results of spectroscopic investigations and Michaelis – Menten analysis show no evidence of intermediate complex formation for all the systems. Based on the empirical results obtained, the outer-sphere mechanistic pathways were proposed for all the reaction systems investigated.

TABLE OF CONTENTS

Title	i
Declaration	ii
Certification	iii
Dedication	iv
Acknowledgment	v
Abstract	vi
Table of contents	viii
List of Figures	xii
List of Tables	xvi
Abbreviations	xvii
CHAPTER ONE	
1.0 Introduction	1
1.1.0 Rate monitoring techniques	2
1.1.1 Conventional methods	2
1.1.2 Monitoring rates of fast reactions	2
1.1.2.1 Flow technique	2
1.1.2.2 Relaxation method	3
1.1.2.3 Resonance technique	3
1.2.0 Theoretical consideration in electron transfer processes	4
1.2.1 Franck – Condon Principle	4
1.2.2 Electron tunneling theory	5
1.2.3 Solvated electron theory	7

1.3.0 Oxidation- reduction(redox)reaction 8

1.3.1 Homonuclear or isotopic electron exchange 8

1.3.2 Heteronuclear electron transfer or cross reactions 8

1.4.0 Points of mechanistic interest in redox reactions 9

1.4.1 Mechanisms of electron transfer reactions 10

1.4.2 The outer-sphere mechanism 10

1.4.3 The inner-sphere mechanism 12

1.5.0 Diagnosis of redox reaction mechanism 14

1.5.1 Rate of redox process versus rate of substitution 14

1.5.2 Identification of the binuclear intermediate 14

1.5.3 Products analyses 15

1.5.4 Reactivity pattern 16

1.5.5 The effects of added ions 16

1.5.6 Activation parameters 17

1.5.7 Use of ambidentate bridging ligand 17

1.5.8 Marcus theory of electron transfer rates 17

1.6 Research objectives 19

CHAPTER TWO

2.0 Literature review 20

2.1 Permanganate as an oxidizing and hydroxylating agent 20

2.2.0 Nicotinic acid 25

2.2.1 Deficiency of nicotinic acid 25

2.2.2 Toxicity of nicotinic acid 26

2.2.3 Reactions of nicotinic acid 27

2.3.0 Amino acids 28

2.3.2 Reactions of amino acids 28

2.4.0 Cysteic acid 31

2.5.0 Aspartic acid 31

2.5.1 Forms of aspartic acid 32

2.5.2 Role of aspartic acid in the biosynthesis of amino acid 32

2.6.0 Tryptophan 33

2.6.1 Role of tryptophan 33

CHAPTER THREE

3.0 Experimental 35

3.1.0 Materials and reagents 35

3.1.1 Preparation of standard solution of potassium permanganate 35

3.1.2 Preparation of standard tetraoxosulphate(VI) acid solution 36

3.1.3 Preparation of standard solution of nicotinic acid 36

3.1.4 Preparation of standard solution of amino acids 36

3.1.5 Preparation of standard solution of salt solution 37

3.1.6 Preparation of standard solution of sodium oxalate 37

3.2.0 Stoichiometric studies 37

3.3 Kinetic measurements 38

3.4 Test for the presence of intermediate complex 41

3.5 Test for free radicals 42

CHAPTER FOUR

4.0 Results 43

4.1	Stoichiometry	43
4.2	Determination of order with respect to reactants	48
4.3	Effect of hydrogen ion concentration on rate of the reactions	61
4.4	Effect of ionic strength of reaction medium on the reaction rate	70
4.5	Effect of added anion on systems investigated	75
4.6	Effect of added cations on systems investigated	75
4.7	Effect of change in dielectric constant of the reaction medium	75
4.8	Free radicals test	90
4.9	Test for intermediate complex formation	90
4.9.1	Spectrophotometric investigation	90
4.9.2	Michaelis-Menten plots	90
4.10	Product analyses	105

CHAPTER FIVE

5.0	Discussion	106
5.1	Permanganate ion–nicotinic acid system	106
5.2	Permanganate ion–L-cysteic acid system	108
5.3	Permanganate ion–L-aspartic acid system	111
5.4	Permanganate ion–L-tryptophan system	112
5.5	Summary and conclusion	115
5.6	Recommendations	117
	References	118

LIST OF FIGURES

Figure 1.1 Electron transfer by penetration of a potential energy barrier 6

Figure 1.2 Energy profile diagram for a redox reaction which occurs by the outer-sphere mechanism 11

Figure 1.3 Energy profile diagram for a redox reaction which occurs by the inner-sphere mechanism 13

Figure 4.1 A plot of absorbance versus mole ratio for the reaction between MnO_4^- and nicotinic acid 44

Figure 4.2 A plot of absorbance versus mole ratio for the reaction between MnO_4^- and L-cysteic acid 45

Figure 4.3 A plot of absorbance versus mole ratio for the reaction between MnO_4^- and L-aspartic acid 46

Figure 4.4 A plot of absorbance versus mole ratio for the reaction between MnO_4^- and L-tryptophan 47

Figure 4.5 A typical pseudo first order plot for the redox reaction between nicotinic acid and permanganate ion 49

Figure 4.6 Plot of $logk_{obs}$ versus log [nicotinic acid] for the redox reaction between permanganate ion and nicotinic acid 50

Figure 4.7 A typical pseudo first order plot for the redox reaction between L-cysteic acidand permanganate ion 51

Figure 4.8 Plot of $logk_{obs}$ versus log [L-cysteic acid] for the redox reaction between L – cysteic acid and permanganate ion 52

Figure 4.9 A typical pseudo first order plot for the redox reaction between L-aspartic acid and permanganate ion 53

Figure 4.10 Plot of log k_{obs} versus log [L-aspartic acid] for the redox reaction between L-aspartic acid and permanganate ion 54

Figure 4.11 A typical pseudo- first order plot for the redox reaction between L- tryptophan and permanganate ion 55

Figure 4.12 Plot of log k_{obs} versus log [L-tryptophan] for the redox reaction between

L- tryptophan and permanganate ion 56

Figure 4.13 Plot of $logk_{obs}$ versus $log[H^+]$ for the redox reaction between nicotinic acid and permanganate ion 62

Figure 4.14 Plot of $logk_{obs}$ versus $log[H^+]$ for the redox reaction between L-cysteic acid and permanganate ion 63

Figure 4.15 Plot of $logk_{obs}$ versus $log[H^+]$ for the redox reaction between L-aspartic acid and permanganate ion 64

Figure 4.16 Plot of $logk_{obs}$ versus $log[H^+]$ for the redox reaction between L-tryptophan and permanganate ion 65

Figure 4.17 Plot of k_2 versus $[H^+]$ for the redox reaction between nicotinic acid and permanganate ion 66

Figure 4.18 Plot of k_2 versus $[H^+]$ for the redox reaction between L-cysteic acid and permanganate ion 67

Figure 4.19 Plot of log k_{obs} versus $log[H^+]$ for the redox reaction between L-aspartic acid and permanganate ion 68

Figure 4.20 Plot of k_2 versus $[H^+]$ for the redox reaction between L-tryptophan and permanganate ion 69

Figure 4.21 Plot of log k_2 versus $I^{½}$ for the redox reaction between nicotinic acid and permanganate ion 71

Figure 4.22 Plot of log k_2 versus $I^{½}$ for the redox reaction between L-cysteic acid and permanganate ion 72

Figure 4.23 Plot of log k_2 versus $I^{½}$ for the redox reaction of L-aspartic acid and permanganate ion 73

Figure 4.24 Plot of log k_2 versus $I^{½}$ for the redox reaction between L-tryptophan and permanganate ion 74

Figure 4.25 Plot of k_2 versus $[NO_3^-]$ for the redox reaction between nicotinic acid and permanganate ion 80

Figure 4.26 Plot of k_2 versus $[NO_3^-]$ for the redox reaction of L-cysteic acid with permanganate ion 81

Figure 4.27 Plot of k_2 versus $[NO_3^-]$ for the redox reaction of L-aspartic acid with permanganate ion 82

Figure 4.28 Plot of k_2 versus $[NO_3^-]$ for the redox reaction of L-tryptophan with permanganate ion 83

Figure 4.29 Plot of $k_2(z^{n+})$ versus $[Li^+]$ for the redox reaction of nicotinic acid with permanganate ion 84

Figure 4.30 Plot of $k_2(z^{n+})$ versus $[Mg^{2+}]$ for the redox reaction of nicotinic acid with permanganate ion 85

Figure 4.31 Plot of $k_2(z^{n+})$ versus $[Li^+]$ for the redox reaction of L-cysteic acid with permanganate ion 86

Figure 4.32 Plot of $k_2(z^{n+})$ versus $[Mg^{2+}]$ for the redox reaction of L-cysteic acid with permanganate ion 87

Figure 4.33 Plot of $k_2(z^{n+})$ versus $[Li^+]$ for the redox reaction of L-aspartic acid with permanganate ion 88

Figure 4.34 Plot of $k_2(z^{n+})$ versus $[Mg^{2+}]$ for the redox reaction of L- tryptophan with permanganate ion 89

Figure 4.35 Plot of $\log k_2$ versus 1/D for the redox reaction of nicotinic acid and permanganate ion 94

Figure 4.36 Plot of $\log k_2$ versus 1/D for the redox reaction of L-aspartic acid and permanganate ion 95

Figure 4.37 Plot of $\log k_2$ versus 1/D for the redox reaction of L-tryptophan and permanganate ion 96

Figure 4.38 Spectra of the reaction mixture between permanganate ion and nicotinic acidafter 2 minutes of reaction 97

Figure 4.39 Spectra of the reaction mixture between permanganate ion and L-cysteic acid after 2 minutes of reaction 98

Figure 4.40 Spectra of the reaction mixture between permanganate ion and L-aspartic acidafter 2 minutes of reaction 99

Figure 4.41 Spectra of the mixture reaction between permanganate ion and L-tryptophan after 2 minutes of reaction 100

Figure 4.42 Michaelis – Menten plot of $1/k_{obs}$ versus 1/[nicotinic acid] for the redox reaction of permanganate ion and nicotinic acid 101

Figure 4.43 Michaelis – Menten plot of $1/k_{obs}$ versus 1/[L-cysteic acid] for the redox reaction of permanganate ion and L-cysteic acid 102

Figure 4.44 Michaelis – Menten plot of $1/k_{obs}$ versus 1/[L-aspartic acid] for the redox reaction of permanganate ion and L-aspartic acid 103

Figure 4.45 Michaelis – Menten plot of $1/k_{obs}$ versus 1/[L-tryptophan] for the redox reaction of permanganate ion and L-tryptophan 104

LIST OF TABLES

Table 4.1 Pseudo-first order and second order rate constants for the reaction between nicotinic acid and MnO_4^-, $[MnO_4^-] = 1.75x10^{-4}$mol dm^{-3}, λ_{max} = 525nm and T = 28.0±1.0°C 57

Table 4.2 Pseudo-first and second order rate constants for redox reaction between $MnO_4^-$and L-cysteic acid, $[MnO_4^-]=1.5\times10^{-4}$ mol dm^{-3}, λ_{max} = 525nm and T= 27.0±1.0°C 58

Table 4.3 Pseudo-first and second order rate constants for redox reaction between $MnO_4^-$and L-aspartic acid, $[MnO_4^-]=1.5\times10^{-4}$ mol dm^{-3}, λ_{max} = 525nm and T= 29.0±1.0°C 59

Table 4.4 Pseudo-first and second order rate constants for redox reaction of $MnO_4^-$and [L-tryptophan], $[MnO_4^-] = 2.0x10^{-4}$ mol dm^{-3}, λ_{max} = 525nm and T= 28.0±1.0°C 60

Table 4.5 Rate constants for the e effect of cations and anions on oxidation-reduction reaction between MnO_4^- and nicotinic acid 76

Table 4.6 Rate constants for the effect of cations and anions on oxidation-reduction reaction between MnO_4^- and L-cysteic acid 77

Table 4.7 Rate constants for the effect of cations and anions on oxidation-reduction reaction between MnO_4^- and L-aspartic acid 78

Table 4.8 Rate constants for the effect of cations and anions on oxidation-reduction reaction between MnO_4^- and L-tryptophan 79

Table 4.9 Effect of change in dielectric constant on the rate constants for nicotinic acid – permanganate ion reaction 91

Table 4.10 Effect of change in dielectric constant on the rate constants for L-aspartic acid – permanganate ion reaction 92

Table 4.11 Effect of change in dielectric constant on the rate constants for L-tryptophan – permanganate ion reaction 93

LIST OF ABBREVIATIONS

T = Temperature

^{o}C = Degree celcius

K^{1} = Electron transmission coefficient

k = Rate constant

h = Planck constant

K = Equilibrium constant

Subt = Substitution

B.D.H = British Drug House

NA = Nicotinic acid

LP = L-tryptophan

H_2P = L-aspartic acid

HR′H = L-cysteic acid

obs = Observed

I = Ionic strength

λ_{max} = Wavelength of maximum absorption

log = Logarithm

D = Dielectric constant

Caled = Calculated

Phen = Phenanthroline

CHAPTER ONE

1.0 INTRODUCTION

Chemical kinetics is a branch of chemistry that deals with the experimental determination of reaction rates from which rate laws are derived. It also includes investigations of how different experimental conditions can influence the speed of a chemical reaction and yield information about the reaction mechanism and transition states, as well as constructing mathematical model that can describes characteristics of a chemical reaction.

A reaction mechanism is a detailed stepwise or step by step sequence of elementary reactions involving molecules, atoms, radicals or ions that occur simultaneously or consecutively and culminate in the observed overall reaction (Cooke, 1979). For proper elucidation of mechanisms, the experimentally determined rate equation, the exact nature of both reactants and products, the presence of any equilibrium and the stoichiometry of the reaction are indispensable (Basolo and Johnson, 1964).

Electron transfer which is the process by which an electron moves from an atom or a chemical species e.g molecules, to another atom or chemical specie, is the only one of many pathways by which redox reactions can occur (Basolo and Pearson, 1967; Burgess, 1978).

Many reactions in inorganic and biological systems involve the electron transfer at one stage or the other and proper understanding of these electron transfer processes helps in the understanding development and eventual effective control of a wide area of science and technology (Iyun, 1982). Numerous biological processes involving electron transfer reactions include oxygen binding, photosynthesis, respiration and detoxification routes. Additionally the process of energy transfer can be formalized as a two electron exchange (two concurrent electron transfer events in opposite directions). In case of small distances

between the transferring molecules. Electron transfer reactions commonly involve transition metal complexes (Greenwood and Earnshaw, 1997; Holleman and Wiberg, 2001).

1.1 Rate monitoring techniques

There are various methods of monitoring the rates of chemical reactions. A particular technique chosen depends on how fast or how slow the reaction occurs.

1.1.1 Conventional methods

These methods are applicable to slow redox reactions. Conventional methods include photometric, spectrometric, radiometric and polarometric. The methods involve the measurement of the concentration or any physical property of one or more of the reactants or products as a function of time. For instance, in some reactions, absorbance of any of the reactants or products could be measured and related directly to the concentration (Wilkins, 1974).

1.1.2 Monitoring rates of fast reactions

Special techniques are employed for fast reactions with half- lives of about a millisecond. Fast reaction techniques can be broadly classified into flow, relaxation and resonance methods.

1.1.2.1 Flow Technique: In the flow method the reactants are mixed as they flow together in a chamber. Different flow techniques can be employed, depending on the treatment given to the reaction after mixing (Caldin, 1974). Common flow methods are discussed below: **Continuous-flow method**: In the continuous-flow method, the reaction mixture flows continuously along an observation tube while conventional monitoring is made either at different points along the observation tube with the flow maintained at constant rate or at a fixed point on the tube with varied flow rate. In either cases a series of values for the extent

of reaction is obtained at different times these values constitute the kinetic data required (Caldin, 1974).

Stopped-flow method: In this method, the reactants (in solution) are forced together through a mixing device and allowed to flow along a tube, and is abruptly stopped so that the solution comes to rest within a few milliseconds. The rate of the flow along the observation tube is such that when the solution is stopped, a segment within 1cm of mixing device has been mixed for only 1-2 milliseconds. Monitoring any reaction taking place in this segment can be done and the signal relayed to the oscilloscope (Caldin, 1974).

Quenched-flow method: In this method the reaction solution is quenched after a predetermined time and the quenched solution is analysed by any conventional method (Caldin, 1974).

1.1.2.2 Relaxation method: This method is used for systems at equilibrium (Eigen and Maeyer, 1963). In these cases the equilibrium is displaced by some external parameters and the readjustment to a new equilibrium position is directly observed. The dependence of a particular equilibrium on a chosen external physical parameters largely determines the method of perturbation used for such equilibrium and hence these methods are referred to as temperature-jump, pressure-jump or electric field-jump (Wilkinson, 1980).

1.1.2.3 Resonance Technique: Both nuclear magnetic resonance (NMR) and electron spin resonance (ESR) techniques have been used to study complex formation (Pearson and Buch, 1962) and aquation of metal ion (Connick and Poulson, 1959) in solution. In cases where NMR and ESR techniques are the methods of choice, the resonance absorption lines are related to the life time of the nucleus in a given spin state and life time of paramagnetic species in a given energy state respectively.

If the life time of these states is reduced by a chemical interaction, it results in line broadening. On addition of increasing amount of a reagent, measurement of the corresponding increase in width of the line due to the second reagent can be made. For instance, H.N.M.R Line broadening has been used to measure the rate of exchange of several mono-donor ligands coordinated to Mn^{II}, Fe^{II} Co^{II}, Ni^{II} and Cu^{II}. (Caldin, 1964; Burgess, 1978).

1.2.0 Theoritical consideration in electron transfer processes

1.2.1 Franck – Condon principle

The principle states that "the motion of nuclei is slow (10^{-13}s) compared to that of the electron (10^{-15}s), and that transfer occurs without an appreciable movement of the nuclei". (Platzman and Franck, 1954; Sutin, 1966). This implies that electron transitions are rapid compared with nuclear motions and electron transfer occurs without significant movement of the atoms. Since electron transfer reactions involve bond breaking and electron formation, Franck – Condon principle must of necessity come into play. However, since the atomic distances between ligands and the metal ions alter the oxidation state of the metal ion, reorganization of the metal-ligand distances for the reactants and products occurs before electron transfer takes place (Candlin *et al*., 1968).

Electron transfer can only take place when ions approach each other. Where the electron transfer step is very rapid, the overall rate is that at which the ions diffuse together to form ion pairs. Franck-Condon Principle presupposes that the electron transfer takes place with the nuclei of the oxidant and reductant virtually stationary. The organization undergone by the reactants before electron transfer occur in such a way that their transition state energies become almost identical and energy change or electron transfer is minimized. The

total change in energy involved in the process can then be represented by equation (1.1) (Marcus, 1956).

$$\Delta G' = \Delta G_t' + \Delta G_i' + \Delta G_o' \qquad (1.1)$$

where $\Delta G_t'$ = association free energy, $\Delta G_i'$ = inner-sphere reorganization energy and $\Delta G_o'$ = outer-sphere reorganization energy.

The principle also assumes that no angular momentum can be transferred to or from the transition state during the act of electron transfer and a restriction is also imposed on the change in spin angular momentum.

1.2.2 Electron tunneling theory

This theory sheds considerable light on the electron transfer process in solution. The theory considers the electronic energy as being low in both reactant and product activated complexes when compared to the classical potential energy barrier to electron migration between these complexes (Weiss, 1954; Marcus, 1956). Therefore, the electronic energy in the reactants and products is not as high as would ordinarily be expected from classical point of view. Hence the electron migrates via a tunneling process whereby it passes through a potential energy barrier rather than over it. The implication is that the electron will be able to travel distances much greater than would correspond to the actual collision of reactants (Basolo and Pearson, 1967).The potential energy diagram, illustrating this barrier linkage is shown in Figure (1.1) below:

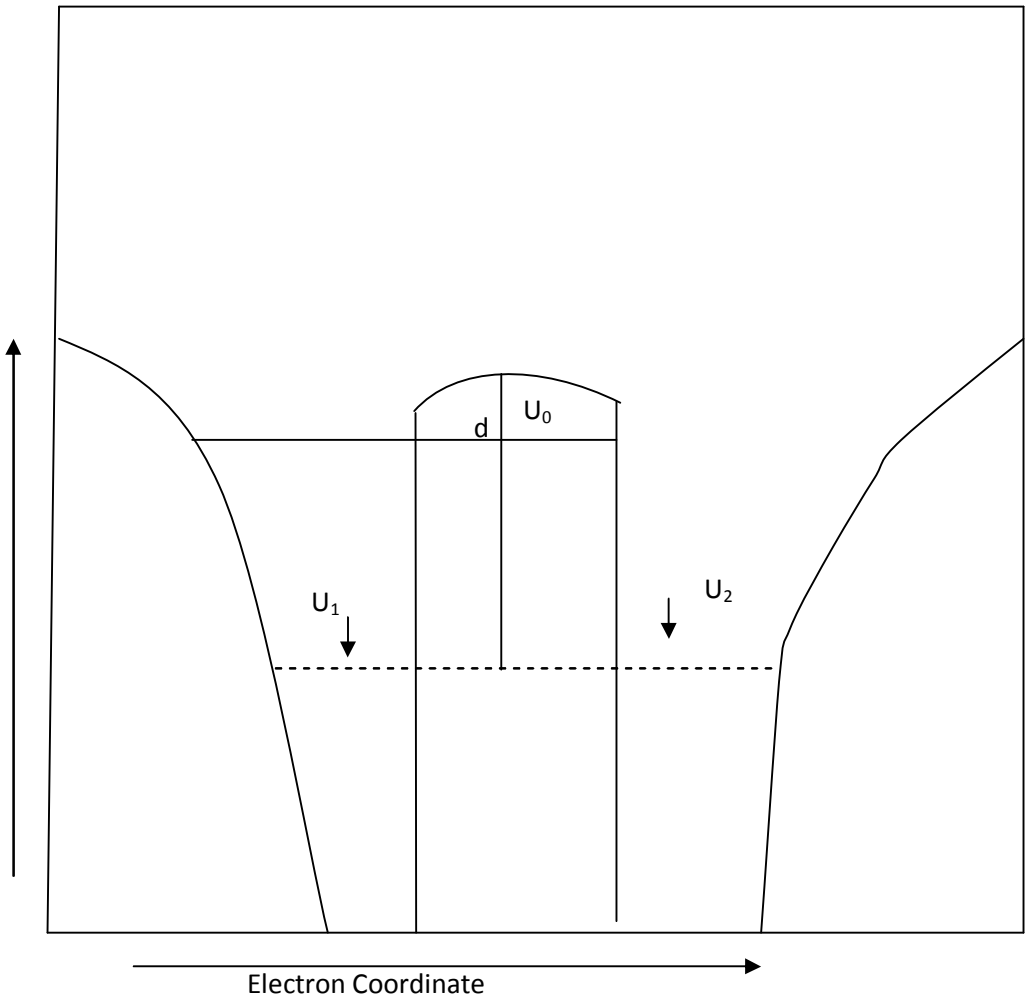


Figure 1.1: Electron transfer by penetration of potential energy barrier

U_1 and U_2 are the ground states of the electrons in cations 1 and 2 respectively,

d = width of barrier at height of penetration, W = kinetic energy of the electron and

U_o = height of the barrier.

The calculation of the electron transmission coefficient as a consequence of the tunneling principle was attempted by Marcus *et al.,* (1954). The results were expressed in terms of transition state theory of chemical kinetics (equation 1.2).

$$k = \frac{KTK^{1}\exp}{h}\left(\frac{-\Delta G_r^{'}}{RT}\frac{\Delta G_e^{'}}{RT}\right) \qquad (1.2)$$

where K^1 = electron transmission coefficient, k = rate constant, K = Boltzman constant, T = absolute temperature, h = Planck constant, R = universal gas constant,

$\Delta G_r^{'}$ = activation free energy for rearrangement of the hydration and coordination shells and

$\Delta G_e^{'}$ = activation free energy for overcoming electric repulsion between the ions.

The transmission coefficient, which always remains less than one, increases, as the exchanging partners come closer together.

1.2.3 Solvated electron theory

This theory attributes the mechanism of electron transfer in solution to the ejection of an electron by the reductant into the solvent (equation 1.3). The solvent then solvates the electron and holds it until the oxidant picks it up (equation 1.4). The possibility that this mechanism operates in aqueous solution is remote, due to the fact that solvated electron with estimated potential of – 2.70V (Latimer, 1952; Burgess, 1978) cannot exist in water without it reducing water (equation 1.5).

$$A + S = A^{+} + S^{-} \qquad (1.3)$$

$$S^{-} + B = [S^{-} + B]^{\#} \longrightarrow S + B \qquad (1.4)$$

where A = reductant,B= oxidant, S= solvent

$$e^{-}_{(ag)} + H_2O \longrightarrow \tfrac{1}{2}H_{2(g)} + OH^{-} \qquad (1.5)$$

1.3.0 Oxidation- reduction(redox) reaction

Redox reactions are those in which the oxidation states of some atoms change. Generally, they can be classified into two broad groups: homonuclear (isotopic) electron exchange reactions and heteronuclear electron transfer or cross reactions (Edwards, 1964).

1.3.1 Homonuclear or isotopic electron exchange

This type of reaction involves the exchange of electrons between two identical metal ion centres in different oxidation states. The reactants and products are the same and identical hence have the same concentrations. The free energy change for such a reaction is mainly due to mixing and is approximately zero (Sharpe, 1982). For example the reactions shown below are homonuclear.

$$*PtCl_6^{2-} + \quad PtCl_4^{2-} \rightarrow PtCl_6^{2-} + \quad *PtCl_4^{2-} \tag{1.6}$$

$$*Fe(phen)_3^{2+} + Fe(phen)_3^{3+} \rightarrow *Fe(phen)_3^{3+} + Fe(phen)_3^{2+} \tag{1.7}$$

Homonuclear electron transfer does not lead to any net chemical change and the equilibrium constant is one since the rate constants are equal for the forward and backward reactions. Isotopic labeling technique is used to monitor slow exchange reactions while NMR spectroscopy is used for fast reaction (Meyer and Taube, 1987; Wilkins, 1974).

1.3.2 Heteronuclear electron transferor cross reactions

This class of reactions involves electron transfer between different metal ion centres. The products are chemically distinct from the reactants (Cooke, 1979).The overall free energy change (ΔG^0) is not equal to zero. In most cases ΔG^0 is less than zero. The reaction can be complementary, if oxidant and reductant undergo equal changes in oxidation states (stoichiometry is 1:1 as for the reactions below).

$$Fe(CN)_6^{4-} + IrCl_6^{2-} \rightarrow Fe(CN)_6^{3-} + IrCl_6^{2-} \tag{1.8}$$

$$Co(en)_3^{3+} + Ru(NH_3)_6^{2+} \rightarrow Co(en)_3^{2+} + Ru(NH_3)_6^{3+} \quad (1.9)$$

The reaction could as well be non-complementary whereby the oxidant and reductant undergo unequal changes in oxidation states (stoichiometry is not 1:1). The reaction

$$Sn^{2+} + 2Fe^{3+} \rightarrow Sn^{4+} + 2Fe^{2+} \quad (1.10)$$

is a good example of such reaction.

For multi- oxidation states changes, mechanistic interest focuses on

(i) How many electrons are transferred in a single step or in a series of univalent changes and (ii) formation of intermediate or otherwise in the process. The oxidation of V^{2+} by Hg^{2+}.

$$Hg^{2+} + V^{2+} \longrightarrow Hg + V^{4+} \quad (1.11)$$

has been documented to be a single step two electron transfer whereas the reaction between I_2 and I_3^- occurs in a series of univalent changes with I_2 as a transient intermediate (Green and Sykes, 1970). Chromium(II) reduction of pentaamine chloroplatinate(IV) (Beattie and Basolo, 1971) and intramolecular electron transfer in some binuclear complexes (Isied and Taube, 1973) have also been reported to occur by direct two electron paths.

1.4.0 Points of mechanistic interest in redox reactions

When undertaking the study of the mechanism of redox reaction. The points of mechanistic interest are:

(i) The stoichiometry of the reaction and the nature (composition) of the activated complex.

(ii) Whether the reaction is accompanied by electron or atoms transfer. If atoms are transferred, which ones are?

(iii) The number of electrons transferred in each single step for a multistep reaction.

(iv) The comparison of the rate of electron transfer with the rate of substitution on the reactant.

(v) For the reactions that are not thermodynamically feasible, what provides the driving force?

(vi) The significance of acid base catalysis when observed.

(vii) Identification or determination of the closeness of approach of the reactants in the activated complex prior to the electron transfer step.

(viii) Identification and isolation of the products formed.

Attempt to address the above points of mechanistic interest have led Taube and his co-workers to establish two outstanding mechanisms for redox reactions. (Taube, 1959, Taube *et al.*, 1953). The two mechanism are the inner-sphere and the outer-sphere mechanisms.

1.4.1 Mechanisms of electron transfer reactions

1.4.2 The outer- sphere mechanism

This mechanism occurs when either or both the oxidant and the reductant are inert to substitution during the time required for oxidation- reduction to take place. The activated complex is designated "the outer-sphere activated complex". In the outer sphere activated complex, the co-ordination sphere of the reaction partners remain intact (although not undisturbed), and the electron given up by the reducing agent must go from the primary bond system of one complex to that of the other.

A typical example of the outer-sphere mechanism is given below:

$$M_1^{II}(H_2O)_6^{2+} + M_2^{III}(NH_3)_5L^{2+} \rightarrow \quad M_1^{III}(H_2O)_5^{3+} + M_2^{II}(NH_3)_5L^{+} \qquad (1.12)$$

Where M_1 and M_2 are different metals with oxidation state of +2 and +3 respectively.

In general the outer-sphere mechanism is thought to occur in four steps. Using the example in above (equation 1.12). The four steps are illustrated as follows

Step I: Formation of a precursor complex

$$M_1^{II}\left(H_2O\right)_6^{2+} + M_2^{III}\left(NH_3\right)_5 L^{2+} \rightleftharpoons \left[\left(H_2O\right)_6 M_1^{II} \,//\, L\, M_2^{III}\left(NH_3\right)_5\right]^{4+} \qquad (1.13)$$

Step 2:Activation of Precursor complex

$$\left[\left(H_2O\right)_6 M_1^{II} \,//\, L\, M_2^{III}\left(NH_3\right)_5\right]^{4+} \rightleftharpoons \left[\left(H_2O\right)_6 M_1^{II} \,//L\, M_2^{III}\left(NH_3\right)_5^{4+}\right]^{\neq} \qquad (1.14)$$

Step 3: Electron transfer and formation of a successor complex

$$\left[\left(H_2O\right)_6 M_1^{II} \,//\, L\, M_2^{III}\left(NH_3\right)_5^{4+}\right]^{\neq} \rightarrow \left[\left(H_2O\right)_6 M_1^{III} \,//L\, M_2^{II}\left(NH_3\right)_5\right]^{4+} \qquad (1.15)$$

Step 4: Decomposition of successor complex to give the final products.

$$\left[\left(H_2O\right)_6 M_1^{III} \,//\, L\, M_2^{II}\left(NH_3\right)_5\right]^{4+} \rightarrow M_1^{III}\left(H_2O\right)_6^{3+} + M_2^{II}\left(NH_3\right)_5 L^{+} \qquad (1.16)$$

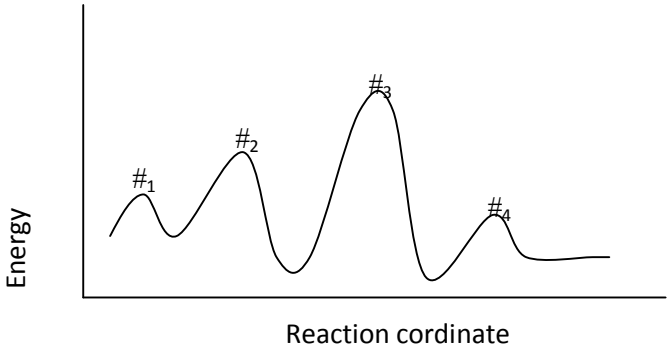


Figure 1.2: Energy profile diagram for a redox reaction which occur by the outer-sphere mechanism

where $\#_1$ = formation of a precursor complex, $\#_2$ = activation of precursor complex, $\#_3$ = electron transfer and formation of a successor complex and $\#_4$ = decomposition of successor complex to give the final products.

Although any of the steps can be the rate determining step, step 3, the electron transfer, is usually the rate determining step.

1.4.3 Inner-sphere mechanism

This type of mechanism involves penetration into the inner-coordination sphere of reactants with the formation of a bridged activated intermediate. (Candlin *et al.*, 1968). Substitution occurs at one of the metal centres to give a ligand- bridged binuclear complex prior to electron exchange process. The two metal centres participating in the reaction are linked by at least one bridging ligand common to their inner coordination shells. The ligand bridge acts as conduction route for transfer of electron from one metal ion to the other. Decomposition of the activated complex, after the electron transfer, yields the products of the reaction. In most cases, the bridging ligand is transferred from its metal centre of origin to the next as can be seen by the typical inner sphere reaction between chromium(II) and cobalt (III) (Candlin and Halpern, 1965).

Typical reactions, that occur through this mechanism include reactions shown by equations(1.17and 1.18) below.

$$\left[Co^{III}(NH_3)_5Cl\right]^{2+} + \left[Cr^{II}(H_2O)_6\right]^{2+} \rightarrow \left[Co^{II}(H_2O)_6\right]^{2+} + 5NH_4^+ + \left[Cr^{III}(H_2O)_5Cl\right]^{2+} \quad (1.17)$$

$$\left[Cr(OH_2)_5Cl\right]^{2+} + \left[*Cr(OH_2)_6\right]^{2+} \rightarrow \left[Cr(OH_2)_6\right]^{2+} + \left[*Cr(OH_2)_5Cl\right]^{2+} \quad (1.18)$$

In general, the inner-sphere mechanism can be represented by the following reaction scheme.

Step 1:Formation of collision complex

$$L_5M^{III}X^{2+} + N^{II}(H_2O)_6^{2+} \rightleftharpoons \left[L_5M^{III}X//N^{II}(H_2O)_6\right]^{4+} \quad (1.19)$$

Step 2:Formation of a bridged precursor complex

$$\left[L_5\ M^{III}\ X\ //\ N^{II}\left(H_2O\right)_6\right]^{4+} \rightleftharpoons \left[L_5M^{III}-X-N^{II}\left(H_2O\right)_5\right]^{4+} + H_2O \qquad (1.20)$$

Step 3: Activation of the precursor complex

$$\left[L_5M^{III}-X-N^{II}\left(H_2O\right)_5\right]^{4+} \rightarrow \left[L_5\ M^{III}-X-N^{II}\left(H_2O\right)_5\right]^{(4+)\neq} \qquad (1.21)$$

Step 4:Electron transfer and formation of successor complex

$$\left[L_5M^{III}-X-N^{II}\left(H_2O\right)_5\right]^{(4+)\neq} \rightarrow \left[L_5\ M^{II}-X-N^{III}\left(H_2O\right)_5\right]^{(4+)\neq} \qquad (1.22)$$

Step 5:Deactivation of activated complex

$$\left[L_5M^{II}-X-N^{III}\left(H_2O\right)_5\right]^{(4+)\neq} \rightarrow \left[L_5\ M^{II}-X-N^{III}\left(H_2O\right)_5\right]^{(4+)\neq} \qquad (1.23)$$

Step 6:Decomposition of Activated Complex

$$\left[L_5M^{II}-X-N^{III}\left(H_2O\right)_5\right]^{(4+)\neq} \rightarrow \left[L_5\ M^{II}\left(H_2O\right)\right]^{2+} + \left[XN^{III}\left(H_2O\right)_5\right]^{2+} \qquad (1.24)$$

Investigation have revealed that the electron transfer step is usually the rate determining step. Typical energy profile for a redox reaction which occurs by the inner-sphere mechanism can be illustrated by Figure 1.3

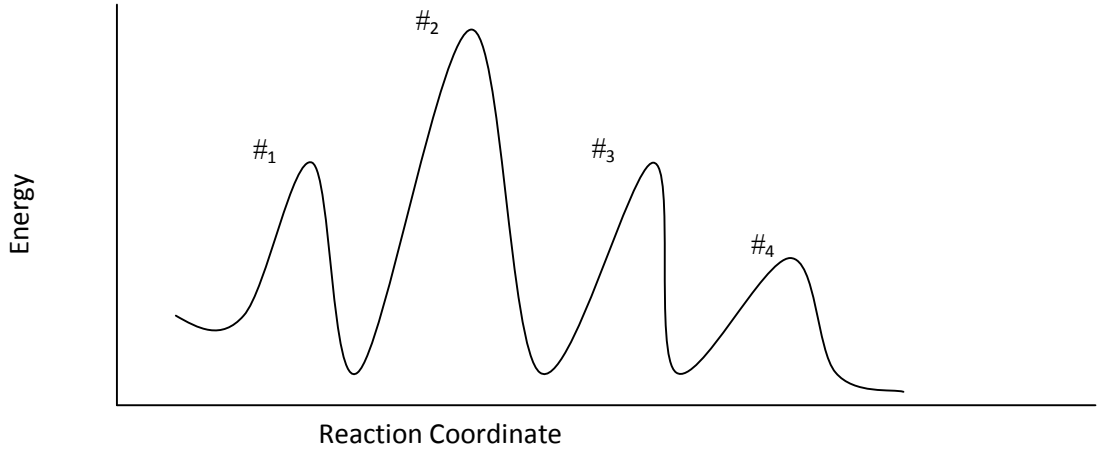


Figure 1.3: Energy profile diagram for a redox reaction which occurs by the inner-sphere

where $\#_1$= Collision complex, $\#_2$= Bridged precursor complex formation,
$\#_3$= Successor complex formation and the act of electron-transfer and
$\#_4$ = Decomposition of successor complex giving the products.

1.5.0 Diagnosis of redox reaction mechanism

The following criteria among others are used in assigning the outer-sphere and the inner-sphere mechanism to redox reactions.

1.5.1 Rate of redox process versus rate of substitution

In the inner-sphere mechanism, substitution into the inner coordination shell of one of the reactant ions precedes electron transfer. Therefore the comparison of the rate of redox process versus rate of substitution into inner coordination shell of the more labile of the reactants ions can be used to assign mechanism to redox reactions.

When $k_{redox} >> k_{sub}$, the outer-sphere mechanism is said to be operating, while if $k_{redox} << k_{sub}$, the inner-sphere mechanism is implicated. If $k_{redox} = k_{sub}$, both the inner-sphere and the outer-sphere mechanism are operating simultaneously

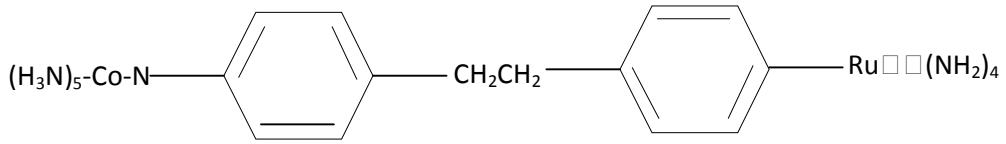
1.5.2 Identification of the binuclear intermediate

The presence of a binuclear intermediate is evidence in support of an inner- sphere mechanism. An example is the reaction VO^{2+} with Cr^{2+} an intermediate $VOCr^{4+}$ was characterized (Espenson, 1965). Its rate of decomposition showed hydrogen ion dependence. The identification of the binuclear intermediate in the inner-sphere mechanism is however possible if the reduced oxidant and the oxidized reductant are relatively inert and the rate of decomposition of the intermediate is slower than the rate of electron transfer.

In some cases where the binuclear intermediate has transient nature, their presence can be inferred indirectly from kinetic data or from empirical, rate law. An example of such

indirectly identified binuclear intermediate include $CrOHV^{5+}$ (Espenson, 1965) and $[OHTiXCo(NH_3)_5]^{5+}$ (Orhanovic and Earley, 1975).

Although the detection of a bridged specie suggests that a reaction may occur by the inner-sphere mechanism, it is not however, a sufficient condition for diagnosing the inner-sphere mechanism. Such intermediates could actually exist and yet the products form directly from such reactants. Taube *et al.*, (1953) have demonstrated such possibilities when they prepared a stable analog of an inner-sphere complex,



and demonstrated that electron transfer occurred independent of the connecting chains.

1.5.3 Products analyses

The transfer of the bridging ligand from one metal ion to another provides an empirical evidence for the operation of the inner-sphere mechanism.

For example the redox reaction involving $Co(NH_3)_5Cl^{2+}$ and Cr^{2+}, the $CrCl^{2+}$ product identified has been associated with the binuclear intermediate $[(NH_3)_5Co\text{-}Cl\text{-}Cr^{4+}]^{\#}$ advancing evidence in favour of the inner-sphere mechanism for the reaction.

These criteria should be used cautiously as:

(i) Atom transfer does not occur in all the inner-sphere reactions (Huchital and Wilkins, 1976) e.g.

$$Co(EDTA)^{2-} + Fe(CN)_6^{3-} \rightarrow Co(EDTA) + Fe(CN)_6^{4-} \qquad (1.25)$$

(ii) The products of some reactions involving reductant such as Fe^{2+}, V^{2+}, Cu^{2+}, Cu^{+}, Eu^{2+} hydrolyses rapidly making detection of MX^{2+} product difficult (X= bridging Ligand).

1.5.4 Reactivity pattern

Below are some of the reactivity pattern that can be used to assign mechanism to redox reactions.

(1) **Reactivity pattern with wide range of reactants**

The comparison of the rate of reaction when similar complexes e.g $Co(NH_3)_5X^{2+}$ ($X=Cl^-,F^-,Br^-$ or NO_3^-) are reacted with a particular reductant gives possible insight into the mechanism that is operating if the rates of the reactions are similar then the outer-sphere mechanism is operating, since this mechanism does not depend on the identity of the bridging ligands. However, when the rates of the reactions depend on the nature of the bridging group, the inner-sphere mechanism is predicted (Sykes, 1967; Shea and Haim, 1973).

(ii) **Relative rates of reaction of hydroxyl and aquo complexes**

The hydroxyl group (OH^-) is a better bridging ligand than water (H_2O). So it is expected that the hydroxyl complexes react faster through the inner-sphere mechanism. Thus where $k_{OH}<<k_{H20}$, the outer-sphere mechanism is said to be operating while converse is true when $k_{OH}>>k_{H20}$

1.5.5 The Effects of added ions

Marked catalysis by added ions have been reported for a variety of reactions known or at least confidently believed, to occur by outer-sphere mechanism. Effects of added anions on known inner-sphere redox reactions are much smaller, hence an examination of the dependence of redox rate on added anion such as chloride, has been used as an indication of mechanism. For instance, in the cases of Yb^{2+} (Christenson and Espenson, 1970) and V^{3+} (Wang and Espenson, 1971).

1.5.6 Activation parameters

The use of activation parameters, $\Delta H^{\neq}$, $\Delta G^{\neq}$ and $\Delta S^{\neq}$ to determine the type of mechanism operating in a particular redox process is of little use, because there seems to be no direct correlation between activation parameters and the type of mechanism (Cotton and Wilkinson, 1980). However change in molar volume of activation ($\Delta V^{\neq}$) has been used in mechanistic diagnosis (Hubbard *et al.*, 1991).

1.5.7 Use of ambidentate bridging ligand

Distinction between the inner-sphere and the outer-sphere mechanism can be made on the basis of difference in the rate of electron transfer observed with symmetrical and unsymmetrical bridging ligands e.g azide, thiocyanate and isothiocyanate complex.

If the ratio of the rate constant for the reduction of azide complex to that for reduction of the thiocyanate complex (k_{N3}^{-}/k_{NCS}^{-}) or for isothiocyanate and thiocyanate complex ($k_{SCN=}k_{NCS}$-) shows no difference or are similar then outer-sphere mechanism should be operating, while the converse is true for reactions of the inner-sphere mechanism (Sutin, 1968; Wang and Espenson, 1971; Espenson, 1965; Candlin *et al.,* 1964).

1.5.8 Marcus theory of electron transfer rates

In the outer-sphere mechanism, the weak interaction between the reactants has permitted its theoretical treatment and the correlation between kinetics and thermodynamic parameters (Sutin, 1966). Probably, the most widely used of treatments is the Marcus theory (Marcus, 1956).

Marcus theory which was initially used for the calculation of absolute rate constants for homonuclear exchange reaction was later extended to cross-reactions. Marcus assumed in his theory small electronic interaction between the reacting species which are treated as

rigid spheres of radii a_1 and a_2, inside which no change of inter atomic distance occurs during the reaction. He further said that when the work term is small, little re-organisation. is involved prior to electron transfer. Marcus therefore predicted that for the cross reaction equation;

$$Ox_1 + Red_2 \rightleftharpoons^{K_{12}} Red_1 + Ox_2 \qquad (1.26)$$

and relative isotopic exchange reaction equation.

$$Ox_1 + {}^*Red_1 \xrightarrow{k_{11}} Red_1 + {}^*Ox_1 \qquad (1.27)$$

$$Ox_2 + {}^*Red_2 \xrightarrow{k_{22}} Red_2 + {}^*Ox_2 \qquad (1.28)$$

Then $K_{12} = (k_{11}\, k_{22}\, k_{12} f)^{1/2}$

where

$$\log f = \frac{(\log K_{12})^2}{4\log \frac{k_{11}k_{22}}{Z^2}} \qquad (1.29)$$

where k_{12} = rate constant for cross reaction, f = transmission coefficient usually assume to be 1, Z = frequency of collision $\approx 10^{11} m^{-1}s^{-1}$ for homogenous reaction, Z= frequency of collision $\approx 10^{11} m^{-1}s^{-1}$ for homogenous reaction, k_{11} and k_{22} = the rate constants for the exchange reactions.

Thus from Marcus equation; theoretical rate constants for electron transfer reaction can be calculated from equation below:

$$k = Ze^{-}\Delta G^{\neq}/RT \qquad (1.30)$$

$\Delta G^{\neq}$= free energy of the cross reaction. A reasonable agreement between k_{caled} and k_{obs} is taken as evidence that the reaction is of the outer sphere type. Marcus theory is now applied in various forms. An example is the linear free energy relationship given by the equation,

$$\Delta G^{\neq}_{12} = 0.5\Delta G^{\neq}_{11} + 0.5\Delta G^{\neq}_{22} + 0.5\Delta G^{0} \qquad (1.31)$$

So that for a series of related reactions a plot of ΔG^{*}_{12} versus ΔG^{0}_{12} is a straight line with a slope of 0.50 if reaction is of the outer sphere mechanism.

1.6 Research objectives

Nicotinic acid which is otherwise called vitamin B_3 is involved in both DNA repair and the production of steroid hormones on the adrenal gland and it is also used for the reduction of cholesterol level in human system (Michael *et al*., 2000; Lehninger*, et al.,* 2000). Amino acids are critical to life and have many functions in metabolism. In biology they are used in plants and micro-organism for the synthesis of pantothetic acid (vitamin B_5), which is a component of coenzyme, in biochemistry, they are important in nutrition. They are also used in food technology and industry for the production of biodegradable plastics, food flavor enhancer, artificial sweetener, cosmetics, biopolymers, corrosion inhibitor, drugs and chiral catalysts (Leuchtenberger, 2005). Potassium permanganate is used in water treatment industry. It is also used biomedically for treatment of gonorrhea, candidiasis, ulcer, dermatitis and fungal infections of hands and feet.

In spite of the uses of these chemicals as enumerated above, there exist insufficient data to really support the oxidation of nicotinic acid and amino acids by potassium permanganate. It is our hope that this research will go a long way to complement the much needed kinetic information relating to the process of oxidation of these biochemical in the human system especially in biomedical industries with view to assigning mechanistic pathways.

CHAPTER TWO

2.0 LITERATURE REVIEW

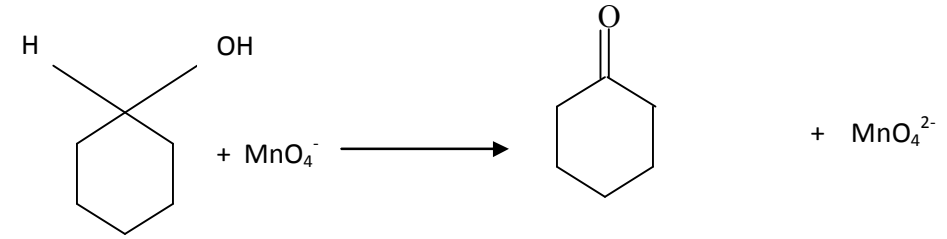
2.1 Permanganate as an oxidizing and hydroxylating agent

Heptavalent manganese as a powerful oxidant and hydroxylating agent has been known for a long time and its chemistry has been reviewed by several authors (Cullis and Ladbury, 1955; Ladbury and Cullis, 1959; Waters, 1958; Stewart and Mocek, 1963). Hiremath *et al.,* (1996) reported that permanganate is widely used as an oxidizing agent in synthetic as well as in analytical chemistry. It has several advantages as an analytical reagent, because it is a strong oxidant and also vividly coloured, thus serving as self indicator. (Insauti *et al*., 1995). The oxidizing abilities of manganese(VII) depend on the pH of the medium (Waters, 1958; Iyun and Ajibade, 1992).

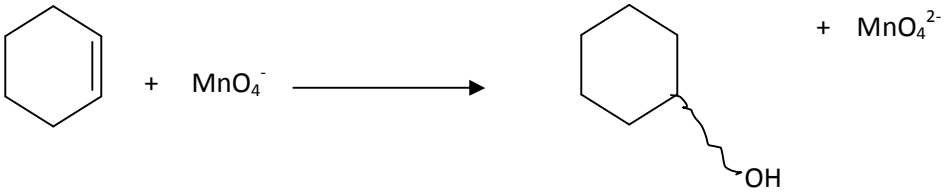
Oxidation of some specific functional groups of organic compounds by permanganate showed that phenols were highly oxidized (He *et al*., 2009 and Jiang *et al*., 2009). Research has also shown that amines and alcohols are readily oxidized by permanganate as well. The reactivity lessens from primary to secondary to tertiary amines and alcohols (Rawalay and Shechter, 1967; Stewart, 1965). It is reported also that alkanes are readily oxidized by permanganate (Stewart, 1965). Benzene rings and their derivatives (toluene and xylenes) are observed to be oxidized slowly by permanganate (Waldemer and Tratnyek, 2006). Functional groups such as amides, carboxylic acid, ketones and aldehydes are observed to be stabled when permanganate is in a neutral solution (Stewart, 1965 and Sharma *et al*., 2008). These typically are the final products for more reactive groups that do oxidize by permanganate. This information can help predict the behaviour of more complex compounds during oxidation by permanganate.

A significant amount of permanganate oxidation research has also been dedicated to the production of manganese(II)oxide. Manganese(II) oxide particles are product of permanganate reduction and are of importance for monitoring permanganate consumption in research and also for their potential deposition during treatment. Studies have shown how reaction condition such as pH affects the production of manganese(II) colloidal particles (Crimi and Siegnist, 2004).

Kolb (1986) studied the permanganate oxidation of cyclohexane, cyclohexene and cyclohexanol. Cyclohexene reacts more rapidly than cyclohexanol, cyclohexane did not react. The secondary alcohol cyclohexanol was oxidized by permanganate to give ketone cyclohexanone. The alkene cyclohexene reacts to give cis-1,2, cyclohexanediol. The permanganate ion was reduced to the green manganate ion. The equations of the reaction are represented as:



(2.1)



(2.2)

The kinetics of the oxidation of mandelic acid (MA) by permanganate ion in aqueous alkaline medium at a constant ionic strength of 1.0 mol dm^{-3} was studied spectrochemically (Panari *et al.,* 1998). The reaction shows first order kinetics in [permanaganate ion] and fractional order dependences in [MA] and [alkali]. Addition of products, manganate and aldehyde had no significant effect on the reaction rate. An increase in ionic strength and a decrease in dielectric constant of the medium increased the rate. The oxidation process in alkaline medium under the conditions employed in the investigation proceeds first by formation of an alkali permanganate complex, which combines with mandelic acid to form another complex. The latter decomposes slowly followed by a fast reaction between the free radical of mandelic acid and another molecule of permanganate ion to give products. The reaction was studied at different temperatures and activation parameters were computed with respect to the slow step of the proposed mechanism.

The kinetics of oxidation of pantothemic acid by permanganate ion in aqueous alkaline medium at constant ionic strength has been investigated spectrophotometrically (Desai *et al.,* 2002). The reaction showed first order kinetic in [MnO_4^-] and an apparent less than unit order dependence each on [pantothemic acid]and [alkali]. Initial addition of products has no significant effect on the rate of the reaction. An increase in ionic strength and decrease in dielectric constant of the medium increase the rate.

Ahmed *et al*., (2003) observed the kinetics of oxidation of chitosan as polysaccharide by permanganate in aqueous perchlorate media at a constant ionic strength. The reaction was found to have second order overall kinetics and to be first order in the concentration of both reactants. The results obtained show that the reaction is acid catalysed. It has been

discovered that potassium permanganate is an effective heterogeneous oxidant, even without resorting to the use of a solid support, if acetonitrile is employed as the solvent.

Rao *et al.,* (2004) discussed the kinetics of oxidation of some monosaccharide viz, D-ribose, D-xylose, D-arabinose, D-glucose, D-fructose, D-galactose, 2-deoxyglucose, and α-methyl glucopyranoside by MnO_4^- in aqueous alkaline medium. The rate of oxidation has been found to be first order both with respect to [oxidant] and [sugar]. The rate is independent of $[OH^-]$ under the experimental conditions of $[OH^-] > 0.5 mol\ dm^{-3}$ where the oxidant is stable. The effect of ionic strength is negligible on the rate. A mechanism involving the formation of a 5 membered cyclic intermediate complex between MnO_4^- and 1, 2-enediol form of sugar is proposed.

Shallangwa *et al.,* (2006), investigated mechanism of oxidation of rosaniline hydrochloride with heptavalent manganese in acidic medium. The stoichiometry of reaction was 1:1 in respect of both oxidant and reductant. The reactions were also found to be first order in both [oxidant] and [reductant] and the rate of reaction displayed negative salt effect. Added anions were observed to have no effect on the reaction system, spectroscopic investigation and Michaelis- Menten plot showed that there was formation of intermediate complex and on the basis of these, the inner-sphere mechanism was proposed for the reaction.

The kinetics and mechanism of oxidation of L-ascorbic acid by permanganate ion in acidic medium has been carried out (Babatunde, 2008). It was observed that two moles of oxidant were consumed by five moles of reductant, the reaction shows dependence on acid concentration and is first order in both oxidant and the reductant. The proposed rate law is

$$-\frac{d}{dt}[MnO^-_4] = (a + b[H^+])[MnO^-_4][H_2A] \qquad (2.3)$$

where a = $2.7 \times 10^{-3} dm^3 mol^{-1} s^{-1}$ and b = $0.38 dm^6 mol^{-2} s^{-1}$.

The results of spectroscopic investigations and kinetic studies did not implicate the formation of intermediate complex. An outer-sphere reaction pathway was proposed for this reaction.

Oxidation of pharmaceuticals and personal care products by permanganate has been evaluated by a spectrophotometric method (Gibson, 2010). In this study thirty-nine compounds were chosen to represent numerous classifications, including beta-blocker cephalosporins, fluoroquinolones, macrolides, non-steroidal anti-inflammatory drugs, phenol structures, polypeptides, sulfonamides, tetracyclines and triazines. The reactivity of each compound was determined by measuring the absorbance of permanganate over time as it reacted with an excess of the compound. The absorbance data fitted into pseudo-first order reaction model that accounted for the growth of manganese dioxide colloids. The most reactive groups that reduced permanganate within minutes at pH 7.0 were the cephalosprins, phenol structures and tetracyclines. The majority of the remaining pharmaceuticals and personal care products were moderately or weakly reactive (reducing permanganate within hours), carbadox, monensin, simetone and tri (2 – carboxyethyl) phosphine were poorly reactive (reducing permanganate over days). Metoprolol was the only selected compound that was determined to be potentially non-reactive (no reaction after one day).

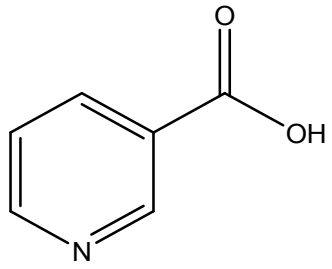
In acidic medium the expected oxidizing species of permanganate ion are mainly Mn(VII), Mn(IV) and Mn(III) (Rao *et al.*, 1979; Rajanna *et al.*, 1996). Several authors have also reported that oxidation by Mn(VII) can undergo scheme similar to the chromic oxidations via an ester-like complex (Cullins and Ladbury, 1955; Wei and Stewart, 1966).

2.2.0 Nicotinic acid

Nicotinic acid otherwise known as vitamin B_3, niacin or pyridine carboxylic acid is a colourless, water-soluble solid, which is a derivative of pyridine, with a carboxyl group (COOH) at the 3-position. It is a precursor to nicotinamide adenine dinucleotide (NAD^+) and nicotinamide adenine dinucleotide phosphate ($NADP^+$) which play essential metabolic roles in living cells. Niacin also involved in deoxyribonucleic acid (DNA) repair and the production of steroid hormones in the adrenal gland. It is one of five vitamins associated with pandemic deficiency diseases such as pellagra (nicotinic acid deficiency), scurvy (vitamin C deficiency), beriberi (thiamin deficiency), rickets (vitamin D deficiency) and night blindness (vitamin A deficiency).

In larger doses nicotinic acid can reverse atherosclerosis by lowering low-density liprotein (LDL) and favourably affecting other compounds (Michael *et al.,* 2000).

Nicotinic acid is structurally shown as



Nicotinic acid

2.2.1 Deficiency of nicotinic acid

Nicotinic acid deficiency is rarely seen in developed countries, but it is usually apparent in conditions of poverty, malnutrition, and chronic alcoholism. It also tends to occur in areas where people eat maize (the only grain low in nicotinic acid) as a stable food (Lagunar and Carpenter, 1951). A special cooking technique called mixtamalization is needed to increase the bioavailabity of nicotinic acid during maize meal/flour production.

Mild vitamin B_3 deficiency has been shown to slow metabolism, causing decreased tolerance to cold. Severe deficiency of nicotinic acid in the diet causes the disease pellagra, which is characterized by diarrhea, dermatitis, and dementia, as well "necklace" lesion on the lower neck, hyper pigmentation, thickening of the skin, inflammation of the mouth and tongue, digestive disturbances, amnesia, delirium and eventually death, if left untreated. Common psychiatric symptoms of nicotinic acids deficiency include irritability, poor concentration, anxiety, fatigue, restlessness, apathy and depression (Pitsavas *et al.,* 2004; Prakash *et al.,* 2008).

2.2.2 Toxicity of nicotinic acid

Pharmacological doses of niacin (1.5-6g per day) often lead to side effect that can include dermatological conditions such as skin flushing and itching, dry skin, and skin rashes including eczema exacerbation and *acanthosis nigricans.*These symptoms are generally related to niacin role as the rate limiting cofactor in the histidine decarboxylase enzyme which converts 1-histidine into histamine H_1 and H_2 receptors mediated histamine is metabolized through a sequences of mono (or di) amine oxidase and catechol-O-methyl transferase(COMT) into methyl histamine which is then conjugate through the liver's CP450 pathways. Persistent flushing and other symptoms may indicate deficiencies in one or more of the cofactors responsible for the enzymatic cascade. Gastro intestinal complaints such as dyspepsia, (indigestion), nausea and liver toxicity, fulminant hepatic failure, have also been reported. Side effects of hyperglycemia, cardiac arrhythmias and "birth defects in experimental animals" have also been reported (Parker *et al.,* 2006; Capuzzi *et al., 2000*). High dose of niacin may also elevate blood sugar, thereby worsening diabetes mellitus. Hyperuricemia is another side effect of taking high dose niacin, and may exacerbate gout.

Mittal *et al*., (2007), reported that niacin at doses used in lowering cholesterol has been associated with birth defects in laboratory animals, with possible consequences, for infant development in pregnant women. Niacin at extremely high doses can have a life-threatening acute toxic reaction. It's extremely high doses can also cause niacin maculopathy, a thickening of the macula and retina, which leads to blurred vision and blindness. This maculopathy is reversible after stopping niacin intake.

2.2.3 Reactions of nicotinic acid

Anders and Karls (1988), studied the reaction of pyridine carboxylic acids with dicyclohexylcarbodiimide and p-nitrophenol. The terminal amino groups of lysine and ornithine were modified in the course of the reaction. In this reaction the p-nitrophenyl esters of 2-pyridine carboxylic (picolinic) acid, 3-pyridinecarboxylic (nicotinic) acid and 4-pyridine carboxylic (isonicotinic) acid were used. The method used consists of adding dicyclohexylcabodiimide (DCC) to a solution of the acids and a 20% excess of p-nitrophenol in N, N-dimethyl formamide (DMF).The results were satisfactory in the case of nicotinic and isonicotinic acid, and the corresponding esters were obtained in a yield of about 60% after recrystallization, but in the case of picolinic acid, however this procedure was not satisfactory and two major products were formed which could be isolated by fractional crystallization from 2-propanol. P-nitrophenyl picolinate was the minor product isolated with a yield of only 16%. The major product isolated with a yield of 32% was N-picolinoyl- N, N' dicyclohexylurea.

Frank and Leslie (1997), studied reductive dechlorination of a 2-chloronicotinic acid under Finkelstein conditions. The process involved nucleophilic displacement of chloride by iodide (as sodium or potassium iodide) in refluxing acetone or methyl ethyl acetone and the reaction was driven by the insolubility of the resultant sodium or potassium chloride in the

acetone solvent. The 5-halo-6-iodonicotinic acids were thus generated from their respective 6-chloro derivatives in acceptable yields.

2.3.0 Amino acids

Amino acids are molecules containing an amine group, a carboxylic acid group and a side chain that varies between different amino acids. The key elements of an amino acid are carbon, hydrogen and nitrogen. They are particularly important in biochemistry where the term usually refers to alpha-amino acids.

The amine and carboxylic acid functional groups found in amino acids allow them to have amphiprotic properties. Carboxylic acid groups ($-CO_2H$) can be deprotonated to become negative carboxylates ($-CO_2^-$), and α-amino groups (NH_2^-) can be protonated to become α-ammonium groups (NH_3^+). This implies that all amino acid has a positive and a negative charge on the same group of atoms. This occurrence is called zwitterions (Simmons and Meisenberg, 2006). For example, aminoethanoic acid (the amino acid glycine) has the formulae $H_2N.CH_2.COOH$. However, under neutral conditions, it exists in the different form of the zwitterions, $^+H_3N.CH_2.COO^-$, which can be regarded as having been produced by an internal neutralization reaction (transfer of a proton from the carboxyl group to the amino group). Aminoethanoic acid, as a consequence, has some properties characteristic of ionic compounds such as high melting point and solubility in water. In acid solutions, the positive ion $^+H_3NCH_2COOH$ is formed. In basic solutions, the negative ion $H_2NCH_2COO^-$ predominates.

2.3.2 Reactions of amino acids

Denis (1911), reported the oxidation of the alanine and tyrosine with alkaline potassium permanganate. The products of the oxidation of alanine with the oxidant were ammonia, carbondioxide, oxalic acid, acetic acid and nitric acids. Whereas the oxidation

products of tyrosine were found to consist of ammonia, carbondioxide, oxalic acid, acetic acid and nitric acid together with traces of an acid which was thought to be p-oxybenzoic acid but which owing to the minute amounts available could not be identified.

Kinetics and mechanism of oxidation of DL-α-alanine by permanganate ion in acid perchlorate media has been discussed (Hassan, 1991).The reaction was found to obey second order kinetics overall with respect to each of the reactants in the slow initial stage, but this was not however maintained throughout the relatively fast final stage of reaction. The added salts lead to the prediction that Mn(II) and or Mn(IV) play a very important role in the reaction kinetics.The products obtained through qualitative analysis conform to the stoichiometric equation below:

$$5CH_3CH(NH_2)COOH + 2MnO_4^- + 11H^+ \longrightarrow CH_3CHO + 5NH_4^- + 2Mn^{2+} + 5CO_2 + 3H_2O \quad (2.4)$$

Iyun and Tinuoye (1988) studied the chromium(VI) oxidation of L–cysteine and observed that three moles of L-cysteine were consumed by one mole of chromium(VI). The reaction conformed to the rate law

$$-\tfrac{1}{3}\frac{d}{dt}[CrO_4^{2-}] = (a + b[H^+])[CrO_4^{2-}][L-\text{cysteine}] \quad (2.5)$$

The rate of reaction was observed to increase with increase in ionic strength but decrease with increase in medium dielectric constant. Addition of $CH_3COO^-$and NO^-_3 enhanced the reaction rate. Spectroscopic and kinetics evidence suggested that a precursor complex is formed prior to the electron transfer step. The inner-sphere mechanism involving a Cr(VI)-sulphur bonded binuclear intermediate was proposed for the reaction.

Kinetics and mechanism of the oxidation of DL-methionine by chromium(IV) in aqueous acidic media has been reported (Iyun and Adeyanju, 2004). The reaction was mildly

catalysed by acid and anions. The rate of the reaction increased slightly with increase in ionic strength of the reaction medium and was inversely dependent on the dielectric constant of the reaction medium. The stoichiometry equation of the reaction was

$$CrO_4^- + 2RSCH_3 + 4H^+ \longrightarrow 2RCH_2S{=}O + Cr^{2+} + 2H_2O \quad (2.6)$$

where $RSCH_2 = CH_2SCH_2CH_2CH(NH_2)COOH$

The reaction kinetics of the autocatalytic oxidation of L-asparagine by permanganate ions has been investigated in moderately strong acid medium using the spectrophotometric technique (Zahedi and Bahrami, 2004). An autocatalytic effect due to Mn^{2+} ions formed as a reaction product was observed, both catalytic and non-catalytic processes were determined to be first order with respect to the permanganate ion, while a first and a fractional order with respect to the amino acid for non-catalytic and catalytic reactions were obtained respectively. The overall rate equation for the process may be written as;

$$-\frac{d}{dt}[MnO_4^-] = k'_1[MnO_4^-] + k'_2[MnO_4^-][Mn^{2+}] \quad (2.7)$$

where k'_1 and k'_2 are pseudo rates constants for non-catalytic and catalytic reactions, respectively.

Song *et al*., (2008) investigated the kinetics and mechanism of oxidation of leucine and alanine by Ag(III) complex in alkaline medium spectrophotometrically. The reaction was in first order with respect to Ag(III) complex and amino acids (leucine, alanine). The second order rate decreased with the increasing in $[OH^-]$. A plausible mechanism was proposed from the empirical kinetic data obtained. The activation parameters were also calculated at 298.2k.

Kinetics and mechanism of oxidation of L-arginine by sodium periodate in alkaline medium has been reported (Sridevi and Vani, 2010). It was found that the reaction is first

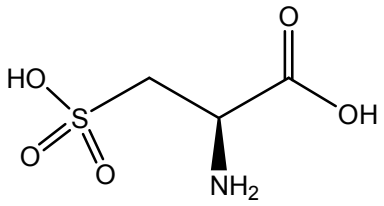
order with respect to [arginine], [OH^-] and [periodate]. The oxidation product of the reaction was found to be α-keto acid. The anionic species of arginine (Arg) was considered to be the reactive species. A suitable mechanism was proposed leading to the rate law.

$$\text{Rate} = -\frac{d}{dt}[\text{periodate}] = \text{kK}[\text{arginine}][OH^-] \quad (2.8)$$

2.4 Cysteic acid

Cysteic acid is an intermediate in cysteine metabolism (Weast, 1981). Cysteine metabolism refers to the biological pathways that consume or create cysteine. The pathways of different amino acids and other metabolites interweave and overlap to creating complex systems. In human cysteine metabolism, L- cysteine is consumed in several ways. It is also consumed in methionine and glutathione metabolism as well as pantothenate/CoA biosynthesis. L-cysteine is converted by enzyme cysteine di-oxygenase to cysteine sulphinic acid or L- cysteic acid.

It is structurally represented as



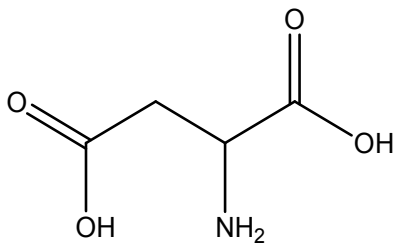
L – cysteic acid

2.5.0 Aspartic acid

Aspartic acid is an α-amino acid with the chemical formular given as $HOOCCH(NH_2)CH_2COOH$. The carboxylate anion, salt, or ester of aspartic acid is known as aspartate. It is a non-essential amino acid which implies that it can be synthesized

(Stryer *et al.,* 2002). It is together with glutamic acid classified as an acidic amino acid with a pka of 4.0.

It is structurally represented as



L – aspartic acid

2.5.1 Forms of aspartic acid

The term "aspartic acid" refers to either of two isomeric forms which are: D-aspartic acid and L-aspartic acid or a mixture of two of these two forms, only "L-aspartic acid" is directly incorporated into amino acid. The biological roles of its counterparts, "D-aspartic acid" are more limited, enzymatic synthesis produced either one of the two forms, but most chemical syntheses produced both forms, "DL-aspartic acid" known as a racemic mixture.

2.5.2 Role of aspartic acid in biosynthesis of amino acids

It is of paramount importance in the metabolism during construction of other amino acids and biochemicals in the citric acids cycle or kreb cycle. Among the biochemicals that are synthesized from aspartic acid are asparagines, arginine, lysine, methionine, threonine, isoleucine and several nucleotides.

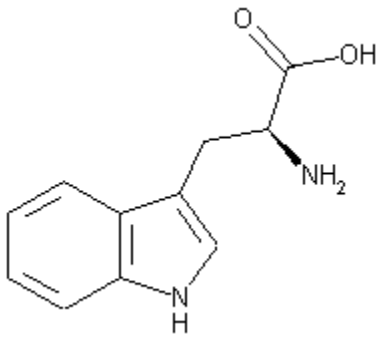
Aspartic acid is used for treatment of chronic fatigue because of the crucial role it plays in generating cellular energy. It moves the coenzyme nicotinamide adenine dinucleotide (NDPH) molecules from the main body of the cell to its mitochondria, where it is used to generate adenosine triphosphate (ATP), the fuel that powers all cellular activity.It sharpened humans mind by increasing concentrations of NADH in the brain, which is

thought to boost the production of neurotransmitters and chemicals needed for normal mental functioning. It also removes excess toxins from the cells, particularly ammonia, which is very damaging to the brain and nervous system as well as the liver (Lehninger *et al.,* 2000).

2.6.0 Tryptophan

Tryptophan is one of the 20 standard amino acids, as well as an essential amino acid in the human diet. Only the L-stereoisomer of tryptophan is used in structural or enzyme proteins, but the D-stereoisomer is occasionally found in naturally produced peptides (Pallaghy, 1999).

It is structurally represented as



L-tryptophan

The distinguishing structural characteristic of tryptophan is that it contains an indole functional group.

2.6.1 Role of tryptophan

Tryptophan has two important functions firstly, a small amount of the tryplophan present in human diet (about 3%) is converted into niacin (vitamin B_3) by the liver, this conversion can help prevent the symptoms associated with niacin deficiency when dietary intake of this vitamin is low (Ikeda *et al.,*1965).

Secondly, tryptophan serves as a precursor for serotonin, a neurotransmitter that help the body to regulate appetite, sleep patterns, and mood, because of its ability to raise serotonin levels. Tryptophan had been used therapeutically in the treatment of a variety of conditions, most notably, insomania, depression, anxiety, headaches, nightmares, obesity, painful premenstrual syndrome and senile dementia (Bell *et al.,* 2001).

CHAPTER THREE

3.0 EXPERIMENTAL

3.1.0 Materials and Reagents

. All reagents used were analar of grade. All reagents and solvents were used without further purification. Distilled water was used in preparing all solutions.

3.1.1 Preparation of standard solution of potassium permanganate

A standard solution of potassium permanganate (BDH, analar) was prepared by weighing 1.98g of the oxidant and dissolving same in 250ml of distilled water. The solution was boiled gently for 30 minutes and then allowed to cool. The solution was then filtered under suction on sintered glass and the filtrate stored in a stoppered chromic acid washed brown bottle. The stoppered bottle was kept in the dark.

The prepared $KMnO_4$ solution was standardized with sodium oxalate according to the procedure reported by Vogel (1961), and which is reproduced below. Some sodium oxalate BDH (analar grade) was dried at 107^0C for about two hours and allowed to cool in a covered vessel in a dedicator, 0.30g of the dry sodium oxalate was accurately weighed into a 600ml beaker, 240ml of freshly prepared distilled water was added and the 12.5ml of concentrated sulphuric acid was added accurately. The mixture was stirred gently until the oxalate dissolved. This solution of oxalate is 1.0mol dm^{-3} and 1.0ml $Na_2C_2O_4$ is equivalent to 0.06701g of $Na_2C_2O_4$.

The permanganate solution was added from a burette at a rate of 25-35ml per minute with constant stirring. The mixture was heated to 60^0C while stirring with a glass rod and the titration completed by adding the permanganate drop wise, until a faint pink colour persists for at least 30seconds. The determination was repeated with the same quantities of sodium oxalate until there were agreements, in terms of observation of faint pink colour that

persisted for at least 30 seconds. The standardized permanganate solution was kept for a long time, but it was restandardized frequently to confirm that there was no decomposition in the system.

Standard solution of 0.02mol dm^{-3} of $KMnO_4$ was prepared based on the procedure described above then $1.75x10^{-4}$ mol dm^{-3}, $1.5x10^{-4}$ mol dm^{-3} and $2.0x10^{-4}$ mol dm^{-3} $KMnO_4$ were obtained from 0.02 mol dm^{-3} by serial dilution method.

3.1.2 Preparation of standard tetraoxosulphate(VI) acid solution

A stock solution of sulphuric acid (analar grade) was made by diluting 98% sulphuric acid of specific gravity 1.84. The sulphuric acid was standardized volumetrically using sodium hydroxide as primary standard and methyl-orange as indicator.

3.1.3 Preparation of standard solution of nicotinic acid

Standard solution of nicotinic acid 0.5 mol dm^{-3} (BDH) was prepared by dissolving 6.16g of the crystal in 100cm^3 of distilled water. This was standardized gravimetrically as follows: 2.00cm^3 of the stock solution was taken and evaporated to dryness in a pre-weighed bottle dried at about 105^oC and cooled in the desiccators until constant weight was obtained. By difference the amount of crystal in 2.00cm^3 was determined after which the mass concentration of the salt and hence its molar concentration was calculated.

3.1.4 Preparation of standard solution of amino acids

Solutions of the amino acids (L-cysteic acid, L-aspartic acid and L-tryptophan) used were prepared by dissolving known amounts of the respective amino acids in known volume of distilled water. All amino acids used were analar grade.

3.1.5 Preparation of standard solution of salt solution

The solutions of Na_2SO_4, Li_2SO_4, NaCl, $NaNO_3$ and $MgSO_4$ were all prepared by dissolving known weight of the respective salt in known volume of distilled water. All salts were analar grade.

3.1.6 Preparation of standard solution of sodium oxalate

Standards solution of sodium oxalate ($Na_2C_2O_4$)with molar mass of 134gmol^{-1} with density of 2.34gcm^{-1} was prepared by dissolving known weight of the oxalate in known volume of distilled water.

3.2.0 Stoichiometric studies

The stoichiometries of the reactions were determined by spectrophotometric titration using the mole ratio method (Ayoko *et al*., 1991a; Lohdip and Iyun, 1993). In all cases the concentration of potassium permanganate was kept constant while that of the nicotinic acid and amino acids were varied as follows;

for MnO_4^- : nicotinic acid

$[MnO_4^-] = 1.75x10^{-4}$ mol dm^{-3}, [nicotinic acid] = $(3.5 – 42) \times10^{-5}$ mol dm^{-3},

$[H^+] = 1.0x10^{-1}$ mol dm^{-3}, I = 5.0×10^{-1} mol dm^{-3} (Na_2SO_4), T= 28.0 ± 1.0^0C and λ_{max} = 525nm.

for MnO_4^-: L-cysteic acid

$[MnO_4^-]= 1.50 x10^{-4}$ mol dm^{-3}, [L-cysteic acid] = $(7.5\text{-}90) \times 10^{-5}$ mol dm^{-3},

$[H^+] = 1.0x10^{-1}$ mol dm^{-3}, I = 5.0×10^{-1} mol dm^{-3} (Na_2SO_4),T= 27.0 ± 1.0^0C and λ_{max} = 525nm.

for MnO_4^-: L-aspartic acid

$[MnO_4^-]= 1.50 x10^{-4}$ mol dm^{-3}, [L-aspartic acid] = $(3.75– 60) \times 10^{-5}$ mol dm^{-3},

$[H^+] = 2.0x10^{-1}$ mol dm^{-3}, I = 1.0 mol dm^{-3} (Na_2SO_4), T= 29.0 ± 1.0^0C and λ_{max} = 525nm.

for MnO_4^-: L-tryptophan

$[MnO_4^-] = 2.0 \times 10^{-4}$ mol dm^{-3}, [L-tryptophan] = $(4.0– 48) \times 10^{-5}$ mol dm^{-3},

$[H^+] = 1.0 \times 10^{-1}$ mol dm^{-3}, I = 5.0. x 10^{-1}mol dm^{-3}(Na_2SO_4),T= 27.0± 1.0^0C and λ_{max} = 525nm.

The reactions were allowed to go to completion for all the systems. This was ascertained by taking the absorbances of the mixtures at intervals. The reactions were taken to be completed when the absorbance remained constant after repeated readings.

The absorbances of the solutions were measured at 525nm, the wavelength of maximum absorption of potassium permanganate, having certified that none of the reactants nor the products absorbed at this wavelength. The stoichiometries, indicated by the point of inflexion were evaluated from the plot of absorbance versus mole ratio of permanganate to respective reductant.

3.3 Kinetic measurements

The rates of the reactions were monitored on a Corning Colorimeter 253 model. The rate of reaction of each reductant (nicotinic acid, L-cysteic acid, L-aspartic acid and L-tryptophan) with permanganate was studied by monitoring decrease in absorbance of the permanganate at 525nm. All kinetic measurements were carried out under pseudo-first order conditions with respective reductant concentration at least 20-fold in excess over the permanganate ion concentration. The conditions under which orders of the reaction with respect to the reactants were determined are as follows:

for MnO_4^-: nicotinic acid

$[MnO_4^-] = 1.75 \times 10^{-4}$ mol dm^{-3}, [nicotinic acid] = (9.0-175) $\times 10^{-3}$ mol dm^{-3},

$[H^+] = 1.0 \times 10^{-1}$ mol dm^{-3}, I = 5.0 x 10^{-1} mol dm^{-3} (Na_2SO_4),T= 28 ± 1^0C and λ_{max} = 525nm.

for MnO_4^-: L-cysteic acid

$[MnO_4^-]$ = 1.50x10^{-4} mol dm^{-3}, [L-cysteic acid] = (4.50 – 95) x10^{-3} mol dm^{-3},

$[H^+]$ = 1.0x10^{-1} mol dm^{-3}, I = 5.0 x 10^{-1} mol dm^{-3} (Na_2SO_4),T= 27.0±1.0^{0}C and λ_{max} = 525nm.

for MnO_4^-: L-aspartic acid

$[MnO_4^-]$= 1.50x10^{-4} mol dm^{-3},[L-aspartic acid] = (7.50 – 75.0) x10^{-3} mol dm^{-3},

$[H^+]$ = 2.0 x 10^{-1} mol dm^{-3}, I = 1.0 mol dm^{-3} (Na_2SO_4),T= 29.0± 1.0^{0}C and λ_{max}= 525nm.

for MnO_4^-: L-tryptophan

$[MnO_4^-]$= 2.0x10^{-4} mol dm^{-3},[L-tryptophan] = (2.0 – 18.0) x 10^{-2} mol dm^{-3},

$[H^+]$ = 1.0x10^{-1} mol dm^{-3}, I = 5.0 x 10^{-1} mol dm^{-3} (Na_2SO_4),T= 28.0± 1.0^{0}C and λ_{max}= 525nm.

The effect of $[H^+]$ on the rate of the reactions was determined under the following conditions;

for MnO_4^-: nicotinic acid

$[MnO_4^-]$ = 1.75x10^{-4} mol dm^{-3},[nicotinic acid] = 8.40x10^{-2} mol dm^{-3},

$[H^+]$= (1.0 – 16.0) x10^{-2} mol dm^{-3}, I = 5.0x10^{-1} mol dm^{-3} (Na_2SO_4),T= 28.0± 1.0^{0}C and λ_{max}= 525nm.

for MnO_4^-: L-cysteic acid

$[MnO_4^-]$ = 1.50x10^{-4} mol dm^{-3}, [L-cysteic acid] = 8.25x10^{-2} mol dm^{-3},

$[H^+]$= (1.0 – 16.0)x10^{-2} mol dm^{-3}, I = 5.0x10^{-1} mol dm^{-3} (Na_2SO_4),T= 27.0± 1.0^{0}C and λ_{max}= 525nm.

for MnO_4^- : L-aspartic acid

$[MnO^-_4]$ = 1.50x10^{-4} mol dm^{-3}, [L-aspartic acid] = 7.50 x10^{-2} mol dm^{-3},

[H+] = (1.0 – 30)x10^{-2} mol dm^{-3}, I = 1.0 mol dm^{-3}(Na_2SO_4),T= 29.0±1.0^{0}C and λ_{max} = 525nm.

for MnO_4^-: L-tryptophan

[MnO_4^-] = 2.0x10^{-4} mol dm^{-3}, [L-trytophan] = 1.80x10^{-2} mol dm^{-3},

[H^+] = (1.0-15.0)x10^{-2} mol dm^{-3}, I = 5.0 x 10^{-1} mol dm^{-3}(Na_2SO_4),T= 28.0±1.0^{0}C and λ_{max} = 525nm.

The effects of ionic strength of reaction medium on the rate constant of the reactions were found by keeping the concentrations of the other reactants constant and varying the concentration of the inert electrolyte(Na_2SO_4) for all the systems studied. The ionic strength of the solutions were adjusted based on the relationship below:

$$I = \frac{1}{2} \sum c_i z_i^2 \qquad (3.1)$$

where Zi is the charge number of an ion (positive for cations and negative for anions).

C_i is the concentration of the ion in solution.

The conditions under which the effects of the ionic strength on the reaction rate were monitored are as follows:

for MnO^-_4: nicotinic acid

[MnO^-_4] = 1.75x10-^{4}mol dm^{-3}, [nicotinic acid] = 8.40x10^{-2} mol dm^{-3},

[H^+] =1.0x10^{-1} mol dm^{-3}, I = (4.0-12)x10^{-1} mol dm^{-3}, T= 28.0± 1.0^{0}C and λ_{max}= 525nm.

for MnO^-_4: L-cysteic acid

[MnO^-_4] = 1.50x$10^{—4}$ mol dm^{-3}, [L-cysteic. acid] = 8.25x10^{-2} mol dm^{-3},

[H^+]= 1.0x10^{-1} mol dm^{-3}, I = (4.0-10)x10^{-1} mol dm^{-3} (Na_2SO_4), T= 27.0±1.0^{0}C and λ_{max}= 525nm.

for MnO^-_4 :L-aspartic acid

$[MnO^-_4] = 1.50x10^{-4}$ mol dm^{-3},[L-aspartic acid] = $7.50x10^{-2}$ mol dm^{-3},

$[H^+]= 2.0x10^{-1}$ mol dm^{-3}, I = $(7.0\text{-}13.0)x10^{-1}$ mol dm^{-3} (Na_2SO_4),T= 29.0 ± 1.0^0C and λ_{max}= 525nm.

for Mno^-_4: L-tryptophan

[MnO-^{4}] = $2.0x10^{-4}$ mol dm^{-3}, [L-trptophan] = $1.80x10^{-2}$ mol dm^{-3},

$[H^+]= 1.0\ x10^{-1}$ mol dm^{-3}, I = $(4.0\text{-}10.0)x10^{-1}$ mol dm^{-3} (Na_2SO_4),

T= 28.0 ± 1.0^0C and λ_{max} = 525nm.

The effect of medium dielectric constant on the reaction rate was observed by carrying out the reaction in medium of varying dielectric constants. The medium dielectric constants were varied by combining water and acetone in different proportion and the dielectric constant of the solutions were calculated using equation below:

$$D = \frac{D_{water}\ xV_{water} + D_{Ace}x\ V_{Ace}}{V_{Total}} \quad (3.2)$$

where D = dielectric constants of the mixture, D_{water} = dielectric constants of water, D_{Ace} = dielectric constants of acetone,V_{water} = volume of water, V_{Ace} = volume of acetone, V_{Total} = the total volume.

3.4 Test for the presence of intermediate complex

Spectrophotometric investigation was carried out on all the systems studied in order to find out whether spectroscopically determinable intermediate complex was formed between permanganate and the respective reductants during the course of each reaction. The spectra of the reaction mixtures were taken over the 400-700nm range, 2 minutes after the

reactions were initiated. The formation of an intermediate complex is indicated by an increase in peak height or shift in λ_{max} of the permanganate.

3.5 Test for free radicals

$5cm^3$ of acrylamide was added to partially oxidized reaction mixture of each reductant and permanganate. This was followed by a large excess of methanol. The acrylamide was also added to a solution of each reductant and permanganate separately. This served as control, formation of gel indicate the presence of free radical.

CHAPTER FOUR

4.0 RESULTS

4.1 Stoichiometry

The results of the stoichiometry showed that one mole of permanganate ion is consumed by one mole of nicotinic acid and L-tryptophan, while two moles of permanganate ion are consumed by five moles of L-cysteic acid and L-aspartic acid respectively. The titration curves from which the stoichiometries were determined are presented in Figures (4.1- 4.4). On the basis of these results, the overall equations for these reactions can be represented by equations (4.1- 4.4)

$$NA + MnO_4^- + nH^+ \longrightarrow Mn^{2+} + \text{other products} \quad (4.1)$$

(where NA represents nicotinic acid):

$$2MnO_4^- + 5HR'H + 6H^+ \longrightarrow 2Mn^{2+} + 5R' + 8H_2O \quad (4.2)$$

(where HR'H represent L – cysteic acid):

$$2MnO_4^- + 5H_2P + 6H^+ \longrightarrow 2\,Mn^{2+} + 5P + 8H_2O \quad (4.3)$$

(where H_2P represent L – aspartic acid)

$$LP + MnO_4^- + nH^+ \longrightarrow Mn^{2+} + \text{other products} \quad (4.4)$$

(where LP represent L – tryptophan)

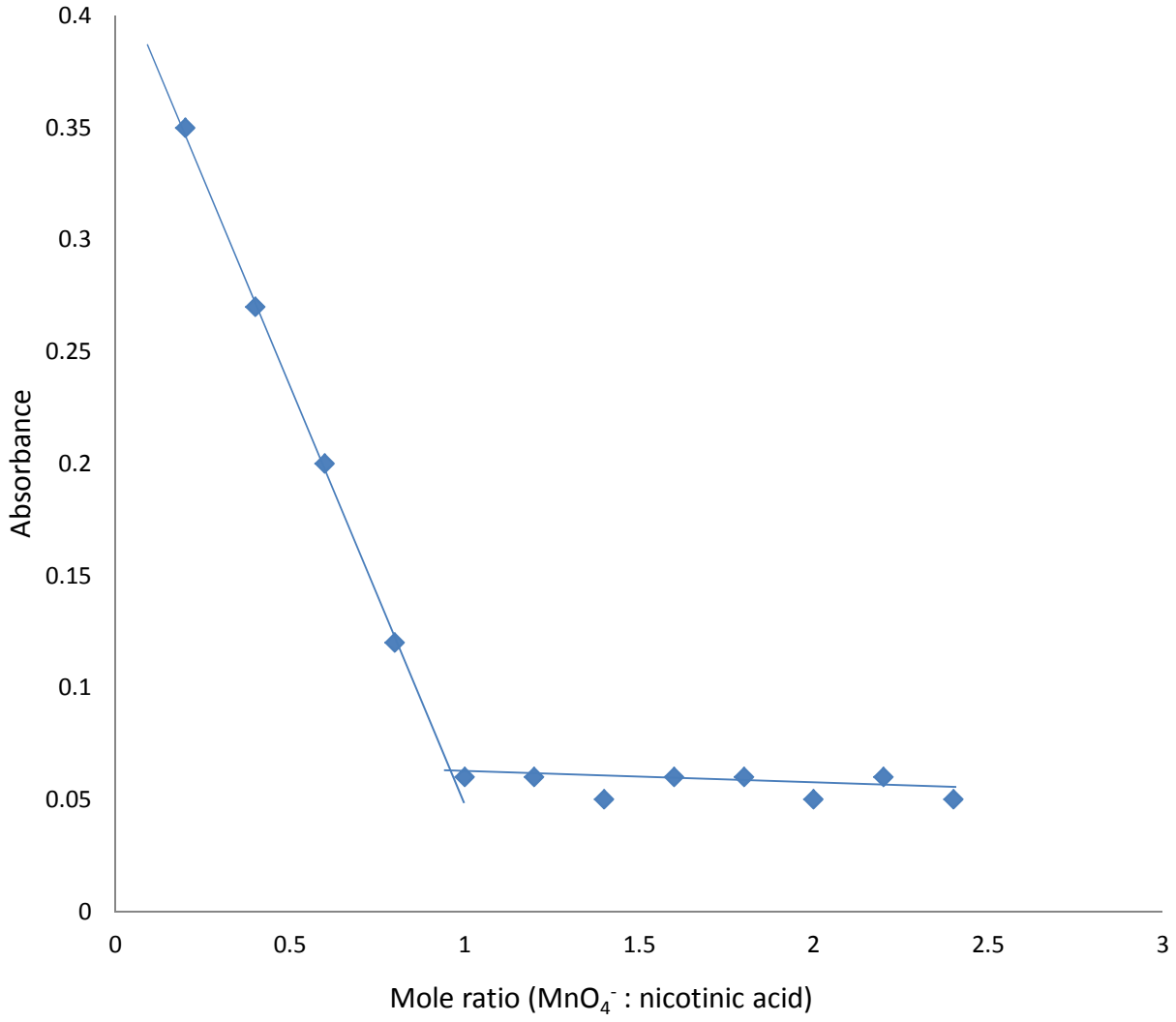


Figure 4.1: A plot of absorbance against mole ratio for the reaction between MnO_4^- and nicotinic acid

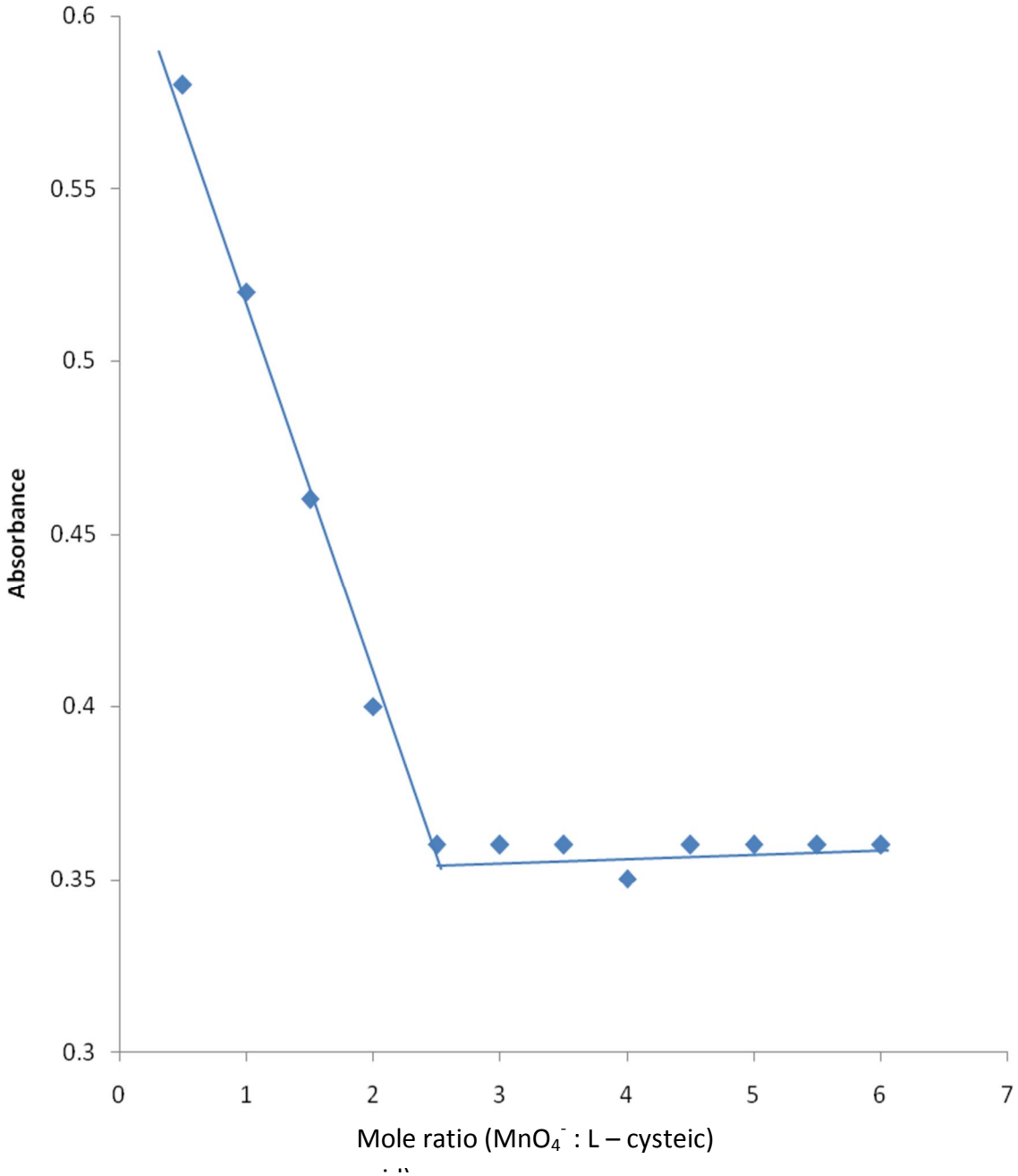


Figure 4.2: A Plot of absorbance against mole ratio for the reaction of MnO_4^- and L- cysteic acid

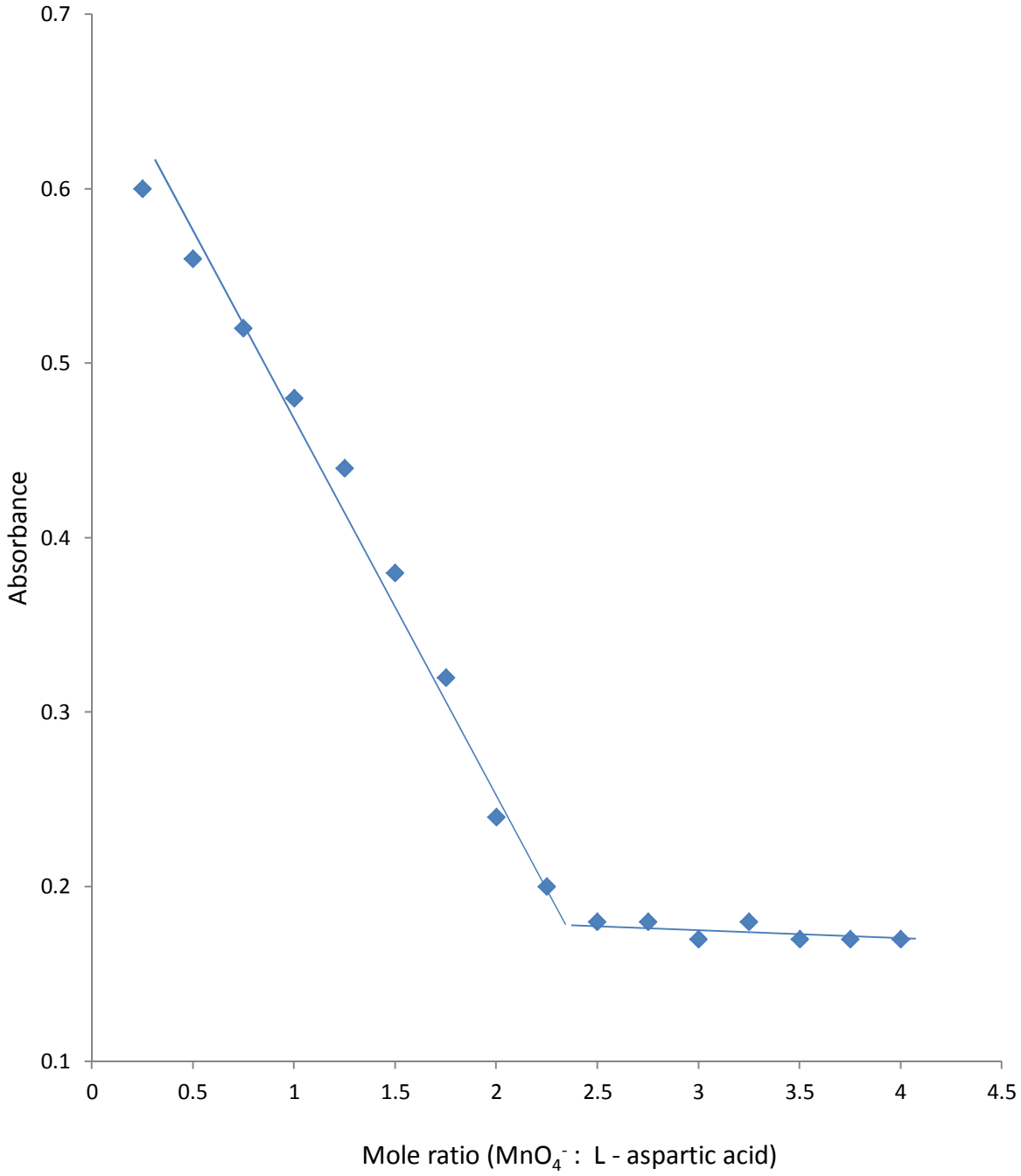


Figure 4.3: A plot of absorbance against mole ratio for the reaction of MnO_4^- and L- aspartic acid

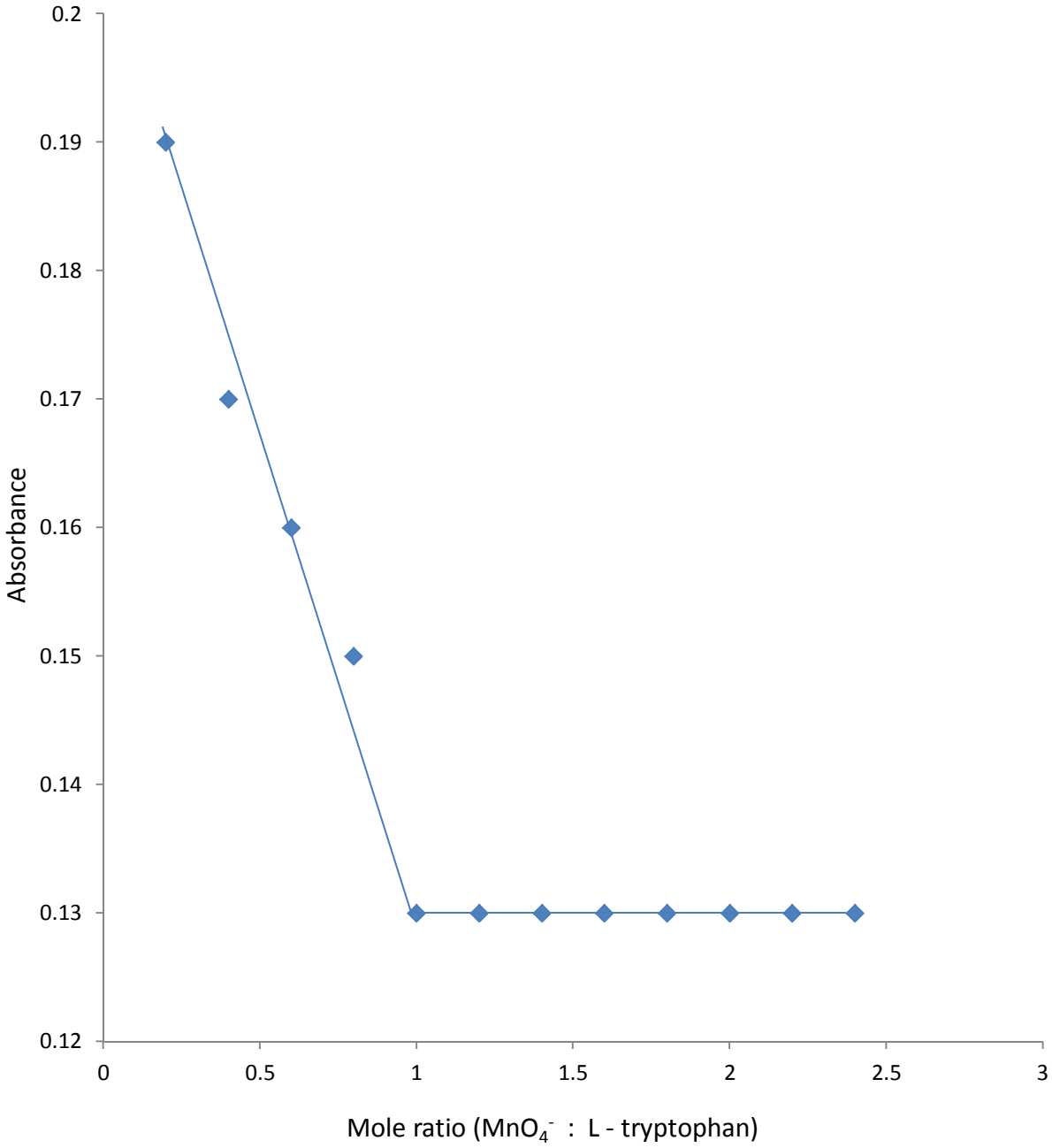


Figure 4.4: A plot of absorbance against mole ratio for the reaction of MnO_4^- and L-tryptophan

4.2 Determination of order with respect to reactants

The pseudo – first order plots of $\log(A_t-A_\infty)$ versus time for all the systems were linear to about more than 75% extent of reaction. This suggests a first order dependence of rate on $[MnO_4^-]$. The typical plots are shown in Figures (4.5- 4.8).The pseudo – first order rate constants, k_{obs} were determined at various initial concentration of each reductant and at constant $[MnO_4^-]$ and $[H^+]$.The order of the reaction for each of the system was obtained from the slope of the plots of $\log k_{obs}$ versus log[reductants] (Figures 4.9-4.12) and are reported in Tables(4.1−4.4). The slopes obtained were 0.96±0.3(MnO_4^-–nicotinic acid), 1.06±0.35(MnO_4^- –L-cysteic acid), 0.98±0.4(MnO_4^- −L-aspartic acid), 1.03±0.41(MnO_4^- −L-tryptophan).These observations showed that the order of the reaction with respect to all [reductants] is one. The reaction is second order overall, the second order rate constants were determined as k_{obs}/[reductants] and were found to be fairly constant (Tables 4.1 - 4.4). These reactions can be fitted into equations (4.5-4.8)

$$-\frac{d}{dt}[MnO_4^-] = k_2[MnO_4^-][\text{nicotinic acid}] \quad (4.5)$$

where $k_2 = (1.72 \pm 0.015)\times10^{-1}$ $dm^3mol^{-1}s^{-1}$, I = 0.5 mol dm^{-3}(Na_2SO_4), T = 28.0 ± 1.0°C and $[H^+]$ = 0.1 mol dm^{-3}.

$$-\frac{d}{dt}[MnO_4^-] = k_2[MnO_4^-][\text{L} - \text{cysteic acid}]$$

(4.6)

where $k_2 = (5.47 \pm 0.07)\times10^{-2}$ $dm^3mol^{-1}s^{-1}$, I = 0.5 mol dm^{-3}(Na_2SO_4), T = 27.0 ± 1.0°C and $[H^+]$ = 0.1 mol dm^{-3}.

$$-\frac{d}{dt}[MnO_4^-] = k_2[MnO_4^-][\text{L} - \text{aspartic acid}] \quad (4.7)$$

where $k_2 = (3.50 \pm 0.06)\times10^{-2}$ $dm^3mol^{-1}s^{-1}$, I = 1.0 mol dm^{-3}, (Na_2SO_4), T = 29.0 ± 1.0°C and $[H^+]$ = 0.2 mol dm^{-3}.

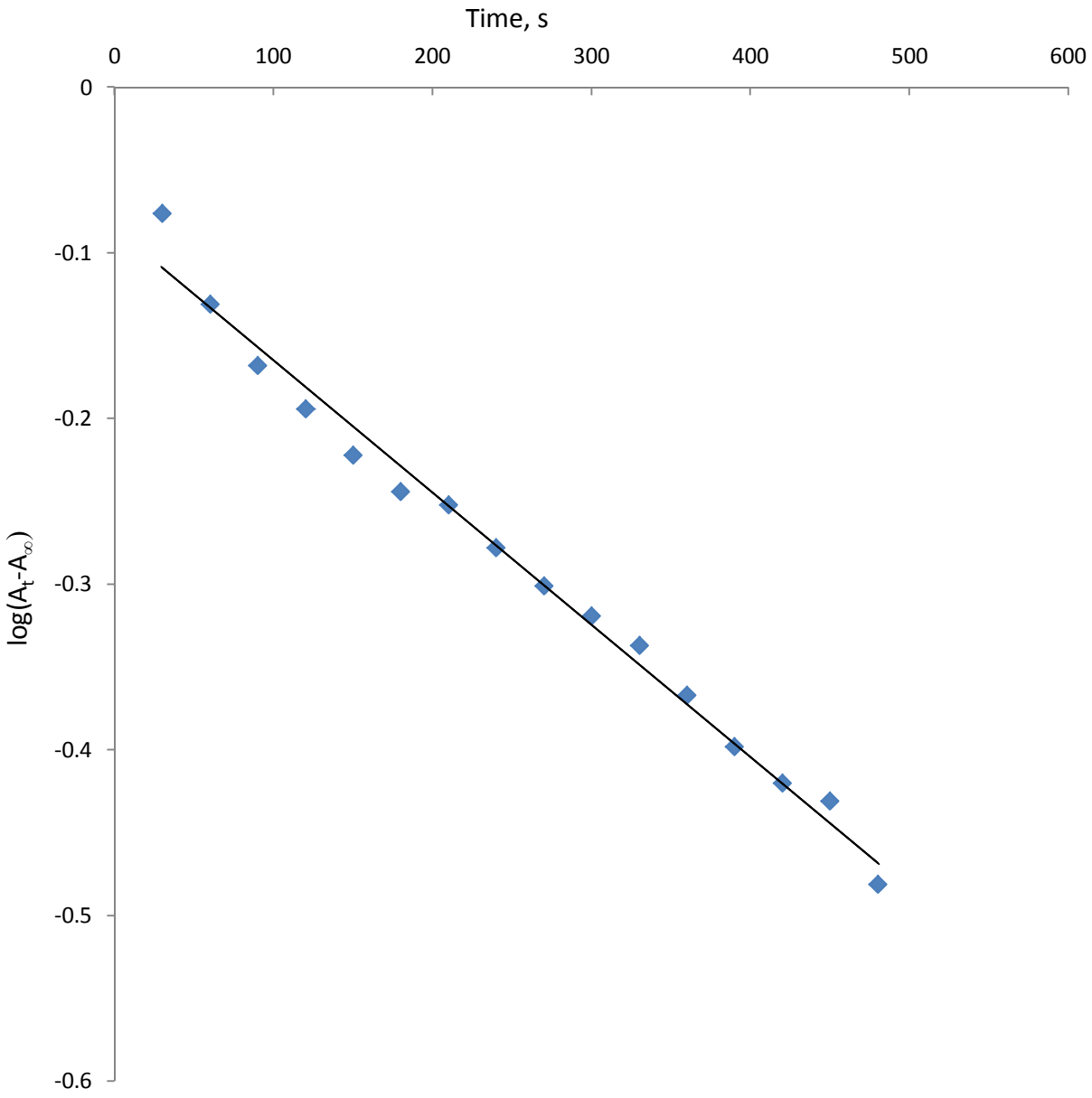


Figure 4.5: A typical pseudo-first order plot for the redox reaction of nicotinic acid and permanganate ion at $[MnO_4^-]$ =1.5x10^{-4}mol dm^{-3}, I = 0.5 mol dm^{-3}, $[H^+]$ = 0.1mol dm^{-3}, [nicotinic acid] = 8.4x10^{-2}mol dm^{-3}, λ_{max} = 525nm and T = 28.0±1.0^{o}C

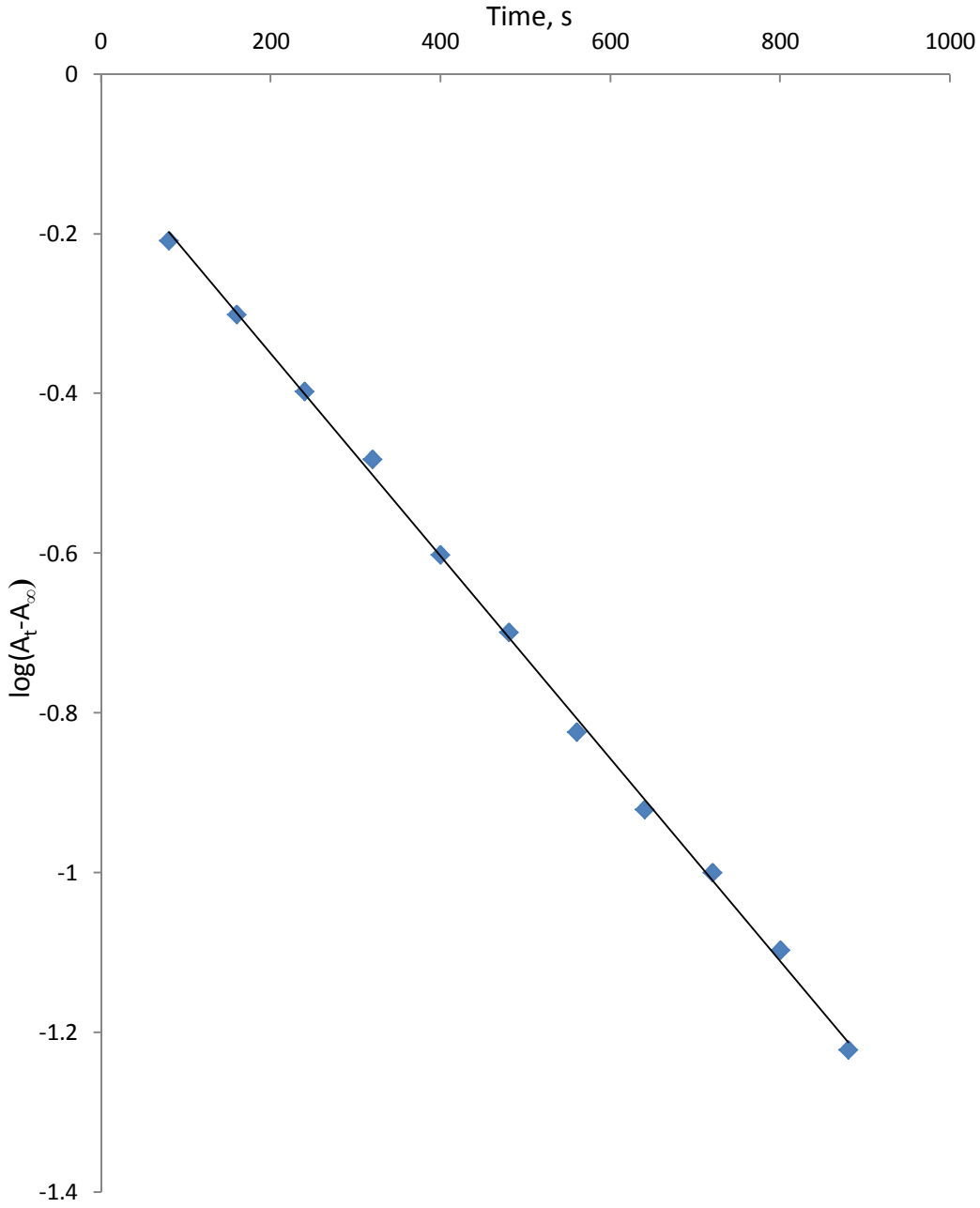


Figure 4.6: A typical pseudo-first order plot for the redox reaction of L – cysteic acid and permanganate ion at $[MnO_4^-] = 1.5x10^{-4}$mol dm^{-3}, I = 0.5 mol dm^{-3}, [L – cysteic acid]=$8.25x10^{-2}$mol dm^{-3}, $[H^+] = 0.1$mol dm^{-3}, λ_{max} = 525nm and T = 27.0±1.0^oC

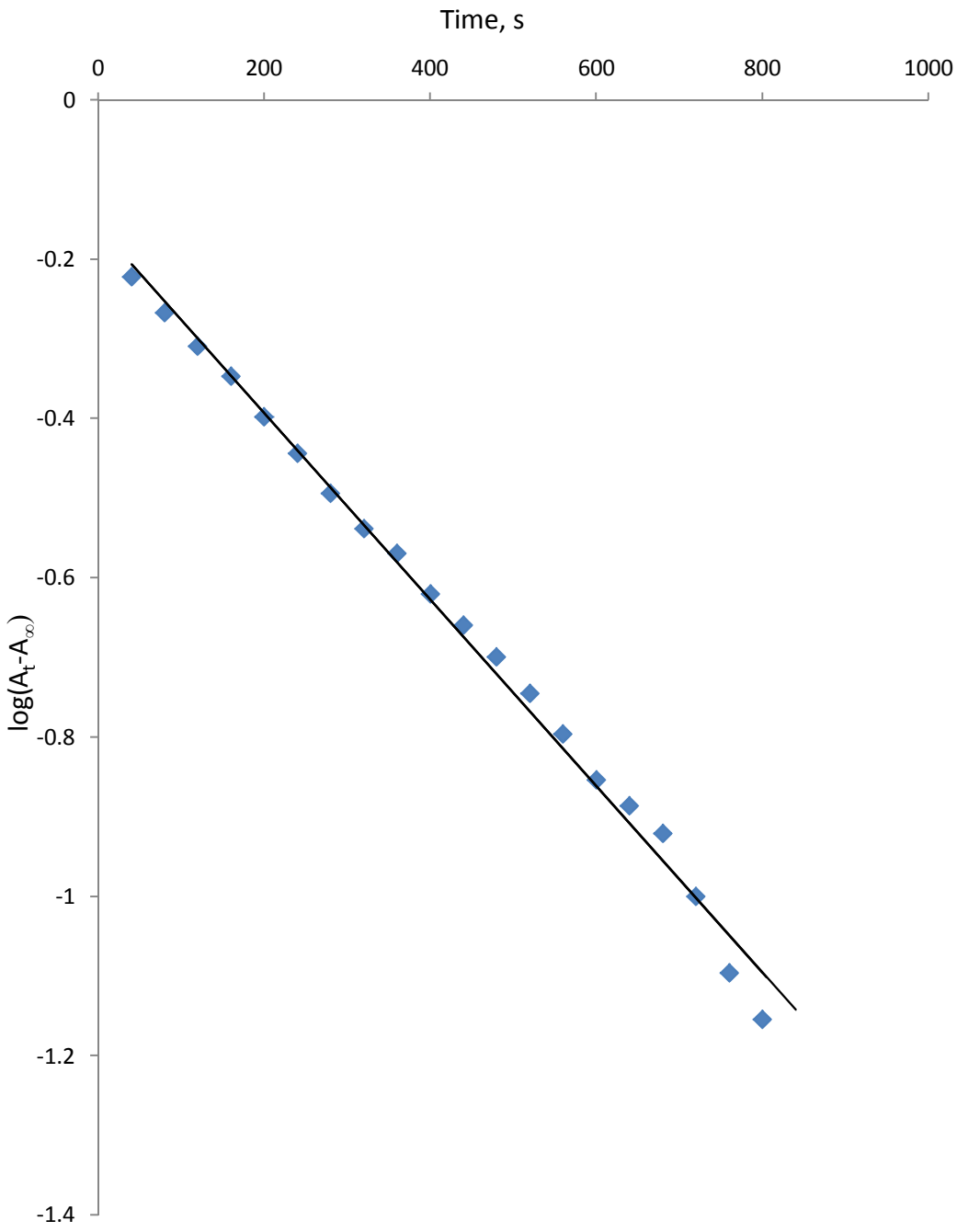


Figure 4.7: A typical pseudo-first order plot for the redox reaction of L – aspartic acid and permanganate ion at $[MnO_4^-] = 1.5x10^{-4}$mol dm^{-3}, I = 1.0 mol dm^{-3}, [L – aspartic acid]=$7.5x10^{-2}$mol dm^{-3}, $[H^+]$ = 0.2mol dm^{-3}, λ_{max} = 525nm and T = 29.0±1.0^{o}C

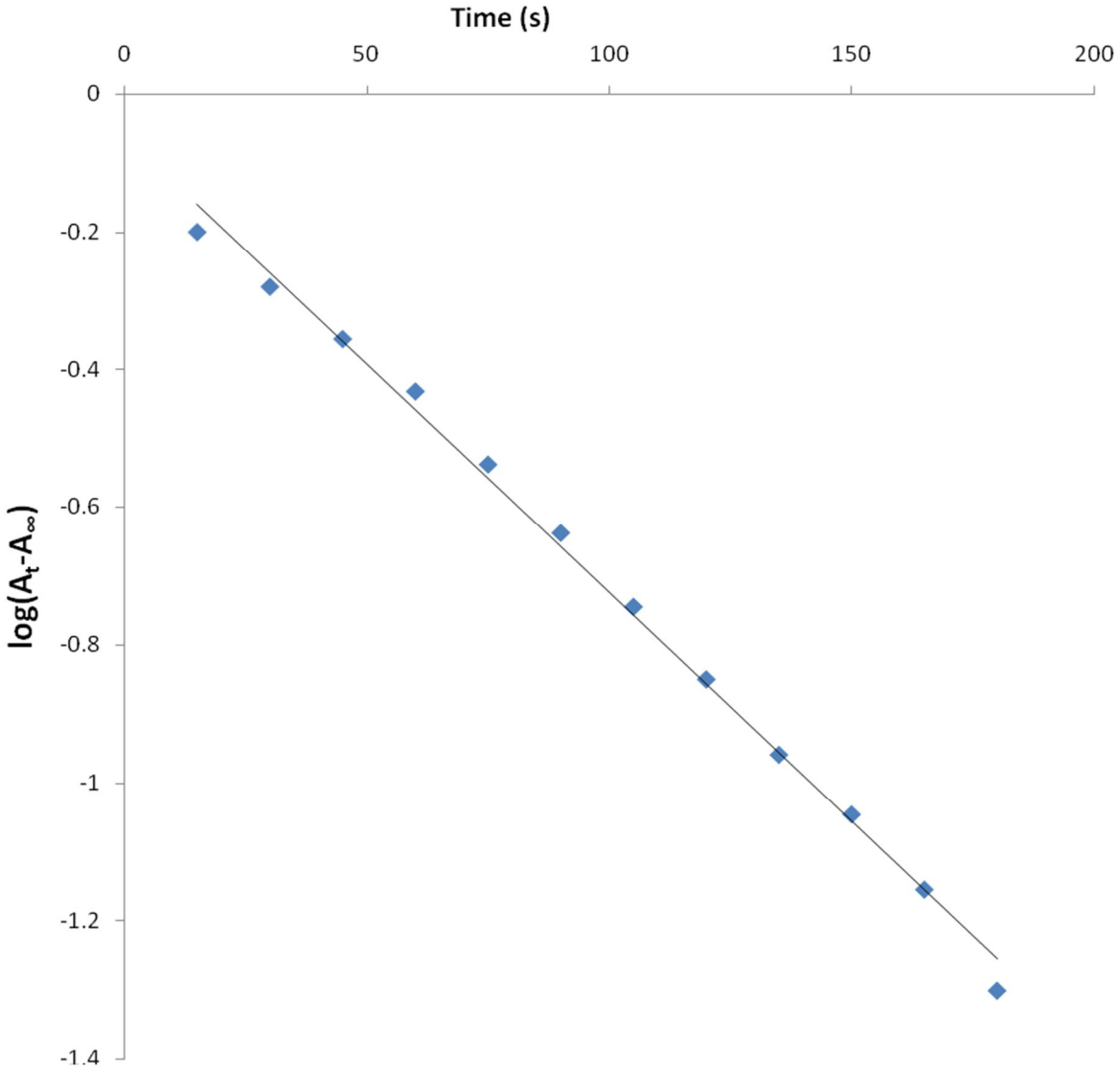


Figure 4.8: A typical pseudo- first order plot for the redox reaction of L – tryptophan and permanganate ion at $[MnO_4^-] = 2.0 \times 10^{-4}$mol dm^{-3}, [L –tryptophan]= 1.8×10^{-2} mol dm^{-3}, $[H^+]$= 0.1mol dm^{-3}, I= 0.5mol dm^{-3}, λ_{max}= 525nm and T= 28.0 ± 1.0^0C

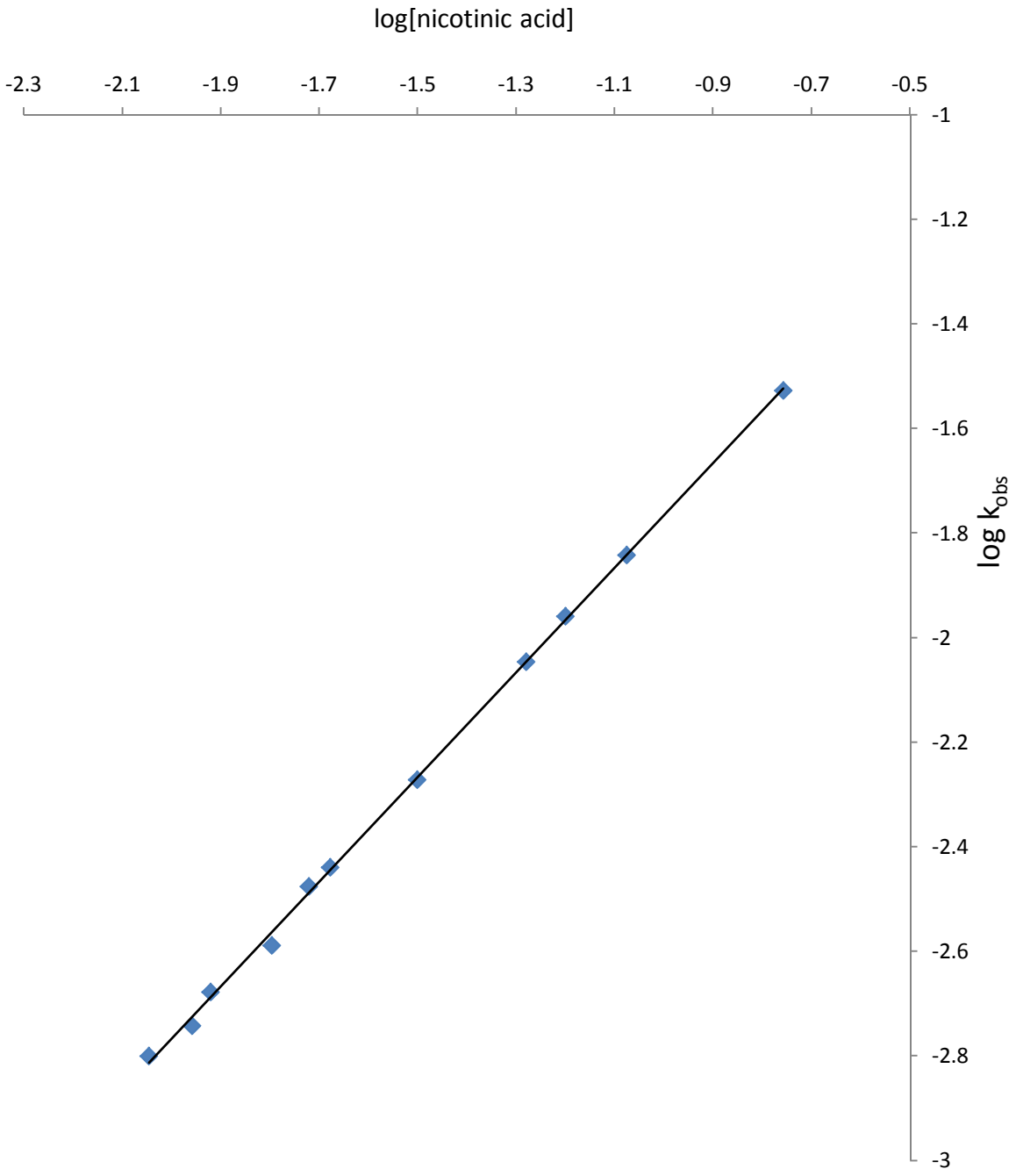


Figure 4.9 : Plot of $\log k_{obs}$ versus log[nicotinic acid] for the redox reaction of permanganate ion and nicotinic acid at $[MnO_4^-] = 1.50 \times 10^{-4}$ mol dm^{-3}, $[H^+] =$ 0.1mol dm^{-3}, I = 0.5 mol dm^{-3} , λ_{max} = 525nm and T = 28.0±1.0°C

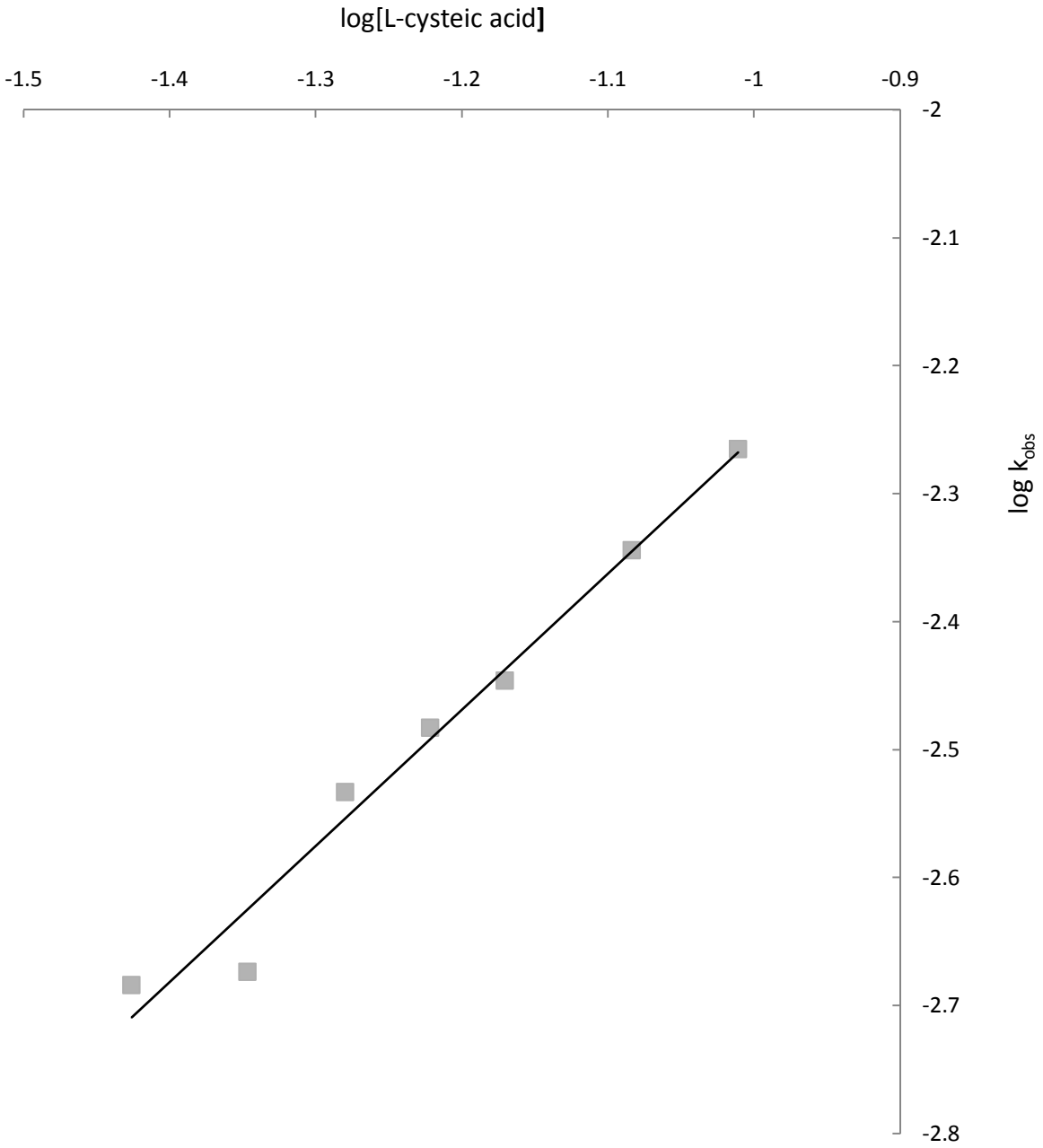


Figure 4.10: Plot of $\log k_{obs}$ versus log [L – cysteic acid] for the redox reaction of L – cysteic acid and permanganate ion at $[MnO_4^-] = 1.5x10^{-4}$mol dm^{-3}, $[H^+] = 0.1$mol dm^{-3}, I = 0.5 mol dm^{-3}, $\lambda_{max} = 525$nm and T = 27.0±1.0°C

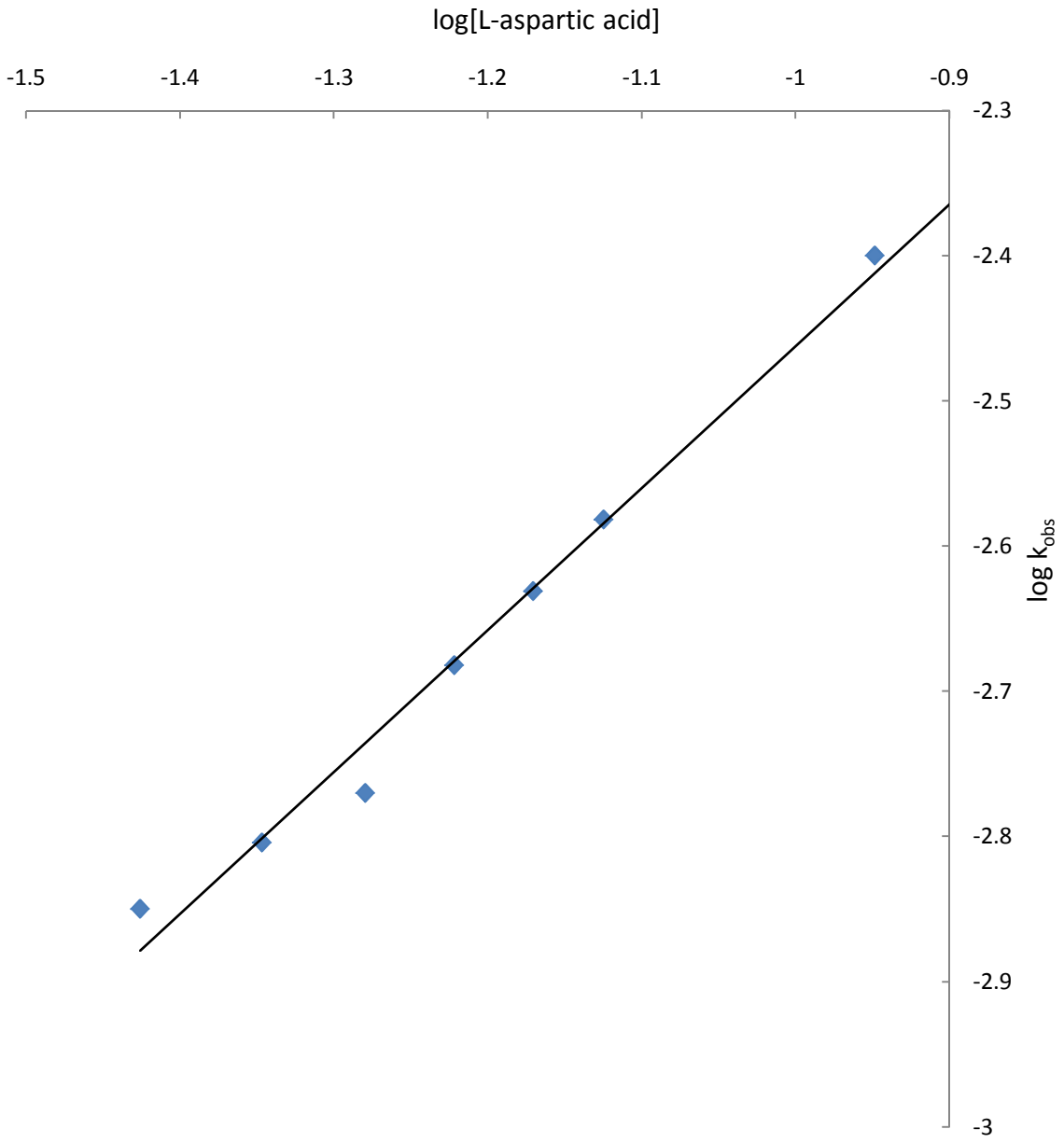


Figure 4.11: Plot of log k_{obs} versus log [L-aspartic acid] for the redox reaction of L – aspartic acid and permanganate ion at $[MnO_4^-] = 1.5x10^{-4}$mol dm^{-3}, $[H^+] = 2.0$ mol dm^{-3}, I = 1.0 mol dm^{-3}, λ_{max} = 525nm and T = 29.0±.01°C

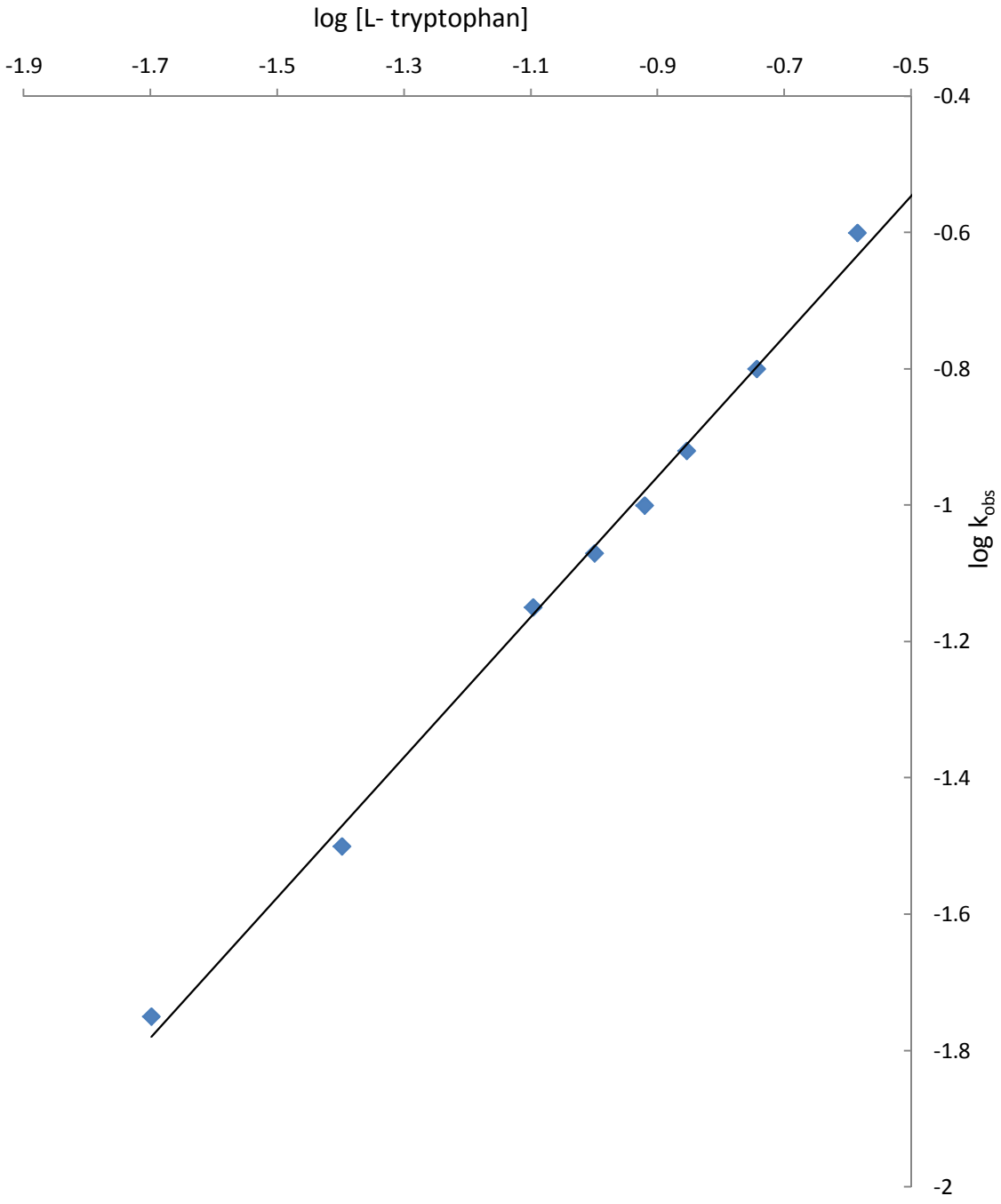


Figure 4.12: Plot of log k_{obs} versus log [L- tryptophan] for the redox reaction of L – tryptophan and permanganate ion at $[MnO_4^-]= 2.0 \times 10^{-4}$mol dm^{-3}, $[H^+]= 0.1$ mol dm^{-3}, I= 0.5mol dm^{-3}, λ_{max} = 525nm and T= 28.0$\pm$1.0^oC

Table 4.1: Pseudo-first order and second order rate constants for the reaction of MnO_4^- and nicotinic acid, $[MnO_4^-] = 1.75x10^{-4}moldm^{-3}$, $\lambda_{max} = 525nm$ and T = 28.0±1.0°C

10^2[nicotinic.acid], $moldm^{-3}$	$10[H^+]$, $mol\ dm^{-3}$	10[I], $moldm^{-3}$	10^3k_{obs}, s^{-1}	$10k_2$, $dm^3.mol^{-1}s^{-1}$
0.90	1.0	5.0	1.55	1.72
1.10	1.0	5.0	1.81	1.74
1.20	1.0	5.0	2.10	1.71
1.60	1.0	5.0	2.58	1.70
1.90	1.0	5.0	3.34	1.73
2.10	1.0	5.0	3.64	1.73
3.15	1.0	5.0	5.34	1.70
5.25	1.0	5.0	9.00	1.71
6.30	1.0	5.0	11.0	1.74
8.40	1.0	5.0	14.0	1.71
17.0	1.0	5.0	29.0	1.70
8.40	0.1	5.0	3.19	0.38
8.40	0.3	5.0	4.79	0.57
8.40	0.6	5.0	9.40	1.12
8.40	0.8	5.0	12.0	1.43
8.40	1.0	5.0	14.0	1.73
8.40	1.2	5.0	16.0	2.00
8.40	1.4	5.0	19.9	2.38
8.40	1.6	5.0	22.7	2.70
8.40	1.0	4.0	16.0	1.92
8.40	1.0	5.0	14.0	1.73
8.40	1.0	6.0	12.0	1.48
8.40	1.0	7.0	11.0	1.31
8.40	1.0	8.0	9.40	1.12
8.40	1.0	9.0	8.30	0.99
8.40	1.0	10.0	7.40	0.88
8.40	1.0	12.0	4.96	0.59

Table 4.2: Pseudo-first and second order rate constants for redox reaction of MnO_4^- and L – cysteic acid, $[MnO_4^-]=1.5 \times 10^{-4}$ mol dm^{-3}, λ_{max} = 525nm and T= 27.0±1.0^{0}C

10^2 [L – cysteic acid], mol dm^{-3}	10 [H^+], mol dm^{-3}	10[I], mol dm^{-3}	$10^3 k_{obs}$, s^{-1}	$10k_2$, dm^{3}mol^{-1}s^{-1}
0.45	1.0	5.0	0.25	5.50
0.75	1.0	5.0	0.42	5.53
2.25	1.0	5.0	1.24	5.45
3.75	1.0	5.0	2.07	5.52
4.50	1.0	5.0	2.12	5.47
5.25	1.0	5.0	2.90	5.58
6.00	1.0	5.0	3.29	5.48
6.75	1.0	5.0	3.57	5.30
8.25	1.0	5.0	4.53	5.50
9.75	1.0	5.0	5.40	5.57
8.25	0.1	5.0	0.45	0.55
8.25	0.4	5.0	1.31	2.19
8.25	0.6	5.0	2.97	3.60
8.25	0.8	5.0	3.62	4.39
8.25	1.0	5.0	4.51	5.47
8.25	1.2	5.0	5.63	6.82
8.25	1.4	5.0	6.11	7.40
8.25	1.6	5.0	7.24	8.78
8.25	1.0	4.0	4.79	5.80
8.25	1.0	5.0	4.54	5.51
8.25	1.0	6.0	4.13	5.00
8.25	1.0	7.0	3.86	4.68
8.25	1.0	8.0	3.51	4.25
8.25	1.0	9.0	3.15	3.82
8.25	1.0	10.0	2.77	3.36

Table 4.3: Pseudo-first and second order rate constants for redox reaction of MnO_4^- and L- aspartic acid, $[MnO_4^-] = 1.5\times10^{-4}$ mol dm^{-3}, λ_{max} = 525nm and T= 29.0 ± 1.0^0C

10^2[L- aspartic acid], mol dm^{-3}	**10 $[H^+]$, mol dm^{-3}**	**[I], mol dm^{-3}**	**10^3k_{obs}, s^{-1}**	**10^2 k_2, $dm^3mol^{-1}s^{-1}$**
0.75	2.0	1.0	0.26	3.48
2.25	2.0	1.0	0.85	3.40
3.75	2.0	1.0	1.38	3.66
4.50	2.0	1.0	1.57	3.49
5.25	2.0	1.0	1.67	3.32
6.0	2.0	1.0	2.08	3.46
6.75	2.0	1.0	2.34	3.47
7.50	2.0	1.0	2.62	3.49
11.25	2.0	1.0	3.97	3.53
7.50	0.50	1.0	0.31	0.42
7.50	1.00	1.0	0.70	0.91
7.50	1.50	1.0	1.53	2.04
7.50	2.0	1.0	2.63	3.51
7.50	2.50	1.0	4.09	5.45
7.50	2.70	1.0	4.53	6.04
7.50	3.00	1.0	6.00	8.10
7.50	2.0	0.7	1.98	2.64
7.50	2.0	0.8	2.10	2.80
7.50	2.0	0.9	2.54	3.38
7.50	2.0	1.0	2.65	3.53
7.50	2.0	1.1	2.86	3.81
7.50	2.0	1.2	3.01	4.02
7.50	2.0	1.3	3.38	4.51

Table 4.4: Pseudo-first and second order rate constants for redox reaction of MnO_4^- and L– tryptophan, $[MnO_4^-] = 2.0x10^{-4}$mol dm^{-3}, T=28.0 $\pm 1.0^0$C, and λ_{max} = 525nm

10^2[L - tryptophan], mol dm^{-3}	**10 $[H^+]$, mol dm^{-3}**	**10[I], mol dm^{-3}**	**$10^2 k_{obs}$, s^{-1}**	**10 k_2, $dm^3mol^{-1}s^{-1}$**
2.0	1.0	5.0	1.74	8.72
4.0	1.0	5.0	3.43	8.57
8.0	1.0	5.0	7.09	8.86
10.0	1.0	5.0	8.61	8.61
12.0	1.0	5.0	10.26	8.55
14.0	1.0	5.0	12.4	8.86
18.0	1.0	5.0	16.0	8.88
26.0	1.0	5.0	23.19	8.92
18.0	0.1	5.0	3.69	2.05
18.0	0.3	5.0	6.50	3.61
18.0	0.5	5.0	9.27	5.15
18.0	0.8	5.0	18.75	7.64
18.0	1.0	5.0	16.02	8.90
18.0	1.2	5.0	18.65	10.6
18.0	1.5	5.0	21.83	12.1
18.0	1.0	4.0	17.30	9.63
18.0	1.0	5.0	16.04	8.92
18.0	1.0	6.0	14.40	8.03
18.0	1.0	7.0	14.06	7.84
18.0	1.0	8.0	13.45	7.47
18.0	1.0	9.0	12.71	7.09
18.0	1.0	10.0	11.16	6.02

$$-\frac{d}{dt}[MnO_4^-] = k_2[MnO_4^-][L-tryptophan] \quad (4.8)$$

where $k_2 = (8.75 \pm 0.014)x10^{-1}$ $dm^3mol^{-1}s^{-1}$, I = 1.0 mol dm^{-3}(Na_2SO_4), T = 28.0 ± 1.0°C and $[H^+] = 0.1$ mol dm^{-3}.

4.3 Effect of hydrogen ion concentration on the rate of the reactions

For all the systems, the rate constants were found to be dependent on the hydrogen ion concentration in the range investigated (Tables 4.1- 4.4). Least square plots of $logk_{obs}$ versus log $[H^+]$ gave straight lines with slopes 0.74±0.28, 1.02±0.4, 1.70±0.2 and 0.7±0.3 for MnO_4^- −nicotinic acid, MnO_4^- −L-cysteic acid, MnO_4^- −L-aspartic acid and MnO_4^- − L-tryptophan systems respectively (Figures 4.13- 4.16).

Also when k_2 were plotted against $[H^+]$ for all the systems (Figures 4.17- 4.20), linear plots were obtained, for MnO_4^- -nicotinic acid, MnO_4^- -L-aspartic and MnO_4^- − L-tryptophan systems intercepts occurred, while in MnO_4^- -L-cysteic acid a straight line graph that passed through the origin was obtained.

The acid dependent rate constant can be represented by equation(4.9) for MnO_4^- −nicotinic acid and MnO_4^- − L-tryptophan reactions and equation(4.10) for MnO_4^- − L-aspartic whereas equation(4.11) is for MnO_4^- -L−cysteic acid reaction.

$$k_2 = a + b[H^+] \quad (4.9)$$

$$k_2 = a + b[H^+]^2 \quad (4.10)$$

$$k_2 = c[H^+] \quad (4.11)$$

where 'a' represents the intercept and 'b' and 'c' represent the slopes of the plots of $k_2$against $[H^+]$. The overall rate equations for the various systems are represented in equations (4.12-4.15)

$$-\frac{d}{dt}[MnO_4^-] = (a + b[H^+])[MnO_4^-][\text{nicotinic acid}] \quad (4.12)$$

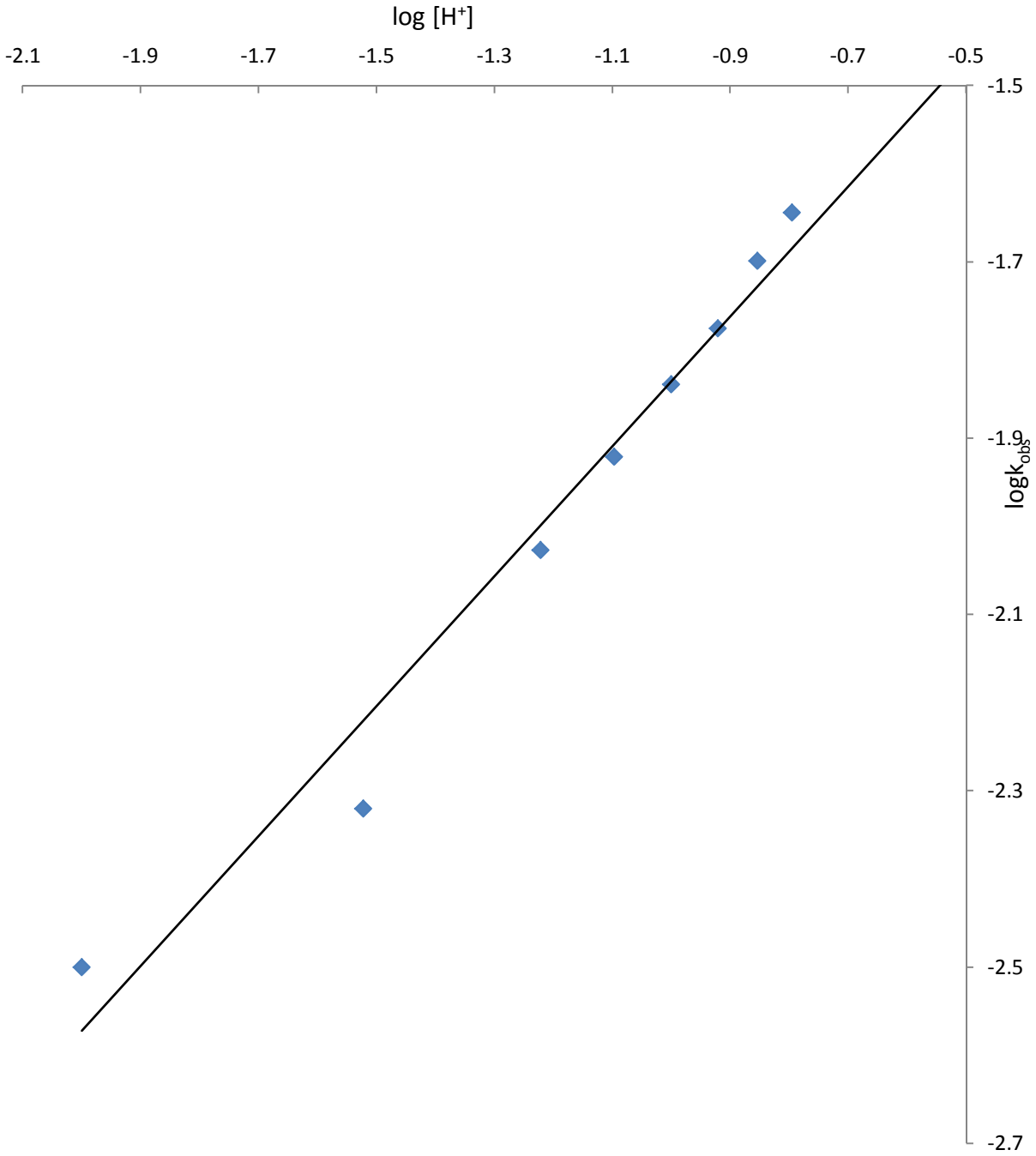


Figure 4.13: Plot of $logk_{obs}$ versus log $[H^+]$ for the redox reaction of nicotinic acid and permanganate ion at $[MnO_4^-]$= 1.5 x10^{-4}mol dm^{-3}, [nicotinic acid]= 8.4x10^{-2} mol dm^{-3}, I = 0.5mol dm^{-3}, λ_{max}= 525nm and T= 28.0$\pm$1.0^{0}C

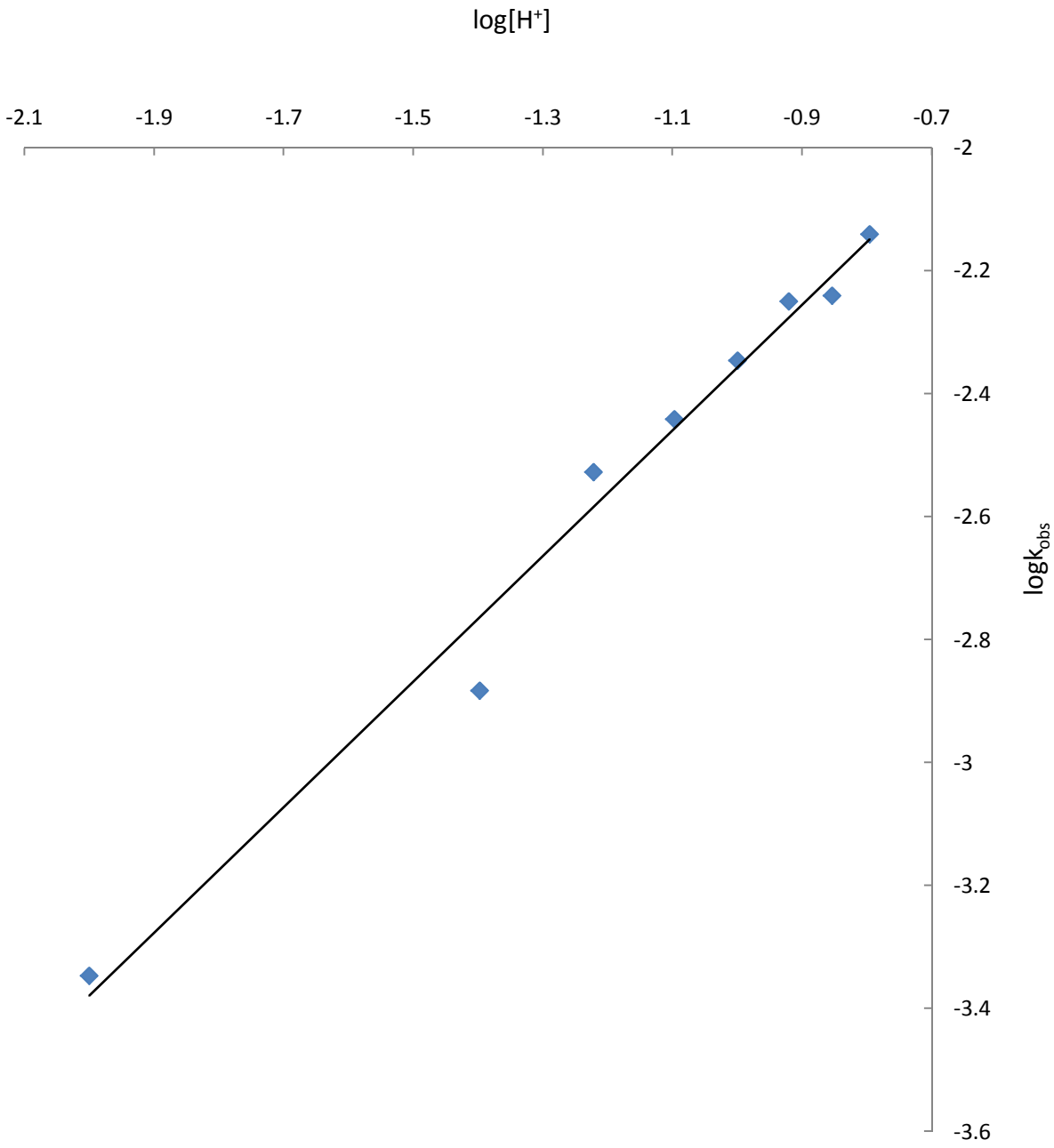


Figure 4.14: Plot of $logk_{obs}$ versus log $[H^+]$ for the redox reaction of L – cysteic acid and permanganate ion at $[MnO_4^-] = 1.5 \times 10^{-4}$mol dm^{-3}, [L – cysteic acid] = 8.25×10^{-2} mol dm^{-3}, $[H^+] = 0.1$mol dm^{-3}, I= 0.5mol dm^{-3}, $\lambda_{max} = 525$nm and $T = 27.0 \pm 1.0^0$C

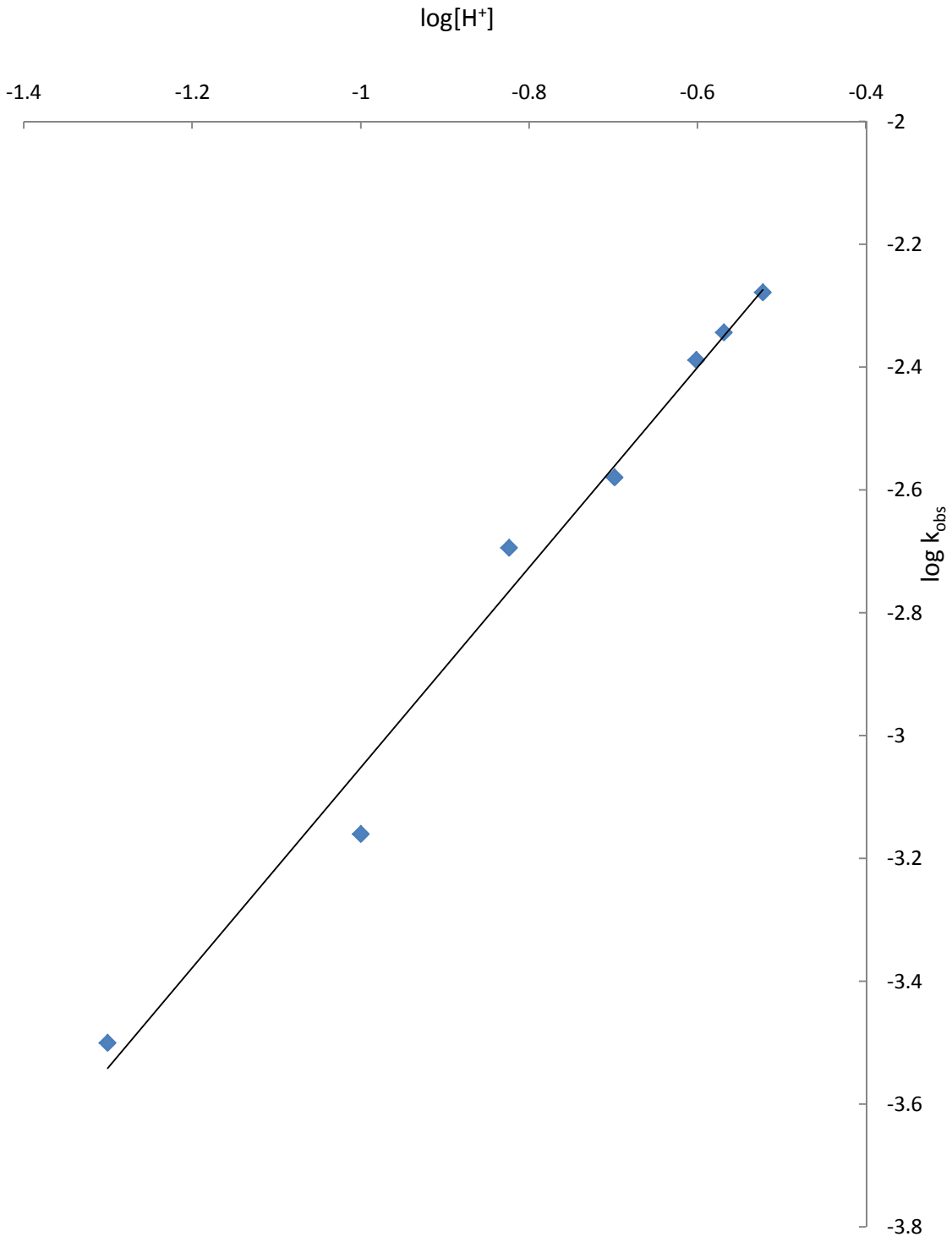


Figure 4.15: Plot of $\log k_{obs}$ versus log $[H^+]$ for the redox reaction of L – aspartic acid and permanganate ion at $[MnO_4^-] = 1.5 \times 10^{-4}$ mol dm^{-3}, [L-aspartic acid] = 7.5×10^{-2} mol dm^{-3}, $[H^+] = 0.2$ mol dm^{-3}, I = 1.0 mol dm^{-3}, λ_{max}= 525nm and T = 29.0$\pm$1.0^{0}C

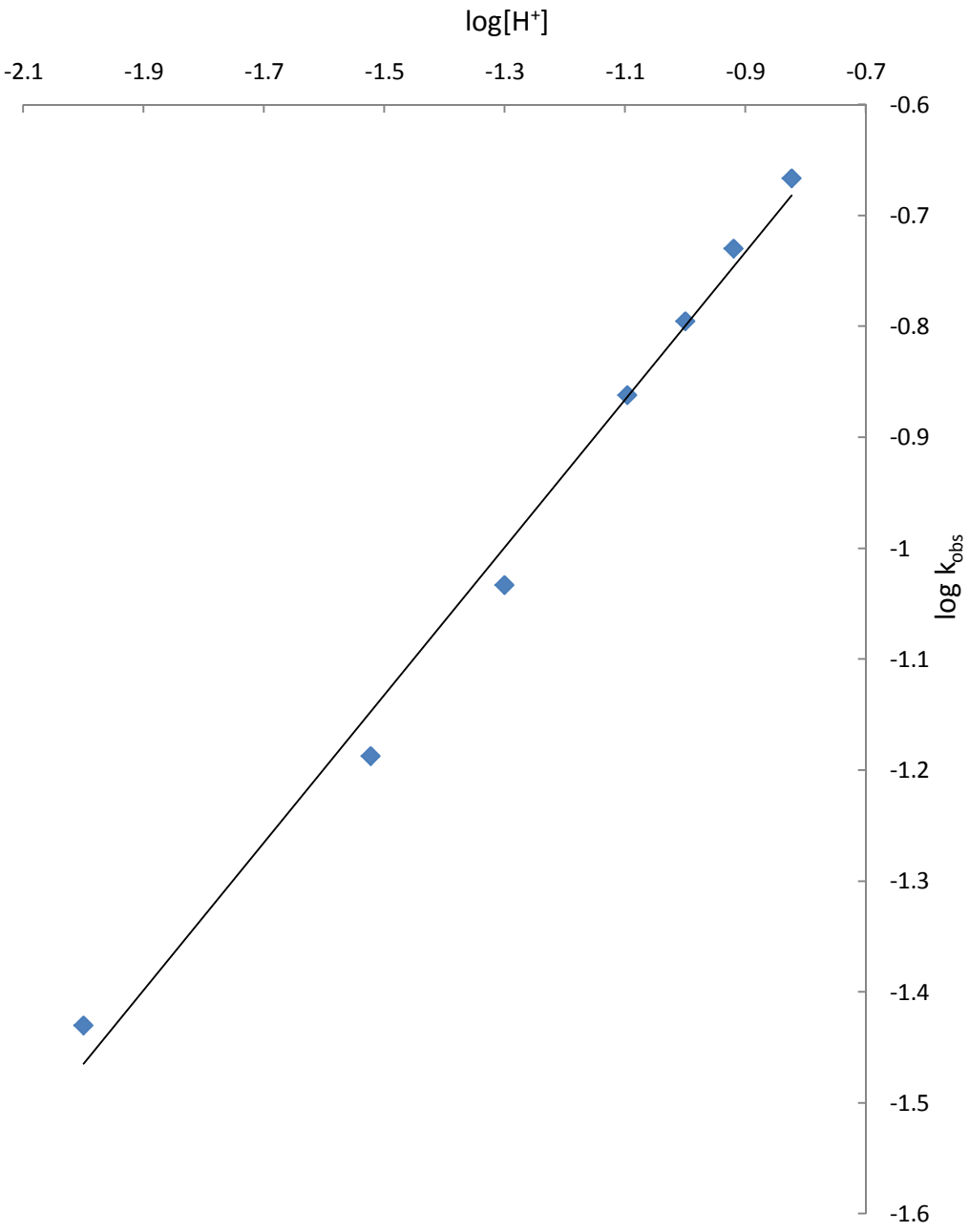


Figure 4.16: Plot of $\log k_{obs}$ versus $\log [H^+]$ for the redox reaction of L – tryptophan and permanganate ion at $[MnO_4^-] = 2.0 \times 10^{-4}$ mol dm^{-3}, [L- tryptophan] = 1.8×10^{-2} mol dm^{-3}, I = 0.5 mol dm^{-3}, $[H^+] = 0.1$ mol dm^{-3}, λ_{max}= 525nm and T = 28.0$\pm$ 1.0^{0}C

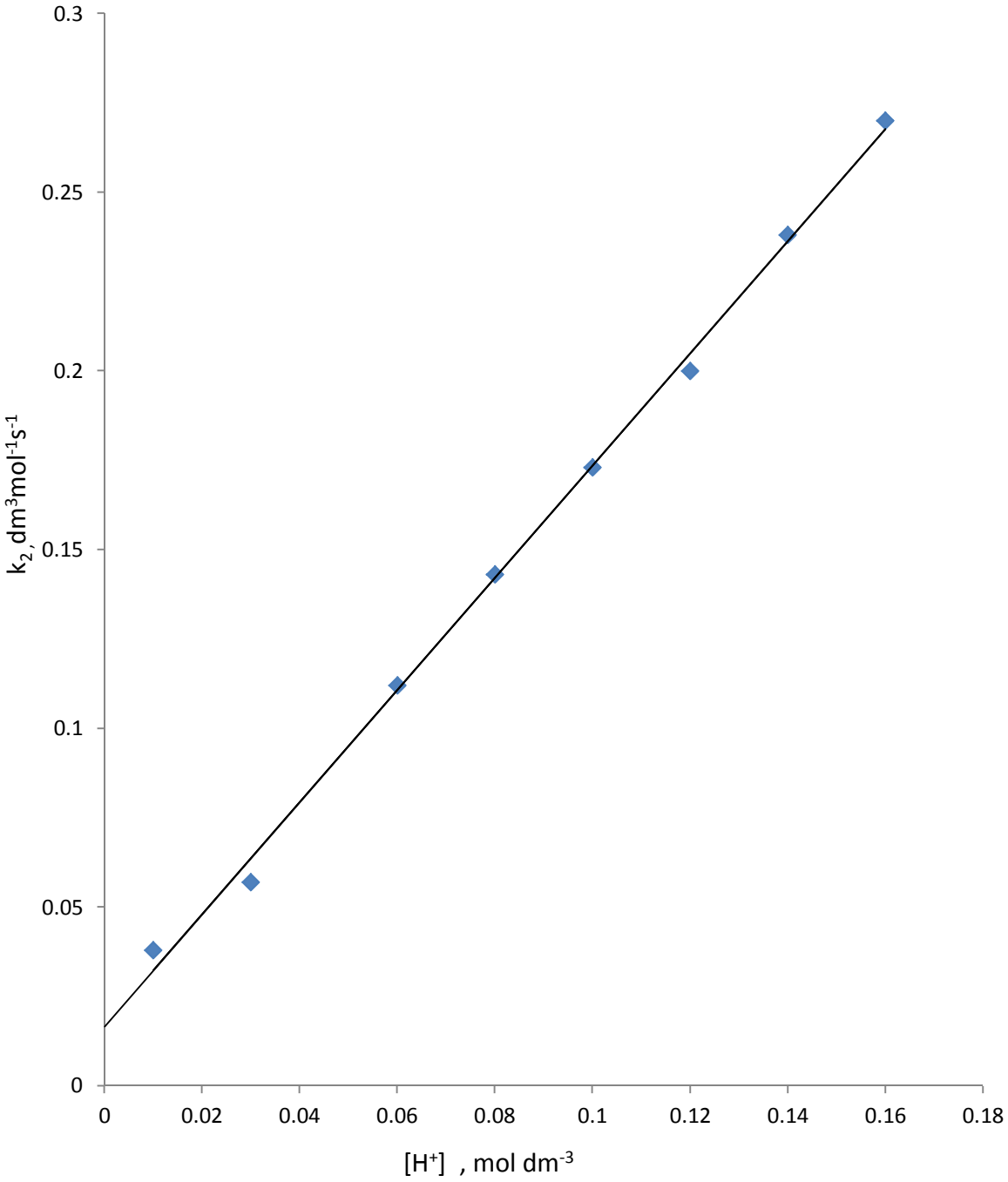


Figure 4.17: Plot of k_2 versus $[H^+]$ for the redox reaction of nicotinic acid and permanganate ion at $[MnO_4^-]$ = 1.5 x10^{-4}mol dm^{-3}, [nicotinic acid] =8.4x10^{-2} mol dm^{-3}, I= 0.5mol dm^{-3} λ_{max}= 525nm and T= 28.0$\pm$1.0^{0}C

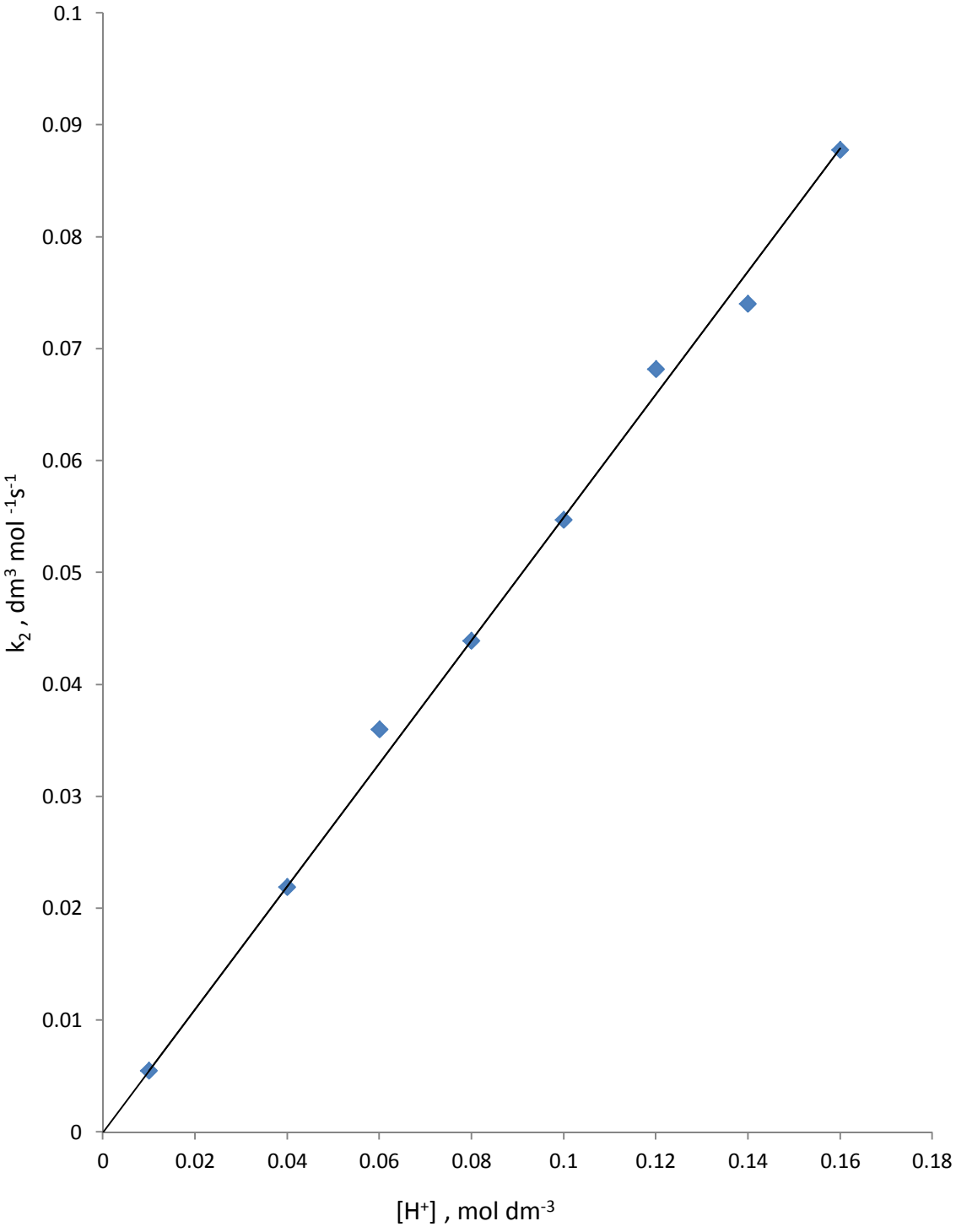


Figure 4.18: Plot of k_2 versus $[H^+]$ for the redox reaction of L– cysteic acid and permanganate ion at [L - cysteic acid] = 8.25×10^{-2} mol dm^{-3}, $[MnO_4^-]$ = 1.5×10^{-4}mol dm^{-3}, I = 0.5mol dm^{-3}, λ_{max} = 525nm and T = 27.0 ± 1.0^0C

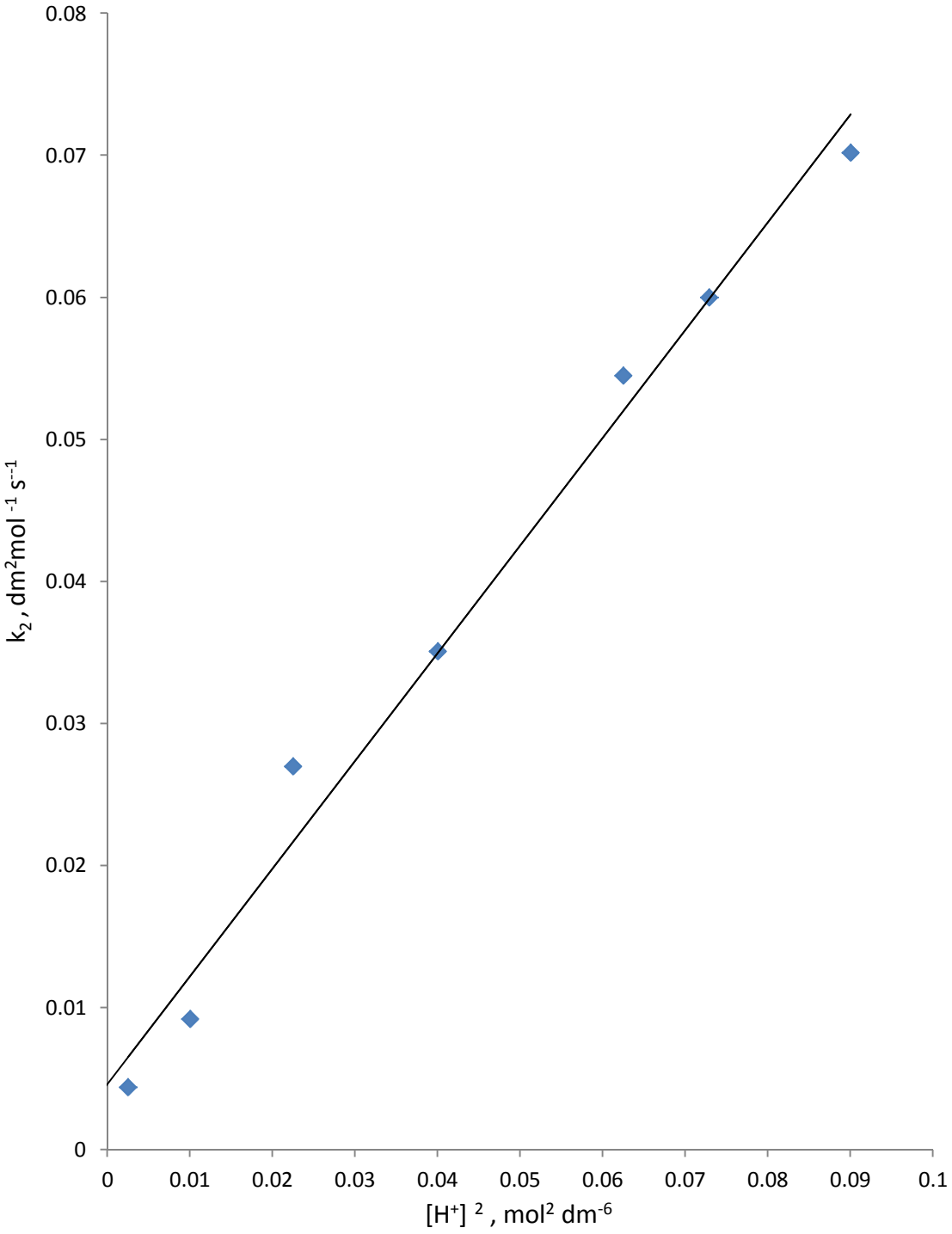


Figure 4.19: Plot of log k_2 versus $[H^+]$ for the redox reaction of L – aspartic acid and permanganate ion at $[MnO_4^-]$ = 1.5 x10^{-4} mol dm^{-3}, [L-aspartic acid] = 7.5x10^{-2} mol dm^{-3}, I = 1.0 mol dm^{-3}, λ_{max} = 525nm and T = 29.0$\pm$1.0^oC

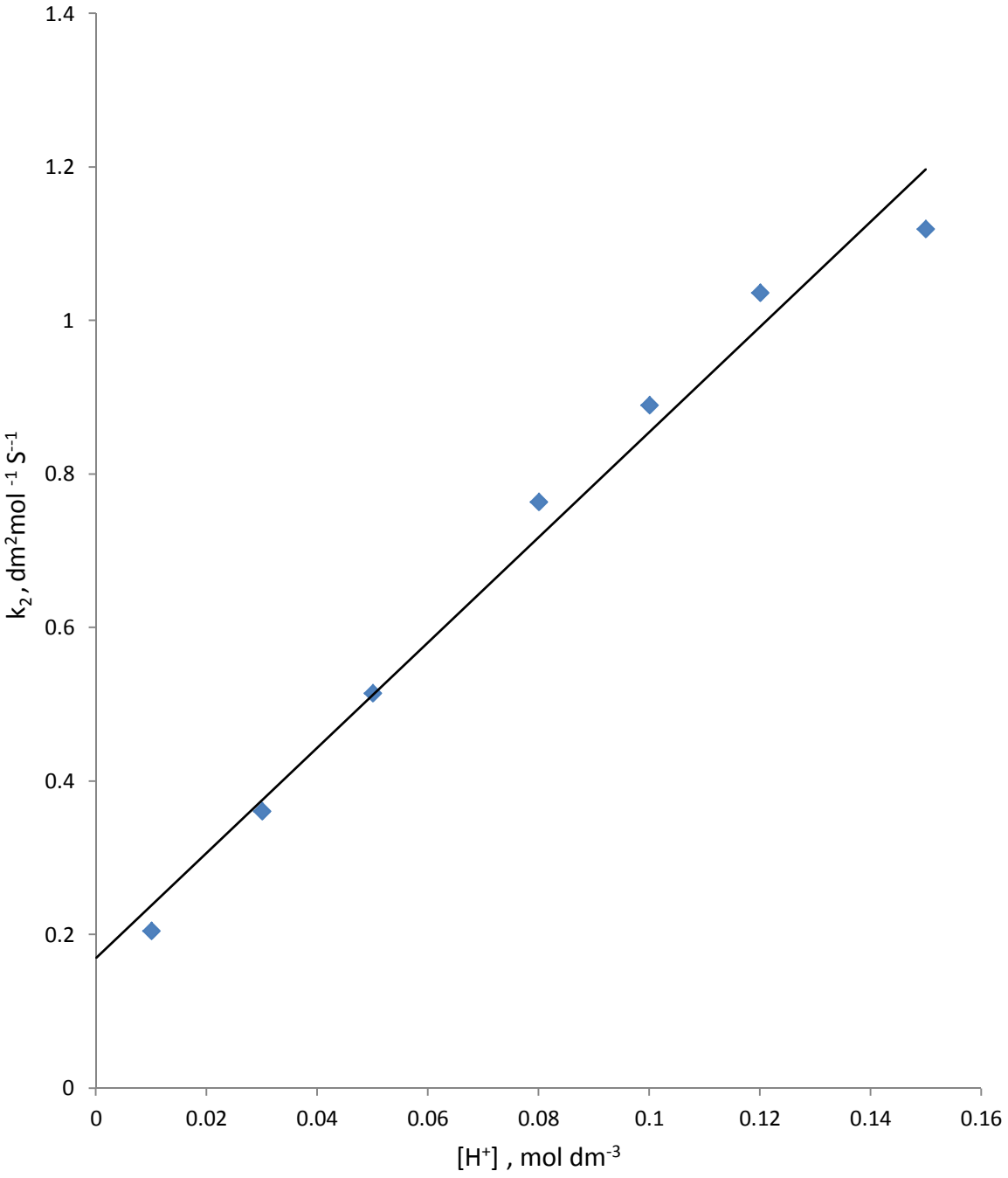


Figure 4.20: Plot of k_2 versus $[H^+]$ for the redox reaction of L– tryptophan and permanganate ion at $[MnO_4^-] = 2.0 \times 10^{-4}$ mol dm^{-3}, [L- tryptophan] = 1.8×10^{-2} mol dm^{-3}, I = 0.5 mol dm^{-3}, λ_{max}= 525nm and T = 28.0$\pm$ 1.0^{0}C

where a = $1.6\times10^{-2}dm^3mol^{-1}s^{-1}$ and b = $1.57dm^6mol^{-2}s^{-1}$ at 28.0±1.0°C.

$$-\frac{d}{dt}[MnO_4^-] = c[H^+][MnO_4^-][L-\text{cysteic acid}] \quad (4.13)$$

where c = $5.4\times10^{-1}dm^6mol^{-2}s^{-1}$ at 27.0±1.0°C.

$$-\frac{d}{dt}[MnO_4^-] = (a + b[H^+]^2)[MnO_4^-][L-\text{aspartic acid}] \quad (4.14)$$

where a = 4.0×10^{-3} $dm^{-3}mol^{-1}s^{-1}$ and b = $7.58\times10^{-1}dm^6mol^{-2}s^{-1}$at 29.0±1.0°C.

$$-\frac{d}{dt}[MnO_4^-] = (a + b[H^+])[MnO_4^-][L-\text{tryptophan}] \quad (4.15)$$

where a = 1.7×10^{-1} $dm^{-3}mol^{-1}s^{-1}$ and b = $6.85dm^6mol^{-2}s^{-1}$ at 28.0±1.0°C.

4.4 The effect of ionic strength

The effect of changing ionic strength on the rate of the reaction was investigated for all the systems studied using Na_2SO_4 with concentrations of other reactants kept constant. The rate constants were found to decrease with increased in ionic strength for MnO_4^- −nicotinic acid, MnO_4^- −L-cysteic acid, and MnO_4^- −L-tryptophan systems, but the rate constant increases as ionic strength increased for MnO_4^- −L-aspartic acid system (Tables 4.1-4.4). The plots of $\log k_2$ versus $I^{1/2}$ were linear for all the systems (Figures 4.21-4.24).The values of the slopes and correlation coefficients for all the systems were found to be -1.07±0.4 and R=0.973, -0.60±0.29 and R= 0.994, +0.76±0.34 and R= 0.980, -0.42±0.22 and R= 0.990, for MnO_4^- − nicotinic acid, MnO_4^- −L-cysteic acid, MnO_4^- −L-aspartic acid and MnO_4^- − L-tryptophan systems respectively.

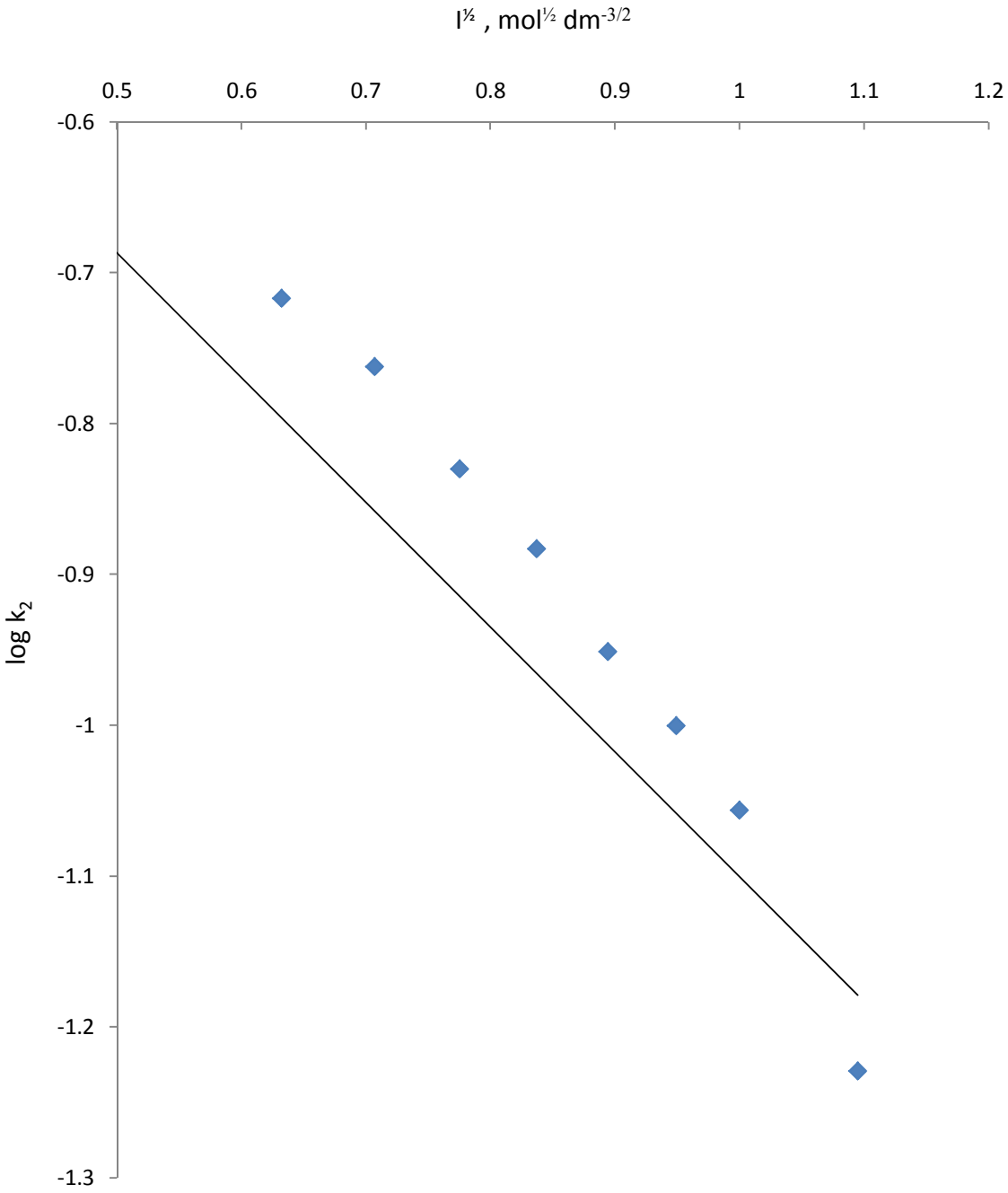


Figure 4.21: Plot of $\log k_2$ versus $I^{1/2}$ for the redox reaction of nicotinic acid and permanganate ionat $[MnO_4^-] = 1.5 \times 10^{-4}$ mol dm^{-3}, [nicotinic acid] = 8.40×10^{-2} mol dm^{-3}, $[H^+] = 0.1$ mol dm^{-3}, λ_{max}= 525nm and T = 28.0$\pm$1.0^{0}C

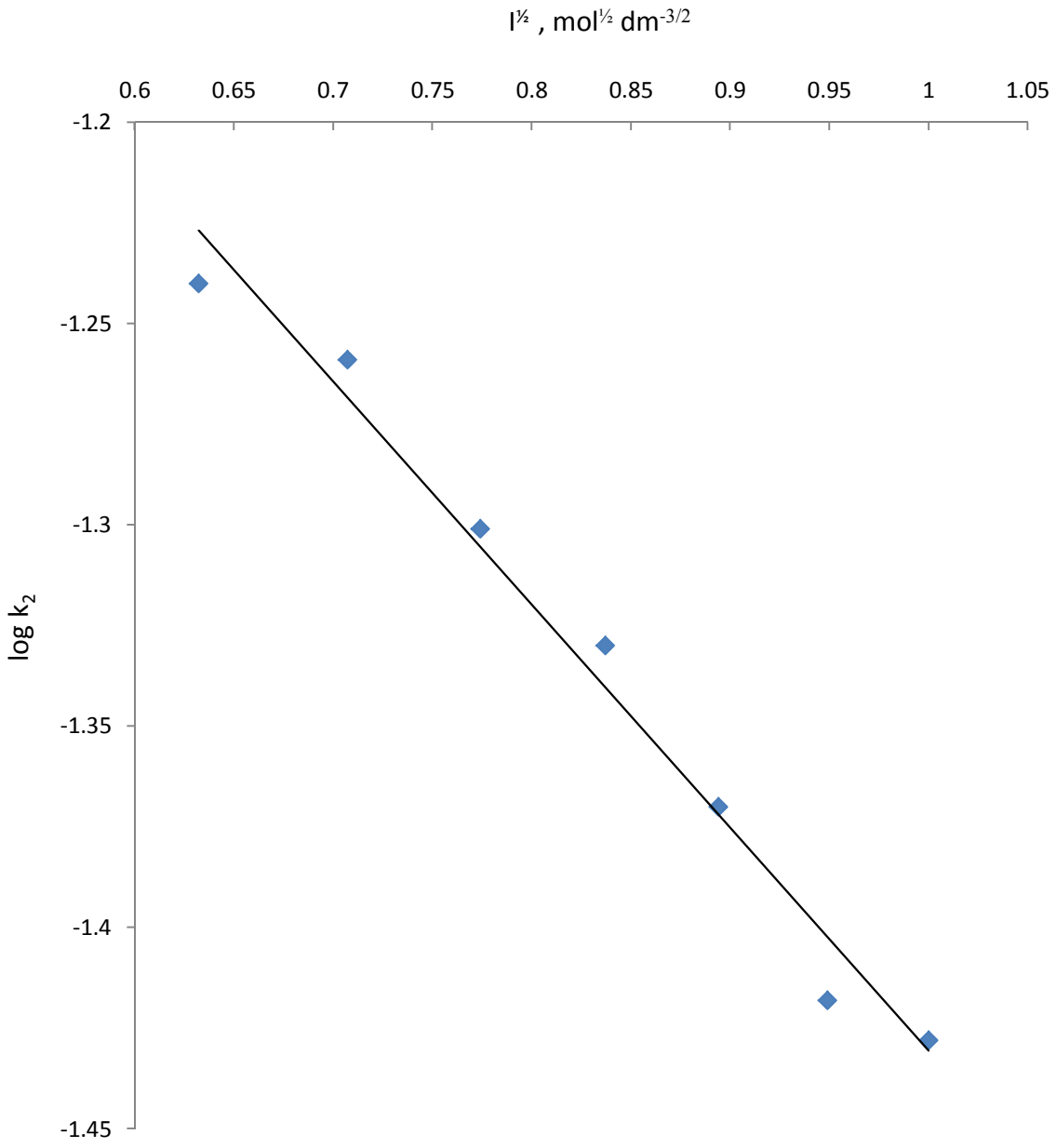


Figure 4.22: Plot of $\log k_2$ versus $I^{1/2}$ for the redox reaction of L – cysteic acid and permanganate ion at $[MnO_4^-]$ = 1.5 x10^{-4} mol dm^{-3}, $[H^+]$ = 0.1 mol dm^{-3}, [L – cysteic acid] = 8.25 x10^{-2} mol dm^{-3}, λ_{max} = 525nm and T = 27.0$\pm$ 1.0^{0}C

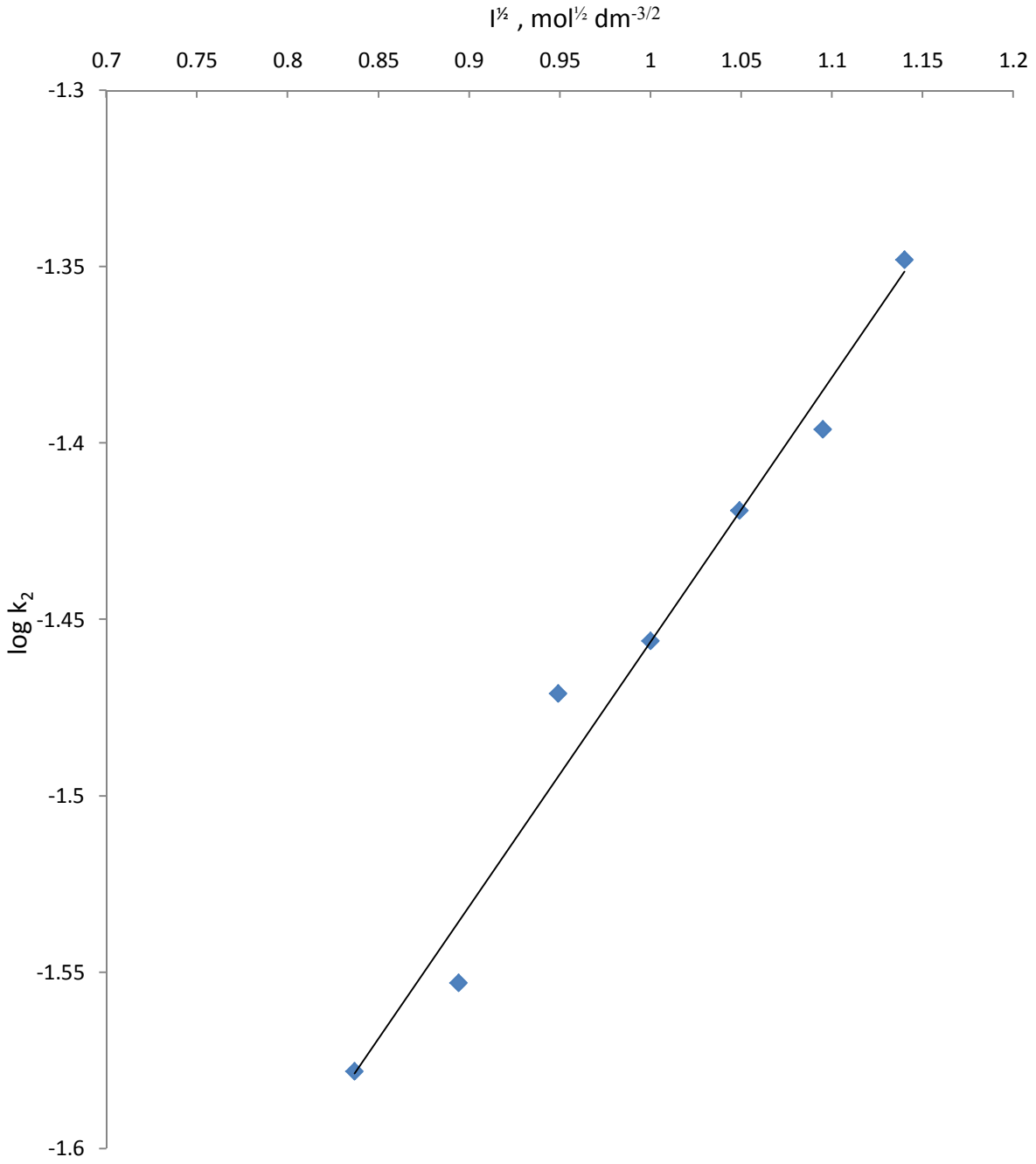


Figure 4.23: Plot of $\log k_2$ versus $I^{½}$ for the redox reaction of L – aspartic acid and permanganate ion at $[MnO_4^-]$ = 1.5 x10^{-4} mol dm^{-3}, [L – aspartic acid] = 7.5x10^{-2} mol dm^{-3}, $[H^+]$ = 0.2 mol dm^{-3}, λ_{max} = 525nm and T = 29.0$\pm$ 1.0^{0}C

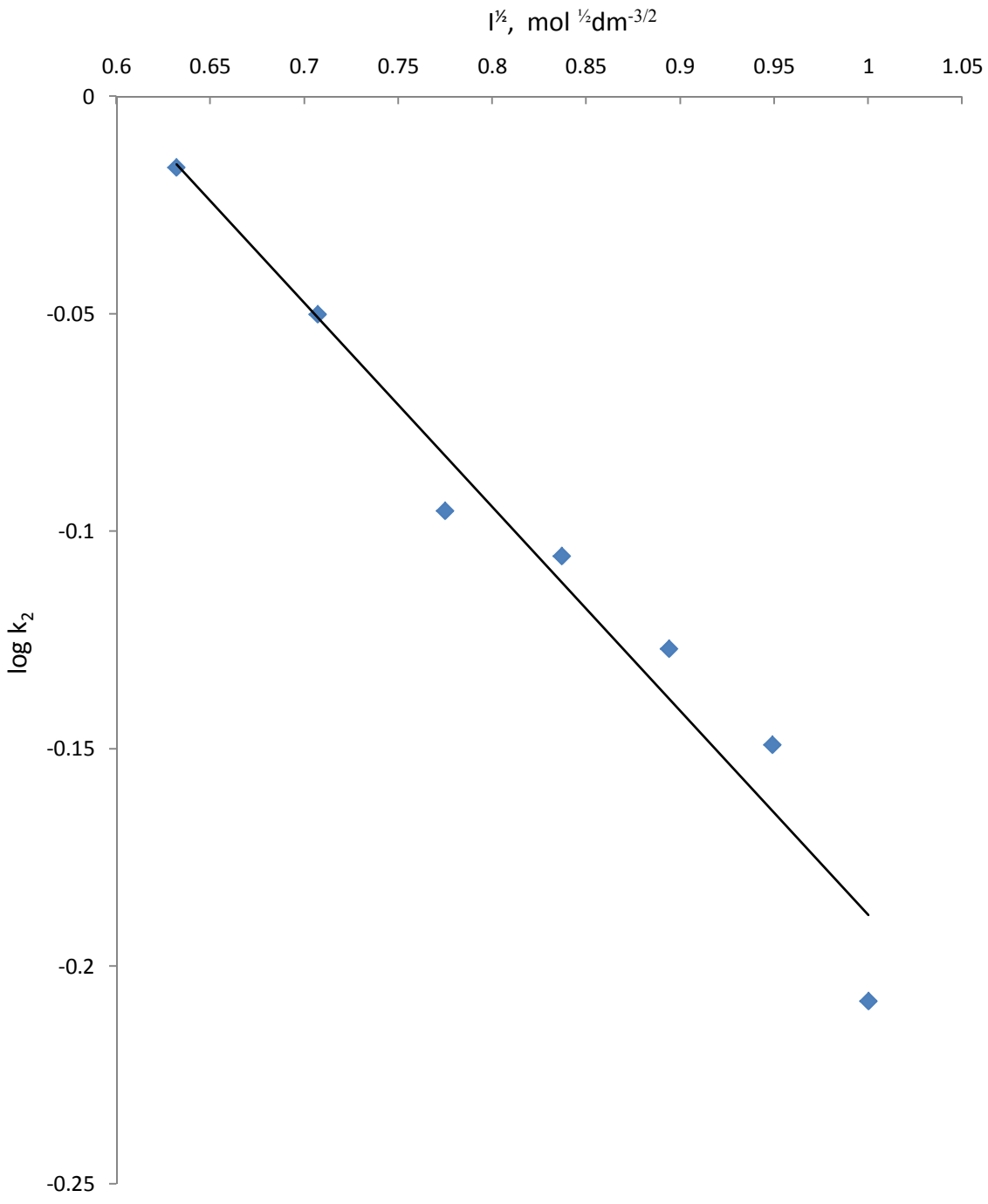


Figure 4.24: Plot of $\log k_2$ versus $I^{1/2}$ for the redox reaction of L – tryptophan and permanganate ion at $[MnO_4^-] = 2.0 \times 10^{-4}$ mol dm^{-3}, [L – tryptophan] = 1.8×10^{-2} mol dm^{-3}, $[H^+] = 0.1$ mol dm^{-3} , $\lambda_{max} = 525$nm and T = 28.0±1.0°C

4.5 Effect of added anion on the systems investigated

The effect of added NO_3^- was investigated and the results presented in Tables (4.5-4.8). It was ascertained that the anion did not react with the oxidant or reductant, all other reactants were kept constant, at constant ionic strength of 0.5 mol dm^{-3} (Na_2SO_4) for MnO_4^- -nicotinic acid, MnO_4^- -L-cysteic acid, and MnO_4^- - L-tryptophan systems and constant ionic strength of 1.0 $moldm^{-3}$ (Na_2SO_4) for MnO_4^- -L-aspartic acid system. It was observed that there was catalysis of the reactions rate when this anion was added in all the systems investigated. When anion-dependent rate constants k(x) was plotted against the concentrations of anion (NO_3^-), linear plots were obtained (Figures 4.25 - 4.28).

4.6 Effect of added cations

The concentrations of all other reactants were kept constant at ionic strength of 0.5 mol dm^{-3} (Na_2SO_4) for MnO_4^- -nicotinic acid, MnO_4^- -L-cysteic acid, and MnO_4^- - L-tryptophan systems and constant ionic strength of 1.0 $moldm^{-3}$ (Na_2SO_4) for MnO_4^- -L-aspartic acid system. It was ascertained that the cations did not react with either reductant or oxidant independently. The addition of Li^+ and Mg^{2+} were observed to alter the rate of the reactions in all the systems investigated. The results are presented in Tables (4.5 – 4.8).
The plots of the cation – dependent rate constant versus $[Z^{n+}]$, where Z^{n+} are Li^+ and Mg^{2+} are presented in Figures(4.29- 4.34).

4.7 Effect of change in dielectric constant of the reaction medium

The effect of medium dielectric constant on the rate constant was investigated using 3% - 15% acetone-water mixture for MnO_4^- - nicotinic acid, 3% - 18% acetone-water mixture for MnO_4^- - L- aspartic acid and 5% - 18% for MnO_4^- - L- tryptophan. The rate of reaction of MnO_4^- - nicotinic acid system and MnO_4^- - L-tryptophan were observed to decrease as the medium dielectric constant decreased. The rate of reaction was found to

Table 4.5: Rate constant for the effect of cations and anions on the redox reaction between MnO_4^- and nicotinic acid, at [nicotinic acid] =$8.4x10^{-2}$mol dm^{-3}, $[MnO_4^-] = 1.75x10^{-4}$ mol dm^{-3}, $[H^+] = 0.1$ mol dm^{-3}, I = 0.5 mol dm^{-3} and T = 28.0$\pm$ 1.0^0C

$10^4[NO_3^-]$, moldm^{-3}	**10^2k_{obs},s^{-1}**	**$10k_2$,dm^{3}mol^{-1}s^{-1}**
5	1.51	1.79
50	2.00	2.38
75	2.07	2.48
100	2.24	2.67
$10^4[Li^+]$		
5	1.34	1.60
50	1.22	1.45
75	1.13	1.35
100	0.97	1.15
$10^4[Mg^{2+}]$		
5	1.32	1.57
50	1.07	1.28
75	0.85	1.01
100	0.52	0.62

Table 4.6: Rate constant for the effect of cations and anions on the redox reaction between MnO_4^- and L – cysteic acid, at $[MnO_4^-] = 1.5x10^{-4}$ mol dm^{-3}, [L- cysteic acid] = $8.25x10^{-2}$ mol dm^{-3}, I = 0.5 mol dm^{-3}, $[H^+]$ = 0.1 mol dm^{-3} and T = 27.0± 1.0^0C

$10^4[NO_3^-]$, mol dm^{-3}	**10^3k_{obs},s^{-1}**	**10^2k_2,$dm^3mol^{-1}s^{-1}$**
5	4.60	5.58
50	5.23	6.34
75	5.68	6.89
100	5.92	7.17
10^4 $[Li^+]$		
5	4.61	5.59
50	5.45	6.60
75	5.65	6.85
100	6.27	7.60
10^4 [Mg^{2+}]		
5	4.64	5.62
50	6.06	7.35
75	7.30	8.85
100	7.59	9.20

Table 4.7: Rate constant for the effect of cations and anions in redox reaction between MnO_4^- and L-aspartic acid, at $[MnO_4^-] = 1.5x10^{-4}$ mol dm^{-3}, [L- aspartic acid] $= 7.50x10^{-2}$ mol dm^{-3}, I = 1.0 mol dm^{-3}, $[H^+] = 0.2$ mol dm^{-3} and T = 29.0 ± 1.0^0C

$10^4[NO_3^-]$, mol dm^{-3}	$10^3k_{obs}, s^{-1}$	$10^2k_2, dm^3mol^{-1}s^{-1}$
5	2.49	3.32
25	2.28	3.04
75	2.06	2.75
100	1.65	2.20
10^4 $[Li^+]$		
5	2.88	3.84
25	3.32	4.43
75	3.57	4.76
100	3.60	4.80
10^4 $[Mg^{2+}]$		
5	2.83	3.77
25	3.16	4.21
75	3.39	4.52
100	3.27	4.36

Table 4.8: Rate constant for the effect of cation and anion on the redox reaction between MnO_4^- and L – tryptophan, at $[MnO_4^-] = 2.0x10^{-4}$ mol dm^{-3}, [L - tryptophan] = 1.8 $x10^{-2}$mol dm^{-3}, I = 0.5 mol dm^{-3}, $[H^+]$ = 0.1 mol dm^{-3} and T = 28.0± 1.0^0C

$10^4[NO_3^-]$, mol dm^{-3}	**10^2k_{obs}, s^{-1}**	**$10k_2$,$dm^3mol^{-1}s^{-1}$**
5	1.60	8.87
25	1.56	8.67
75	1.51	8.39
100	1.47	8.16
10^4 [Mg^{2+}]		
5	1.61	8.94
25	1.63	9.06
75	1.67	9.28
100	1.7	9.44

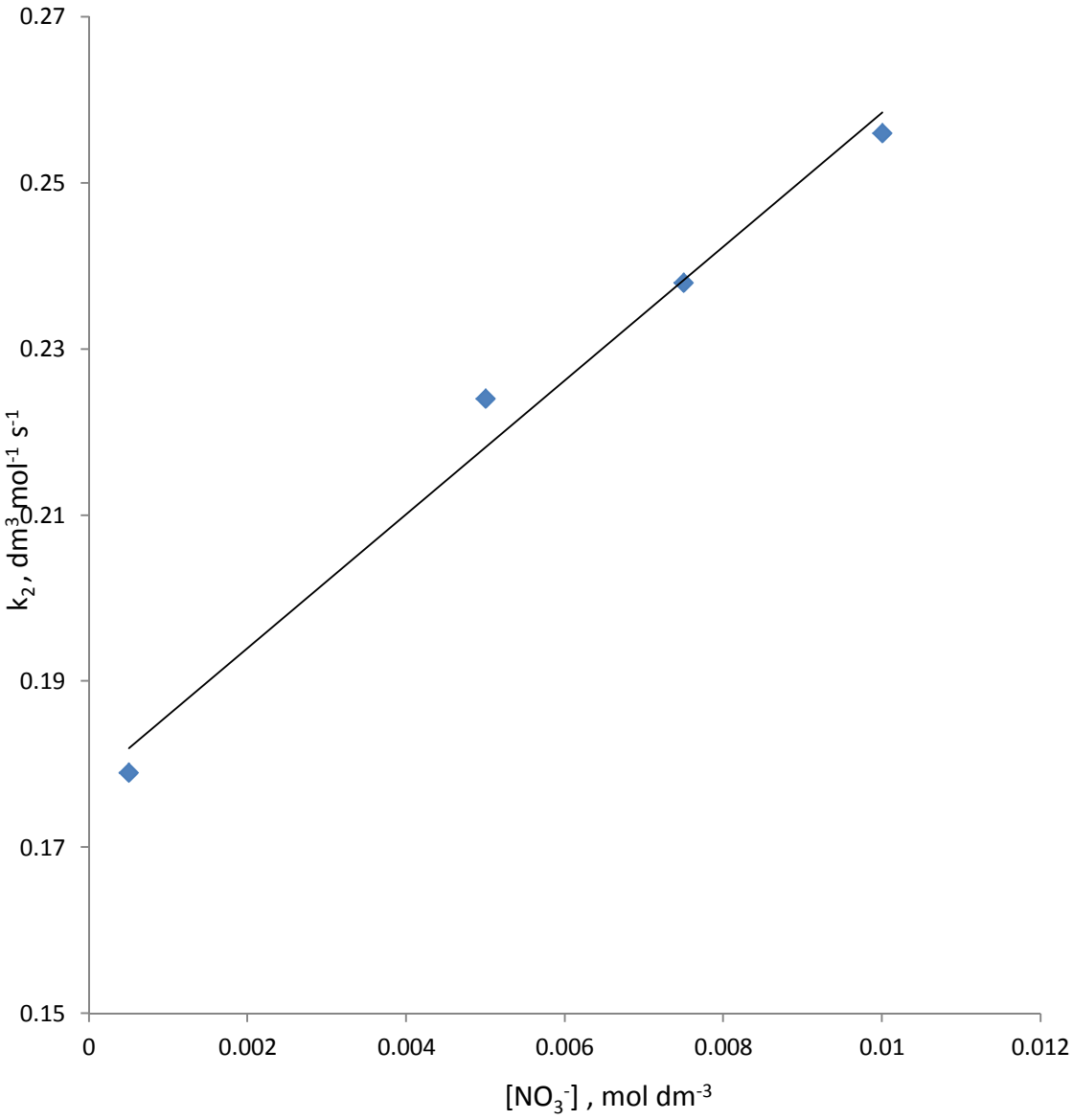


Figure 4.25: Plot of k_2 versus $[NO_3^-]$ for the redox reaction of nicotinic acid and permanganate ion at $[MnO_4^-]$ = $1.5x10^{-4}$mol dm^{-3}, [nicotinic acid] = $8.4x10^{-2}$mol dm^{-3}, $[H^+]$ = 0.1mol dm^{-3}, I = 0.5 mol dm^{-3}, λ_{max} = 525nm and T = 28.0±1.0°C

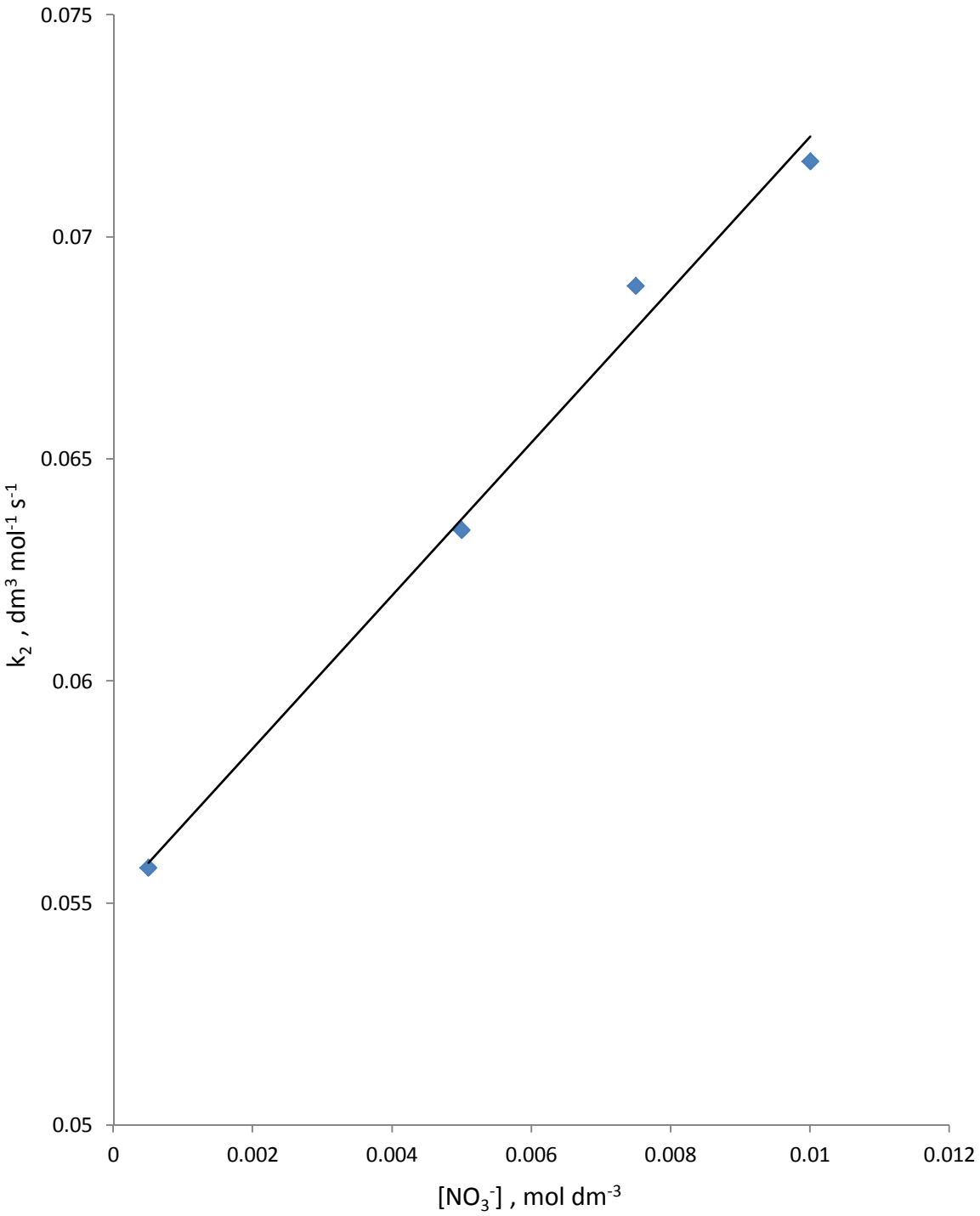


Figure 4.26: Plot of k_2 versus $[NO_3^-]$ for the redox reaction of L – cysteic acid and permanganate ion at $[MnO_4^-] = 1.5x10^{-4}$mol dm^{-3}, [L – cysteic acid] = $8.25x10^{-2}$mol dm^{-3}, $[H^+] = 0.1$moldm^{-3}, I = 0.5 mol dm^{-3}, λ_{max} = 525nm and T = 27.0±1.0^oC

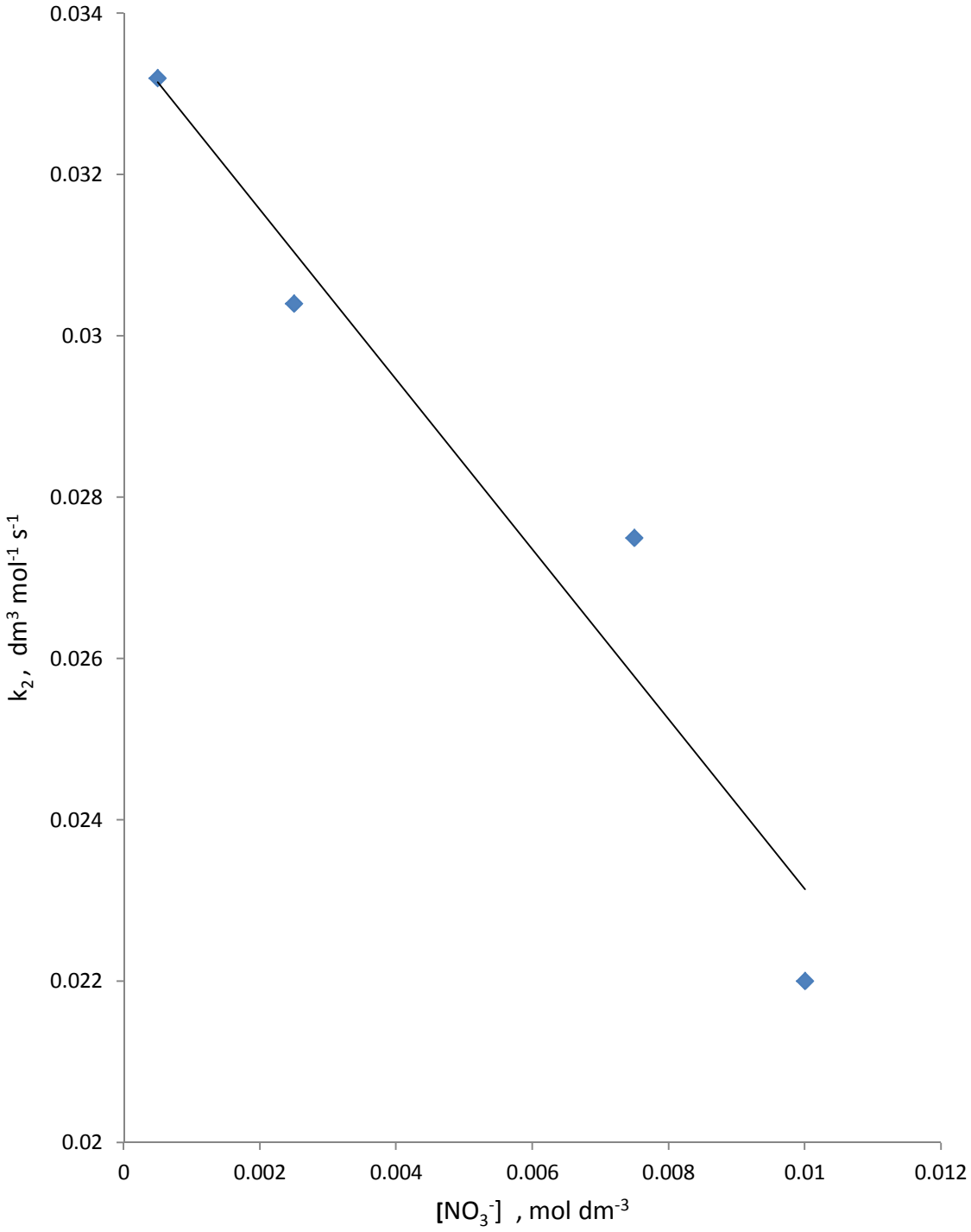


Figure 4.27: Plot of k_2 versus $[NO_3^-]$ for the redox reaction of L – aspartic acid and permanganate ion at $[MnO_4^-] = 1.5x10^{-4}$mol dm^{-3}, [L – aspartic acid] = $7.5x10^{-2}$mol dm^{-3}, $[H^+] = 0.2$mol dm^{-3}, I = 1.0 mol dm^{-3}, λ_{max} = 525nm and T = 29.0±1.0^{o}C

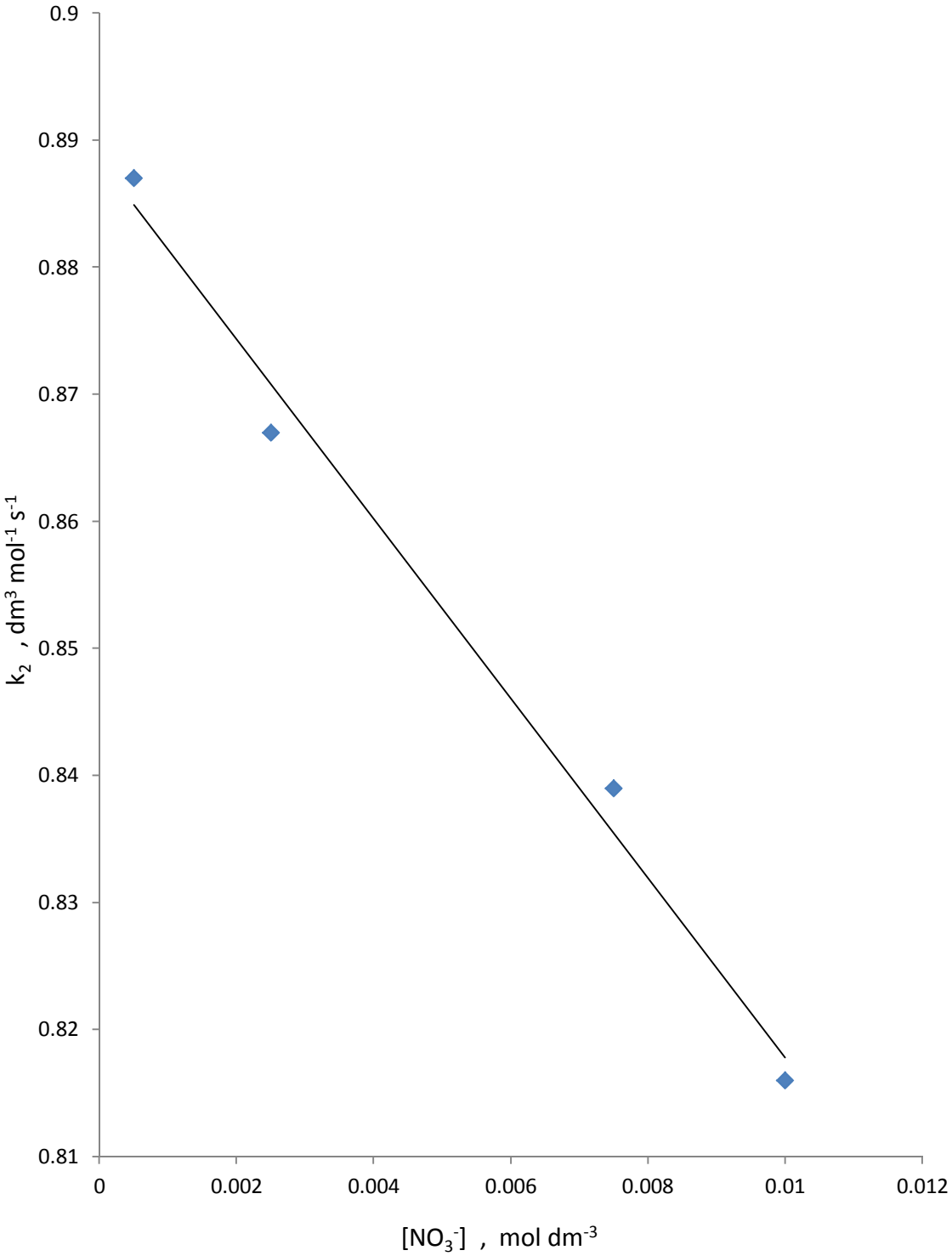


Figure 4.28: Plot of k_2 versus $[NO_3^-]$ for the redox reaction of L- tryptophan and permanganate ion at $[MnO_4^-] = 2.0 \times 10^{-4}$mol dm^{-3}. [L- tryptophan]= 1.8×10^{-2} mol dm^{-3}, $[H^+] = 0.1$ mol dm^{-3} I= 0.5mol dm^{-3}, λ_{max}= 525nm and T= 28.0$\pm$1.0^{O}C

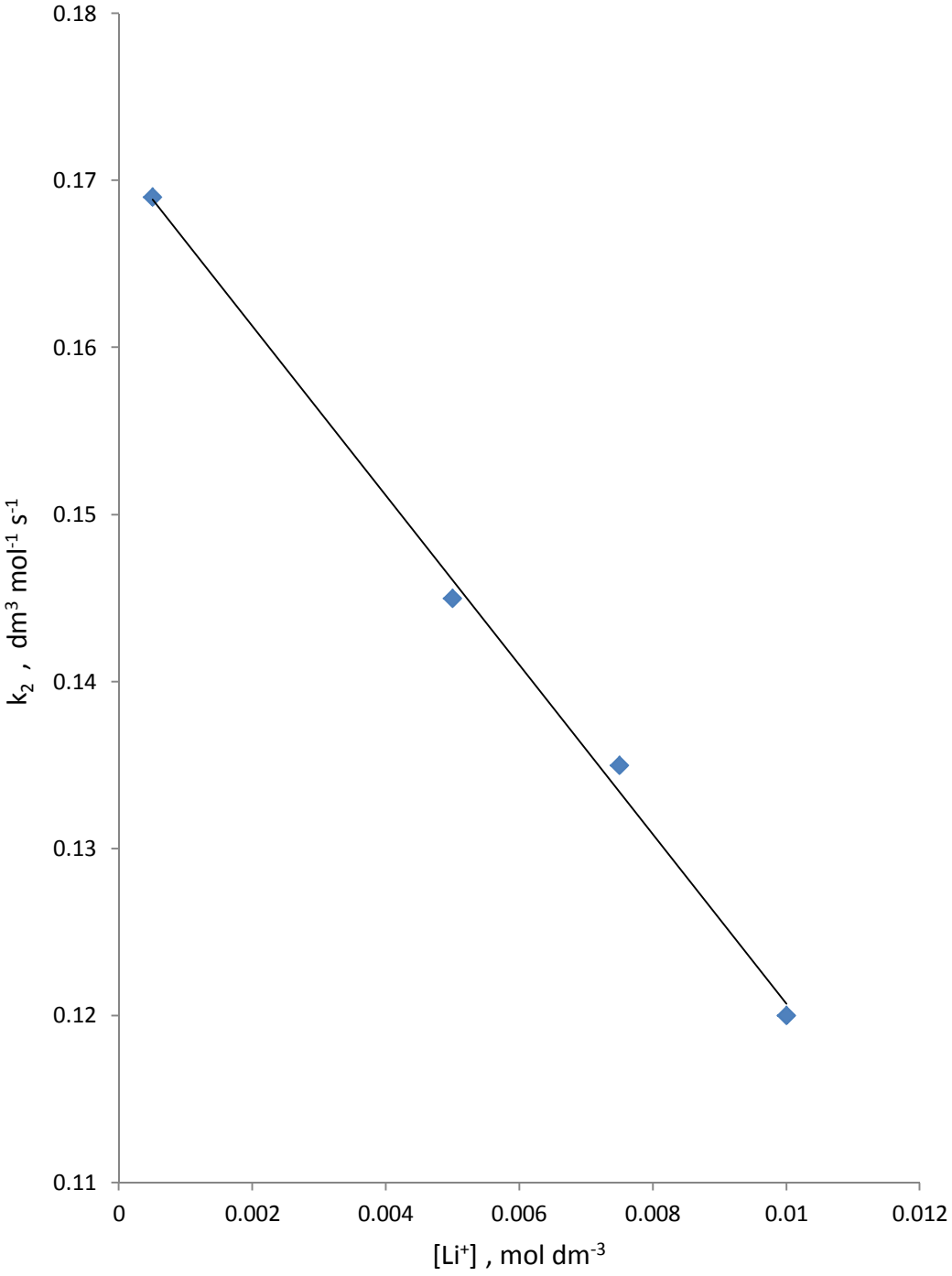


Figure 4.29: Plot of $k_2(z^{n+})$ versus $[Li^+]$ for the redox reaction of nicotinic acid and permanganate ion at $[MnO_4^-] = 1.5x10^{-4}$mol dm^{-3}, [nicotinic acid]= $8.4x10^{-2}$mol dm^{-3}, $[H^+] = 0.1$mol dm^{-3}, I = 0.5 mol dm^{-3}, λ_{max} = 525nm and T = 28.0±1.0^{o}C

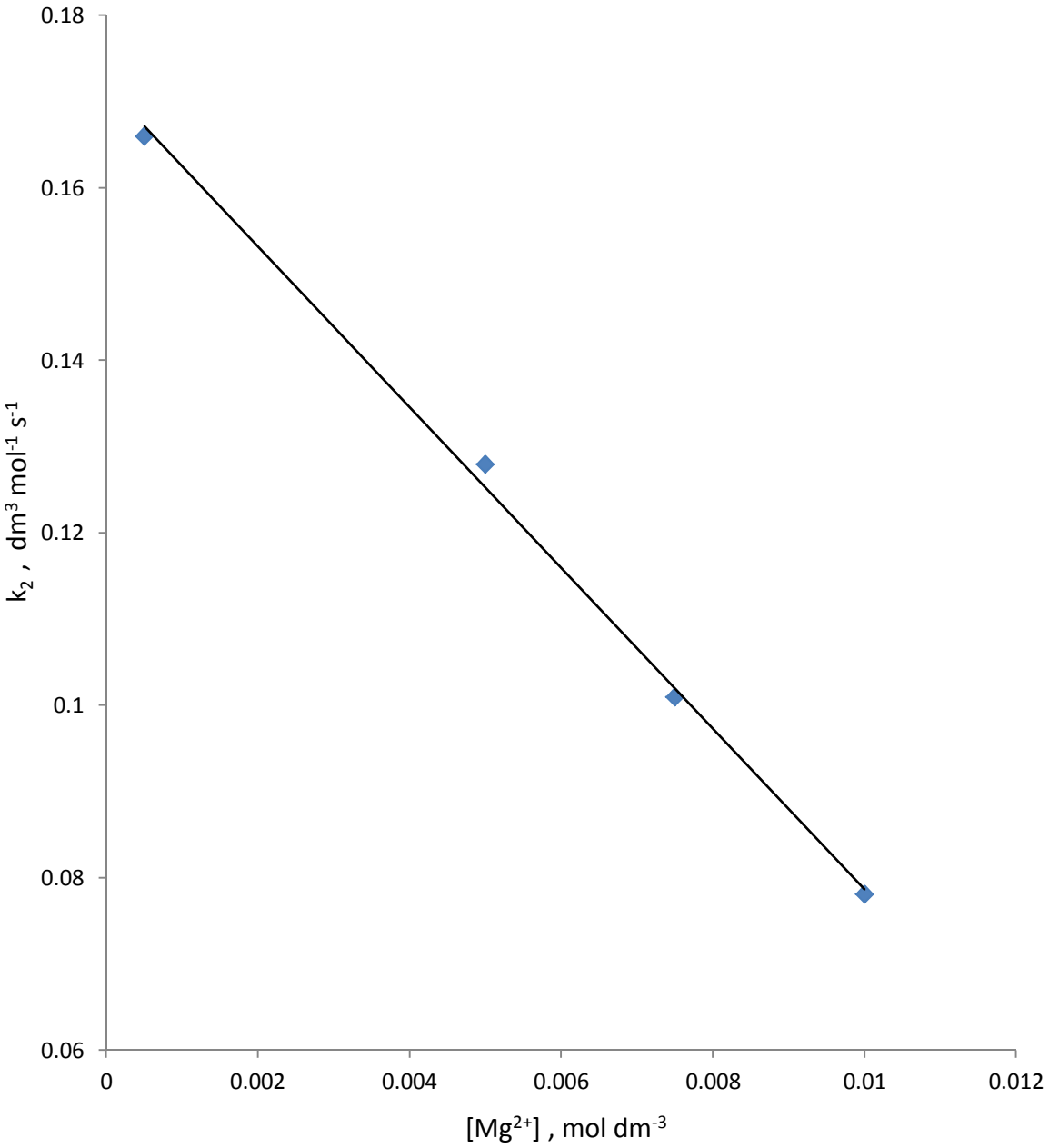


Figure 4.30: Plot of $k_2(z^{n+})$ versus $[Mg^{2+}]$ for the redox reaction of nicotinic acid and permanganate ion at $[MnO_4^-] = 1.5x10^{-4}$mol dm^{-3}, [nicotinic acid]= $8.4x10^{-2}$mol dm^{-3}, $[H^+] = 0.1$mol dm^{-3}, I = 0.5 mol dm^{-3}, λ_{max} = 525nm and T = 28.0±1.0°C

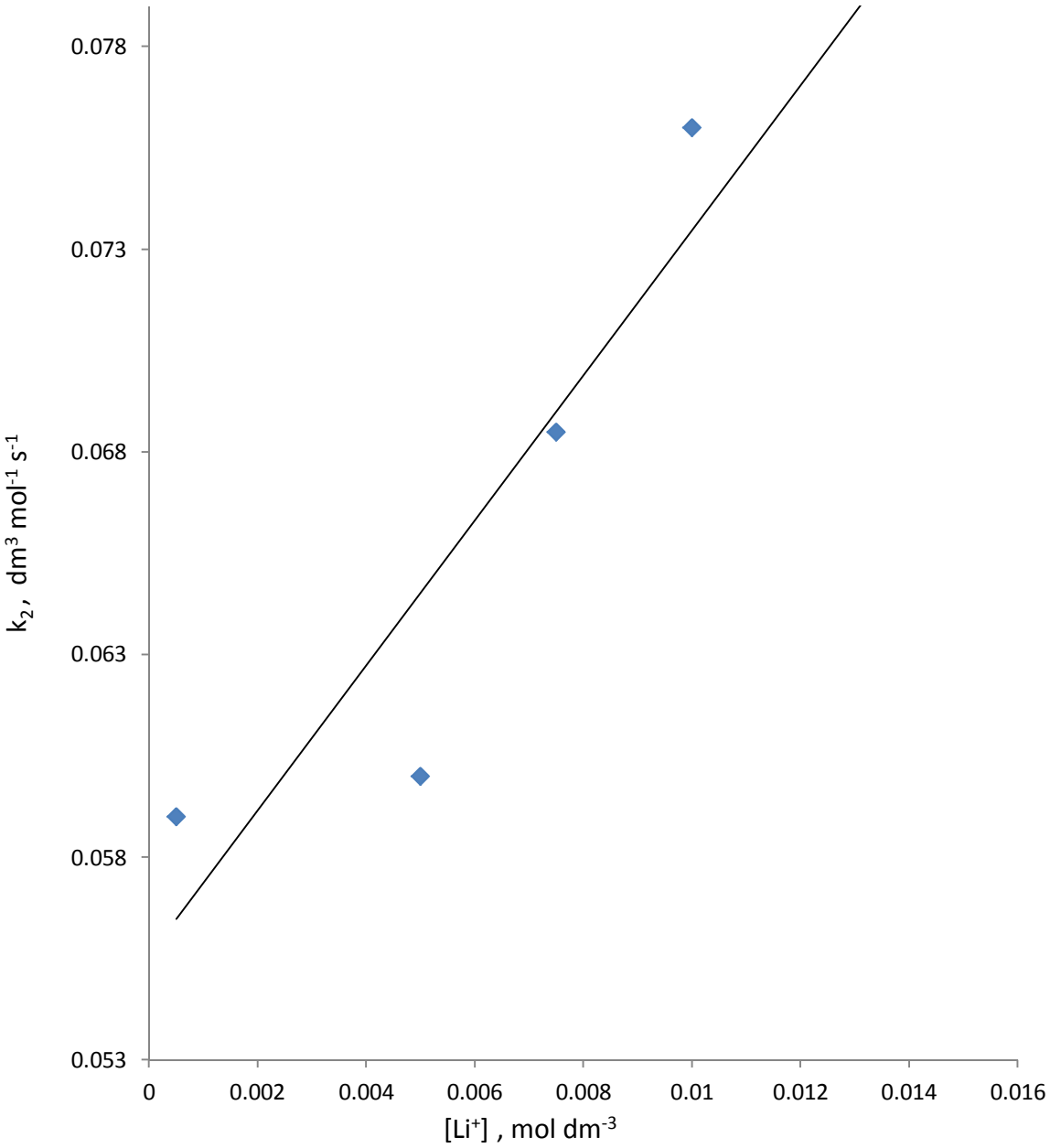


Figure 4.31: Plot of $k_2(z^{n+})$ versus $[Li^+]$ for the redox reaction of L – cysteic acid and permanganate ion at $[MnO_4^-] = 1.5x10^{-4}$mol dm^{-3}, [L– cysteic acid]= $8.25x10^{-2}$mol dm^{-3}, $[H^+] = 0.1$mol dm^{-3}, I = 0.5 mol dm^{-3}, λ_{max} = 525nm and T = 27.0±1.0^{o}C

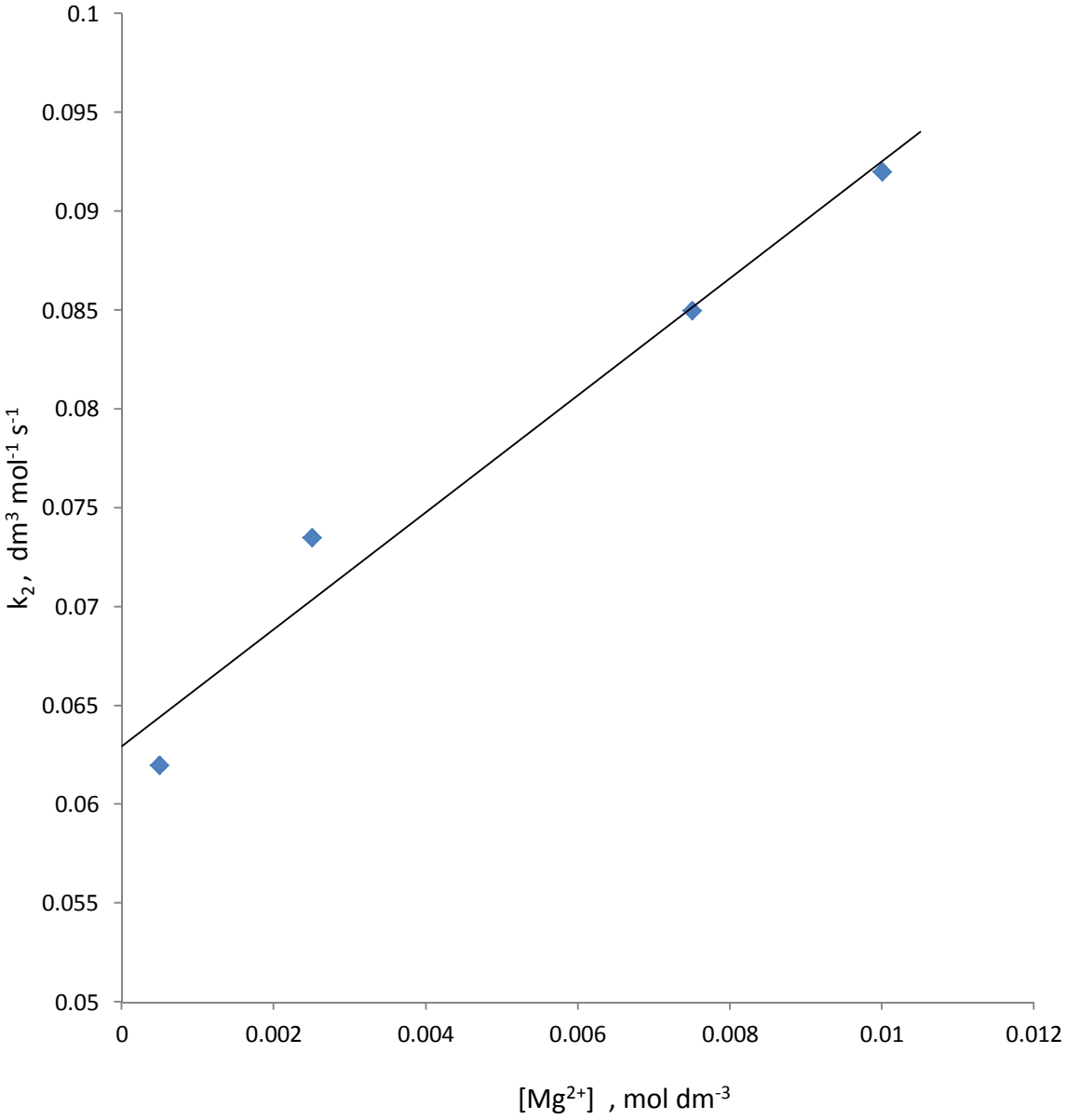


Figure 4.32: Plot of $k_2(z^{n+})$ versus $[Mg^{2+}]$ for the redox reaction of L – cysteic acid and permanganate ion at $[MnO_4^-]$= $1.5x10^{-4}$mol dm^{-3}, [L–cysteic acid]= $8.25x10^{-2}$mol dm^{-3}, $[H^+]$ = 0.1mol dm^{-3}, I = 0.5 mol dm^{-3}, λ_{max} = 525nm and T = 27.0±1.0^oC

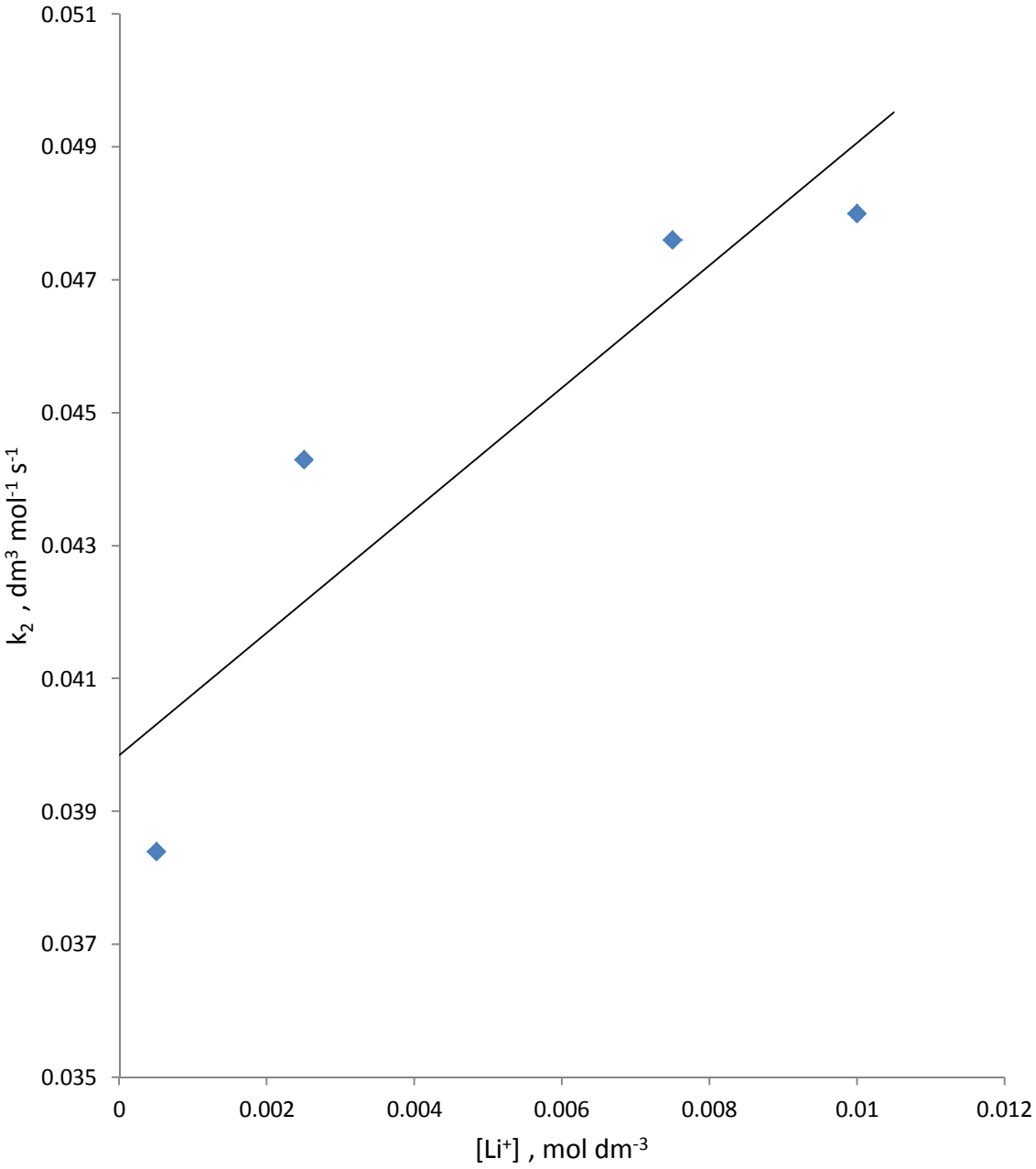


Figure 4.33: Plot of $k_2(z^{n+})$ versus $[Li^+]$ for the redox reaction of L – aspartic acid and permanganate ion at $[MnO_4^-] = 1.5x10^{-4}$mol dm^{-3}, [L – aspartic acid]= $7.5x10^{-2}$mol dm^{-3}, $[H^+] = 0.2$mol dm^{-3}, I = 1.0 mol dm^{-3}, λ_{max} = 525nm and T = 29.0±1.0^{o}C

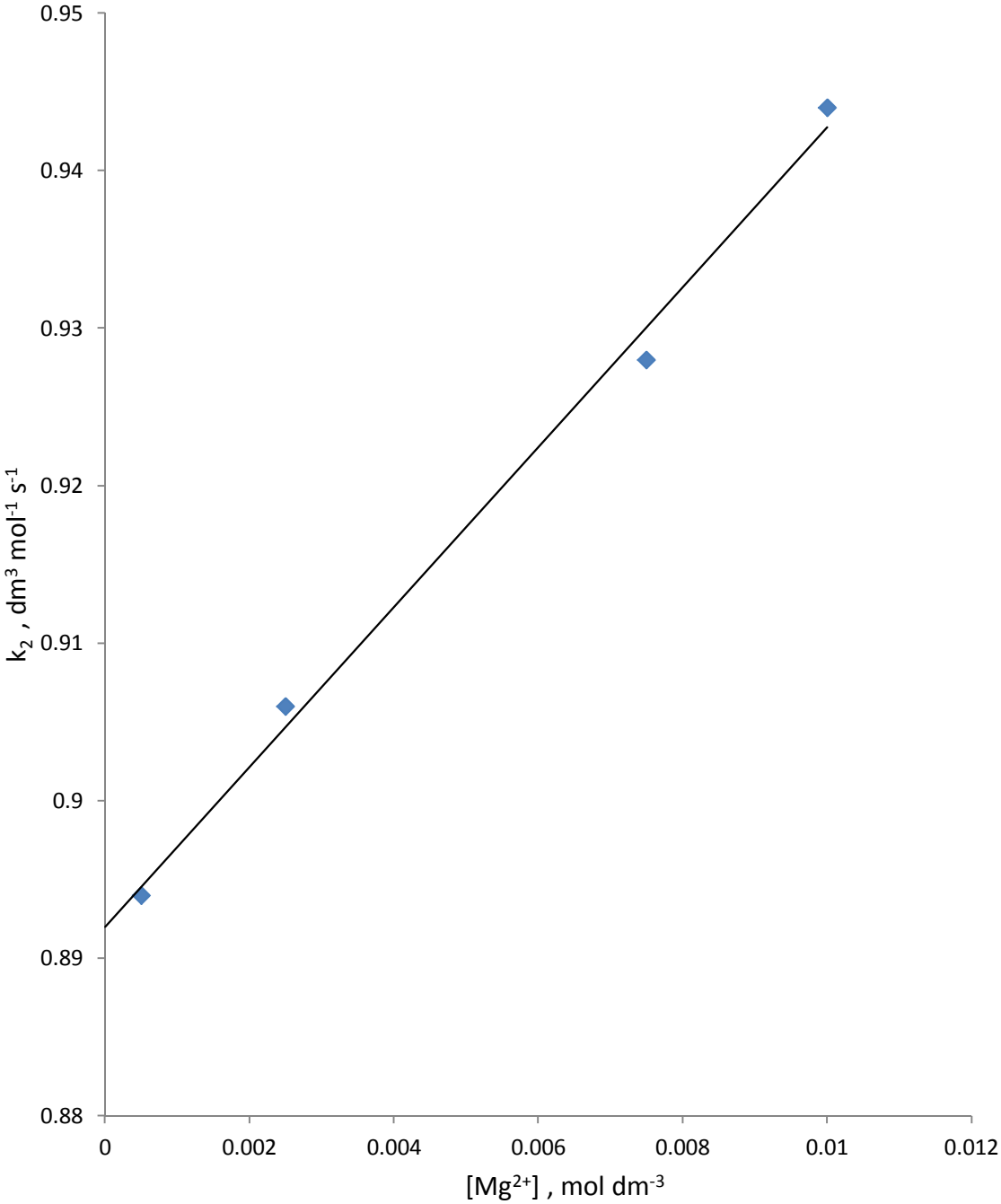


Figure 4.34: Plot of $k_2(z^{n+})$ versus $[Mg^{2+}]$ for the redox reaction of L- tryptophan and permanganate ion at $[MnO_4^-]= 2.0 \times 10^{-4}$mol dm^{-3}. [L- tryptophan]= 1.8×10^{-2} mol dm^{-3}, $[H^+] = 0.1$ mol dm^{-3}, I= 0.5mol dm^{-3} λ_{max}= 525nm and T = 28.0±1.0^{o}C

increase as the medium dielectric constant decrease in MnO_4^- - L – aspartic system. The results are presented in Tables (4.9 – 4.11).Typical plots of $logk_2$ versus 1/D (where D = dielectric constant) for the three aforementioned systems above are shown in Figures (4.35 – 4.37).There was no noticeable change in the rate constants for MnO_4^- - L – cysteic acid system.

4.8 Free radicals test

Acrylamide was added to a partially oxidized reaction mixtures of the reactions systems, of MnO_4^- - nicotinic acid, MnO_4^-- L – cysteic acid, MnO_4^- L – aspartic acid and MnO_4^-- L – tryptophan, then followed by a large excess of methanol, there was no gel formation in all the systems. This probably suggests that no free radical was formed in all the reaction systems.

4.9 Test for intermediate complex

4.9.1 Spectrophotometric investigation

Spectrophotometric investigation were carried out in order to find out whether any spectroscopically determinable intermediate complex were formed in the course of the redox reaction of permanganate ion with all the reductants.The electronic spectra of the reaction mixtures after two minutes over a range of 400 – 700nm. A similar run was made for the permanganate alone. From the spectra (Figures 4.38 – 4.41) there was no significant shift in λ_{max} for all the systems investigated. This suggested that the formation of intermediate complex is not implicated in all the systems investigated.

4.9.2 Michaelis – Menten plot

Plots of $1/k_{obs}$ versus 1/[red] gave straight lines for all the systems and are presented in Figures (4.42 – 4.45). The lines passed through the origin for all the systems without any intercept, except MnO^-_4 – L-aspartic acid system which has small intercept on vertical axis.

Table 4.9: Effect of change in dielectric constant on rate constant for nicotinic acid – permanganate ion reaction at [nicotinic acid]=8.4×10^{-2}mol dm^{-3}, $[MnO_4^-] = 1.75 \times 10^{-4}$mol dm^{-3}, $[H^+] = 0.1$ mol dm^{-3}, I = 0.5 mol dm^{-3}, λ_{max}= 525nm and T= $28.0 \pm 1.0^{O}C$

D	**10^2 k_{obs},s^{-1}**	**$10k_2$,dm^3 mol^{-1} s^{-1}**
79.20	1.39	1.66
78.00	1.35	1.61
76.20	1.32	1.57
75.00	1.28	1.52
73.80	1.23	1.47
72.00	1.19	1.42

Table 4.10: Effect of change in dielectric constant on rate constant for L – aspartic acid – permanganate ion reaction at $[MnO_4^-]= 1.5x10^{-4}$ mol dm^{-3}, [L- aspartic acid] $= 7.50x10^{-2}$ mol dm^{-3}, I = 1.0 mol dm^{-3}, $[H^+]$ = 0.2 mol dm^{-3}, λ_{max} = 525nm and T= 29.0±1.0^{O}C

D	**10^3 k_{obs},s^{-1}**	**10^2k_2,dm^3 mol^{-1} s^{-1}**
79.17	2.66	3.55
78.00	2.68	3.58
76.20	2,76	3.68
75.00	2.81	3.74
72.00	2.93	3.90
70.80	3.05	4.06

Table 4.11: Effect of change in dielectric constant on rate constant for L – tryptophan – permanganate ion reaction at $[MnO_4^-]= 2.0x10^{-4}$ mol dm^{-3}, [L- tryptophan] = $1.8 x10^{-2}$ mol dm^{-3}, I = 0.5 mol dm^{-3}, $[H^+]$ = 0.1 mol dm^{-3}, λ_{max}= 525nm and T= $28.0\pm1.0^{O}C$

D	**10^2 k_{obs},s^{-1}**	**$10k_2$,dm^3 mol^{-1} s^{-1}**
78.00	1.52	8.44
76.80	1.49	8.28
75.00	1.45	8.05
73.80	1.41	7.83
72.00	1.37	7.61
70.80	1.32	7.33

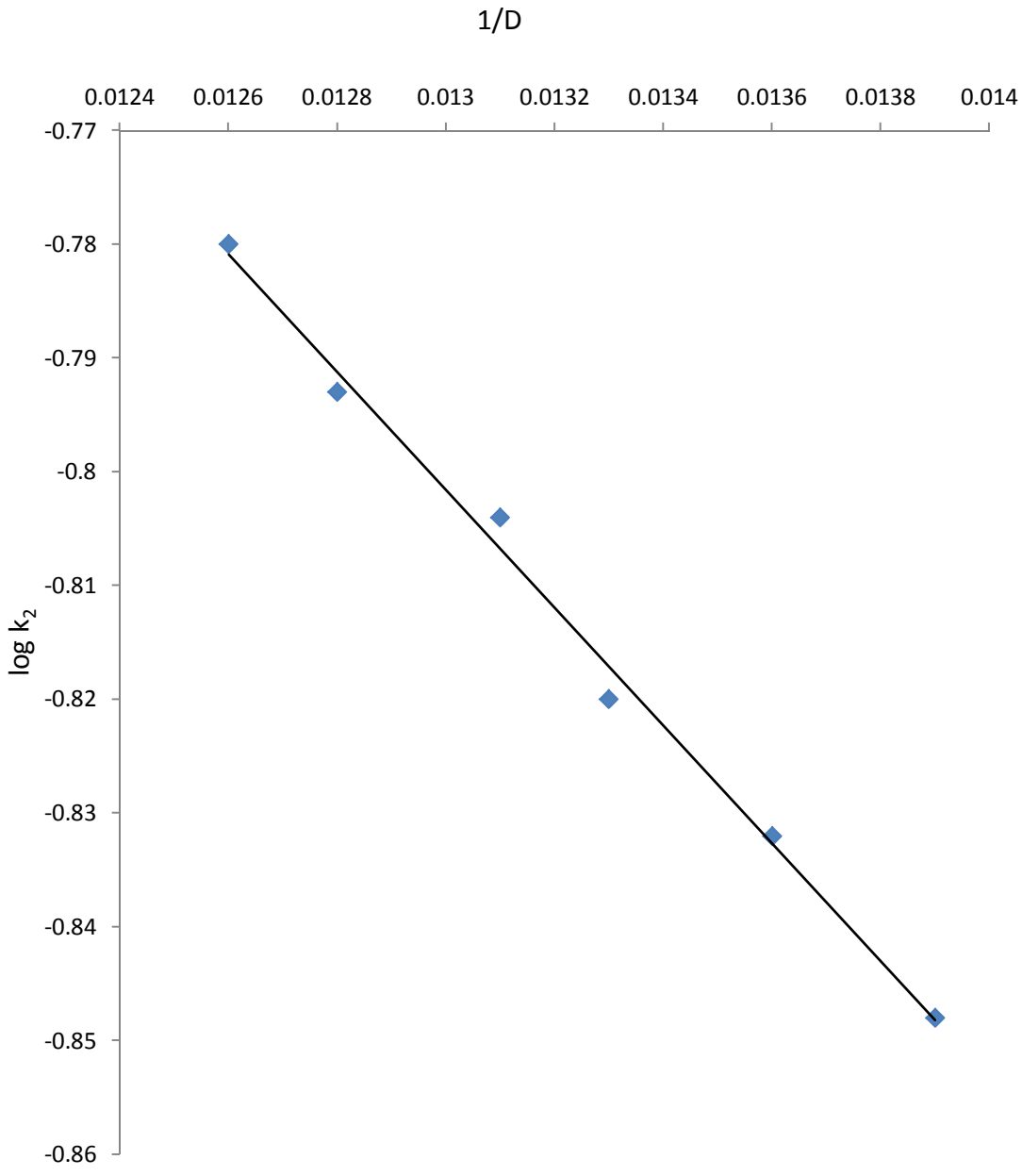


Figure 4.35: Plot of k_2 versus 1/D for the redox reaction of nicotinic acid and permanganate ion at $[MnO_4^-] = 1.5x10^{-4}$mol dm^{-3}, [nicotinic acid] = $8.4x10^{-2}$mol dm^{-3}, $[H^+] = 0.1$mol dm^{-3}, I = 0.5 mol dm^{-3}, λ_{max} = 525nm and T = 28.0±1.0^{o}C

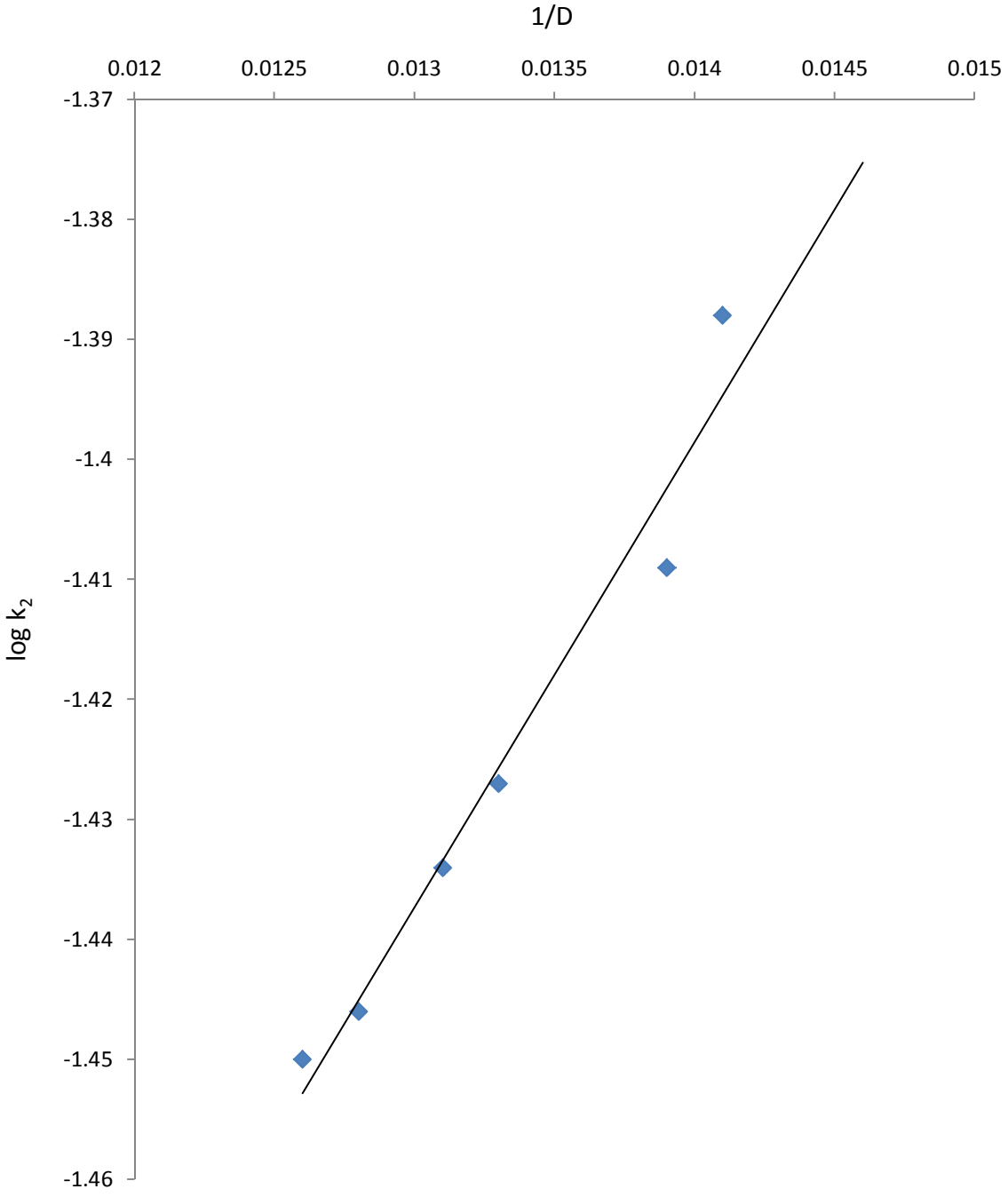


Figure 4.36: Plot of k_2 versus 1/D for the redox reaction of L – aspartic acid and permanganate ion at $[MnO_4^-] = 1.5x10^{-4}$mol dm^{-3}, [L – aspartic acid] = $7.5x10^{-2}$mol dm^{-3}, $[H^+] = 0.2$mol dm^{-3}, I = 1.0 mol dm^{-3}, λ_{max} = 525nm and T = 29.0±1.0^oC

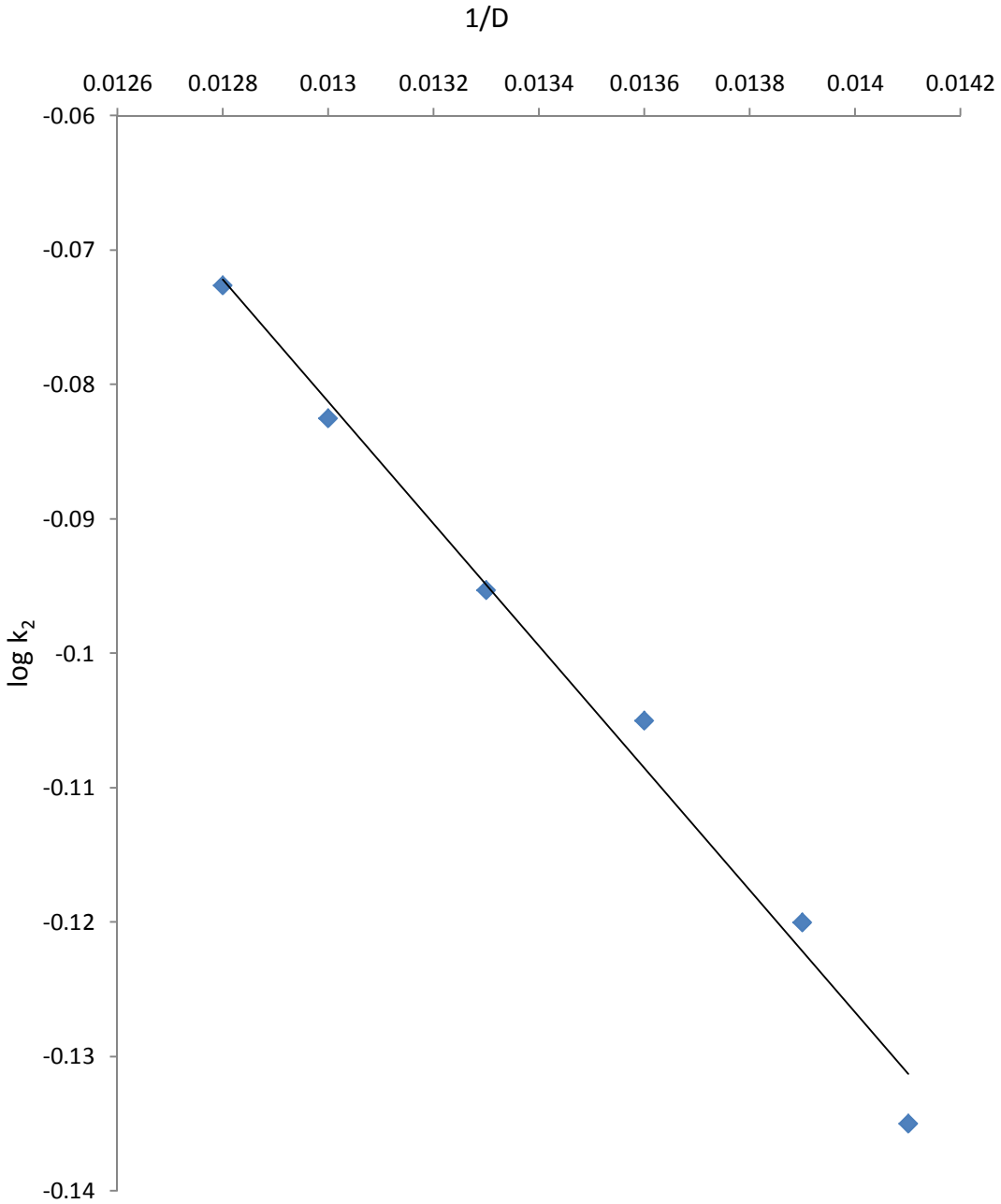


Figure 4.37: Plot of k_2 versus 1/D for the redox reaction of L- tryptophan and permanganate ion at$[MnO_4^-]$ = 2.0 x10^{-4}mol dm^{-3}. [L- tryptophan]= 1.8×10^{-2} mol dm^{-3}, $[H^+]$ = 0.1 mol dm^{-3} I= 0.5mol dm^{-3}, λ_{max}= 525nm and T= 28.0±1.0^{0}C

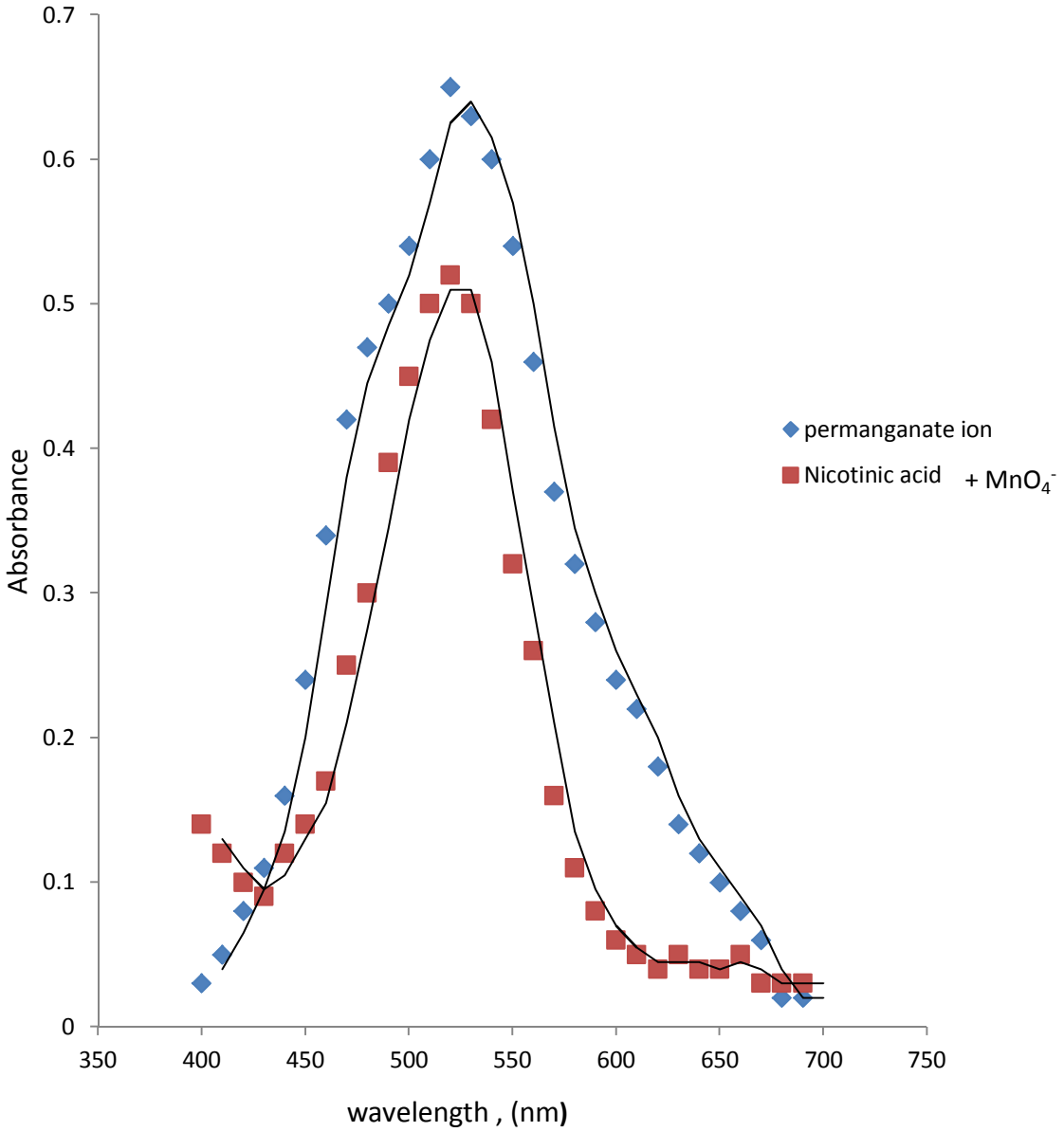


Figure 4.38: Spectra of the redox reaction mixture of permanganate ion and nicotinic acid after 2 minutes of reaction

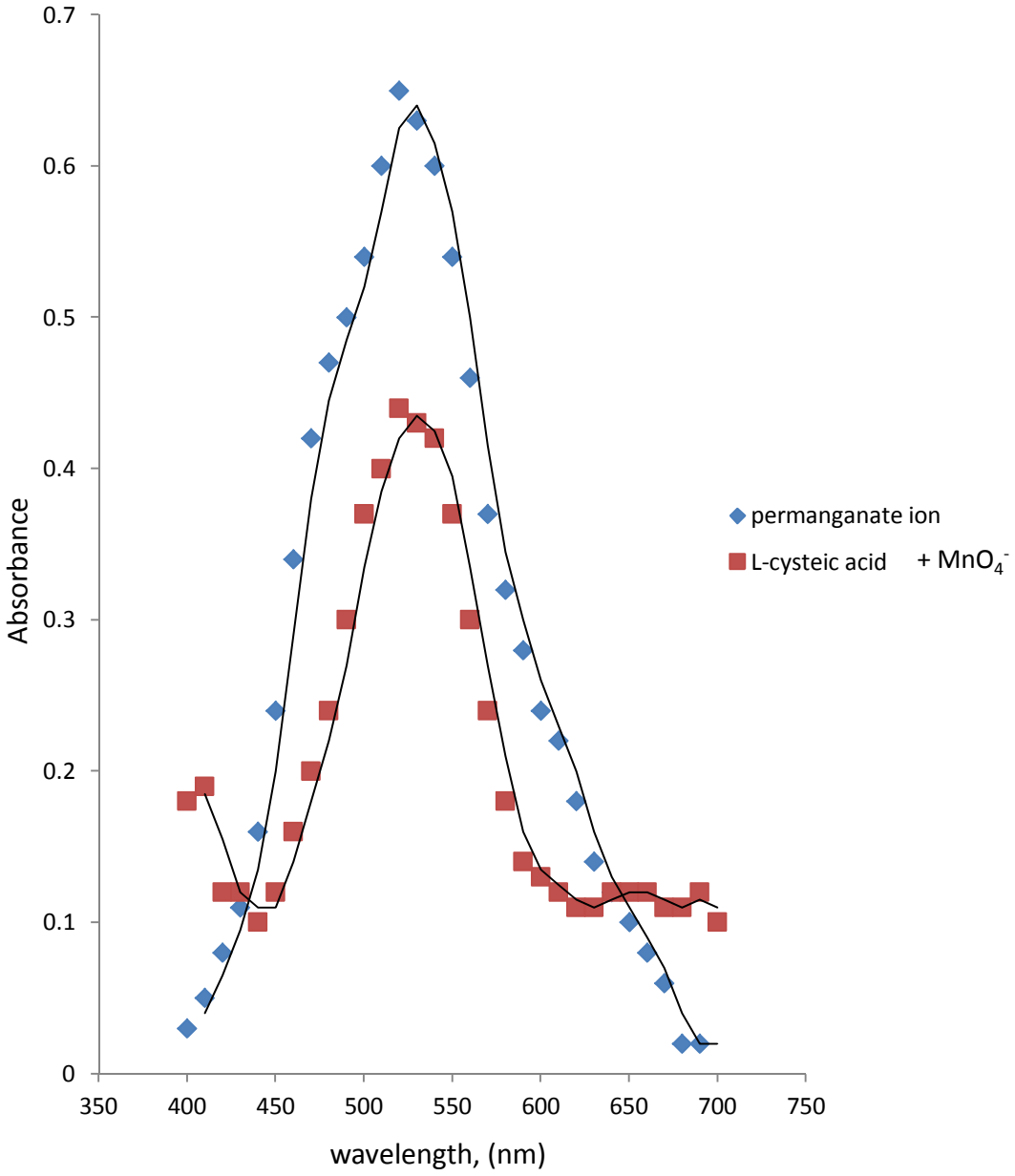


Figure 4.39: Spectra of the redox reaction mixture of permanganate ion and L –cysteic acid after 2 minutes of reaction

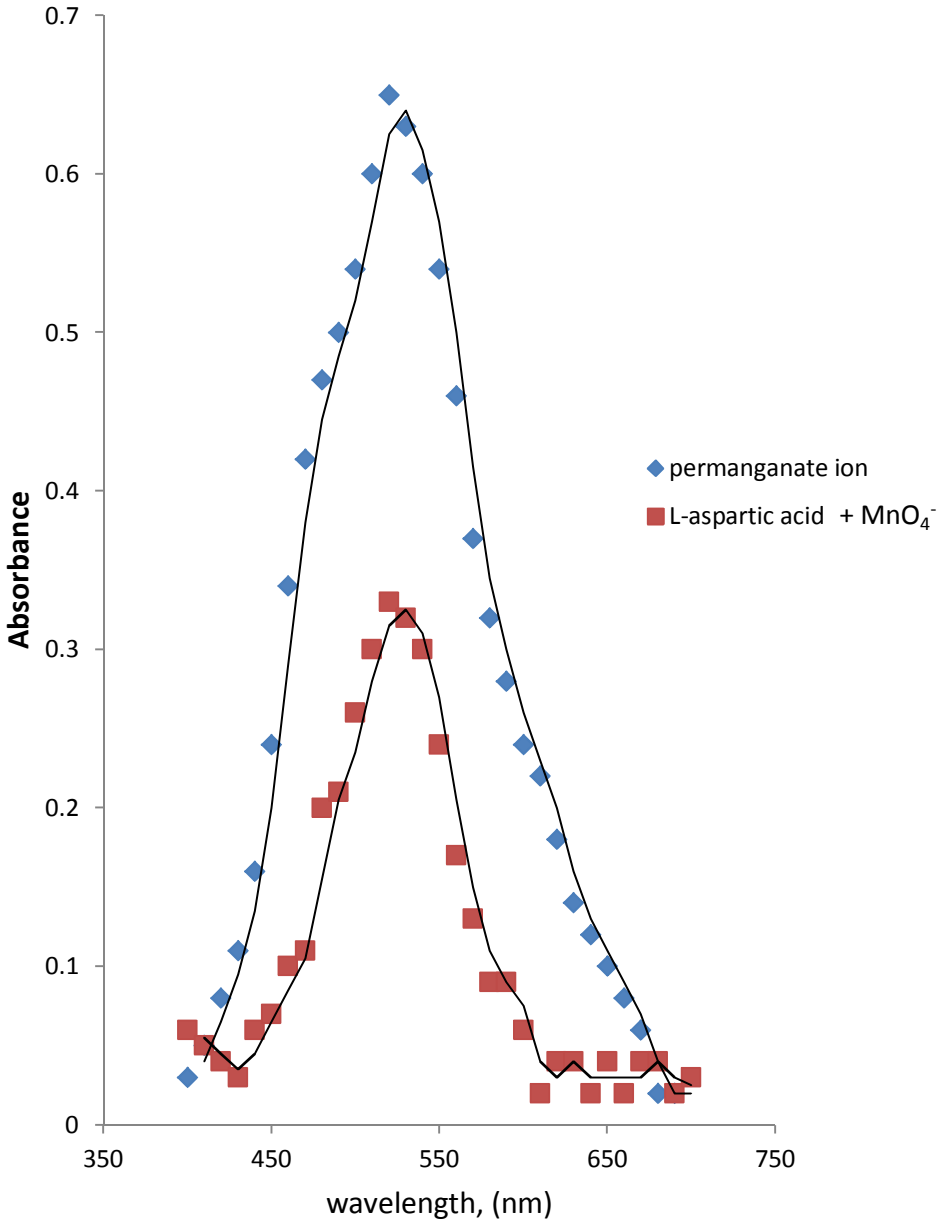


Figure 4.40: Spectra of the redox reaction mixture of permanganate ion and L– aspartic acid after 2 minutes of reaction

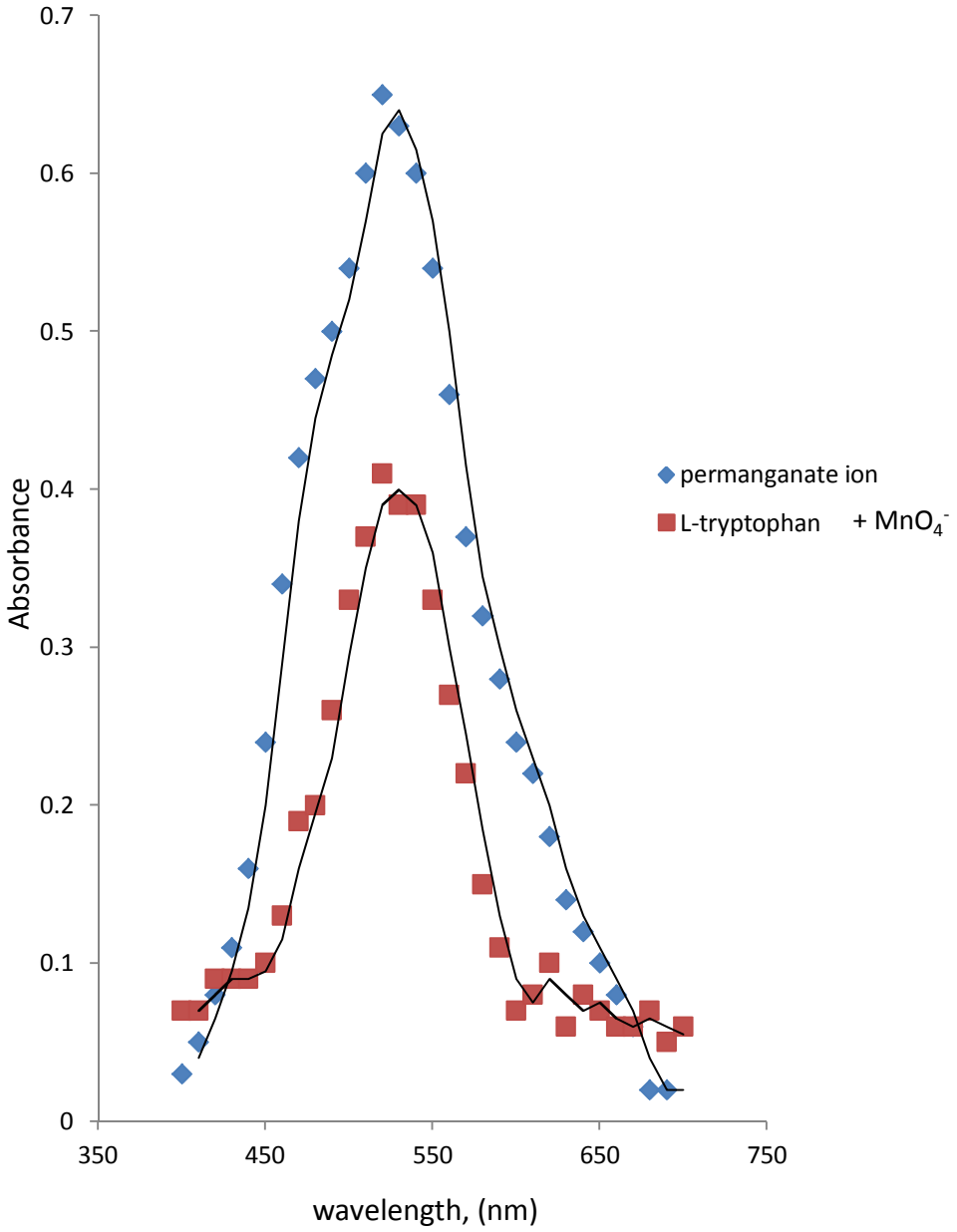


Figure 4.41: Spectra of the redox reaction mixture of permanganate ion and L– tryptophan acid after 2 minutes of reaction

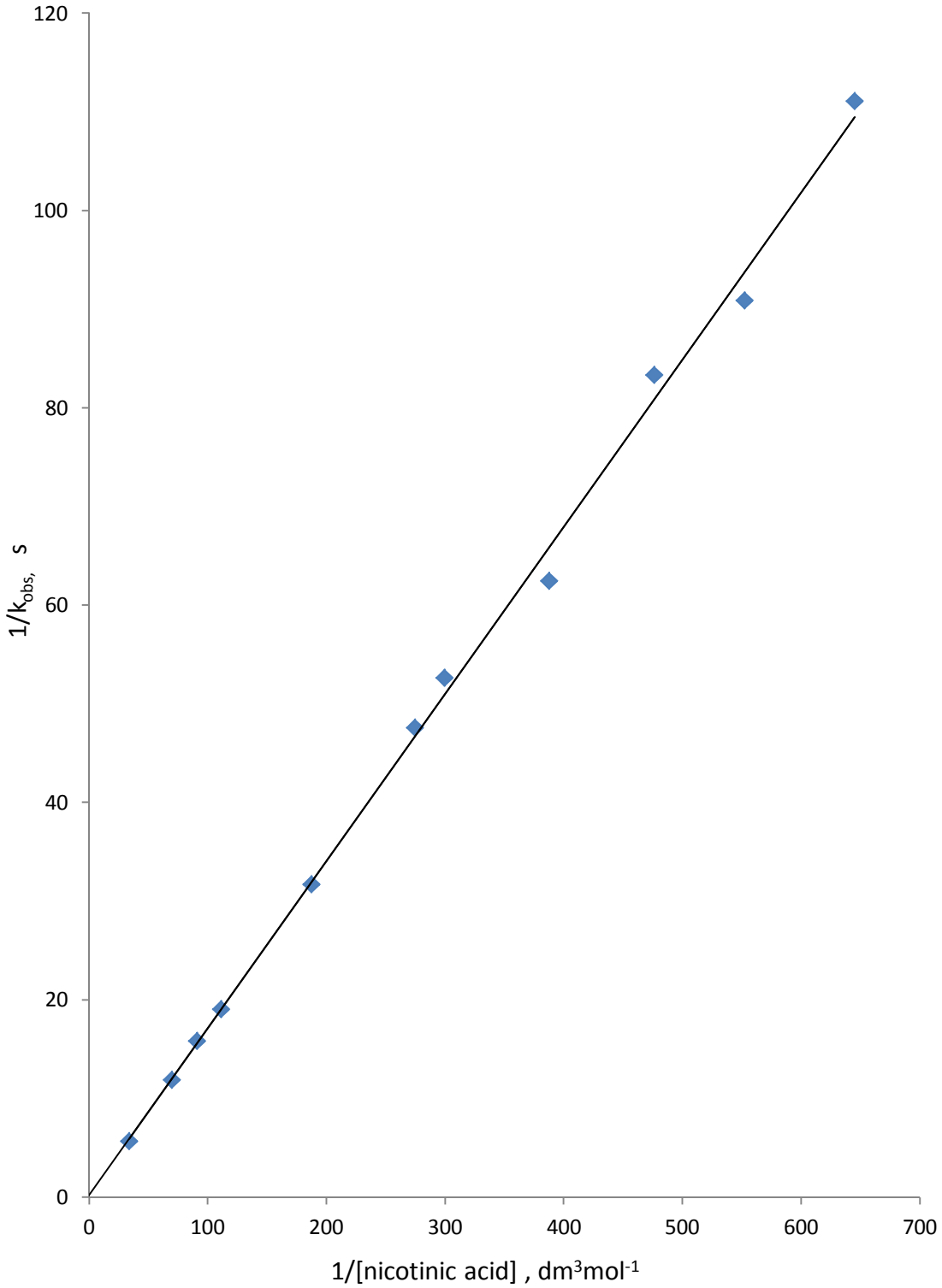


Figure 4.42: Michaelis – Menten plot of $1/k_{obs}$ versus 1/[nicotinic acid] for the redox reaction of permanganate ion and nicotinic acid

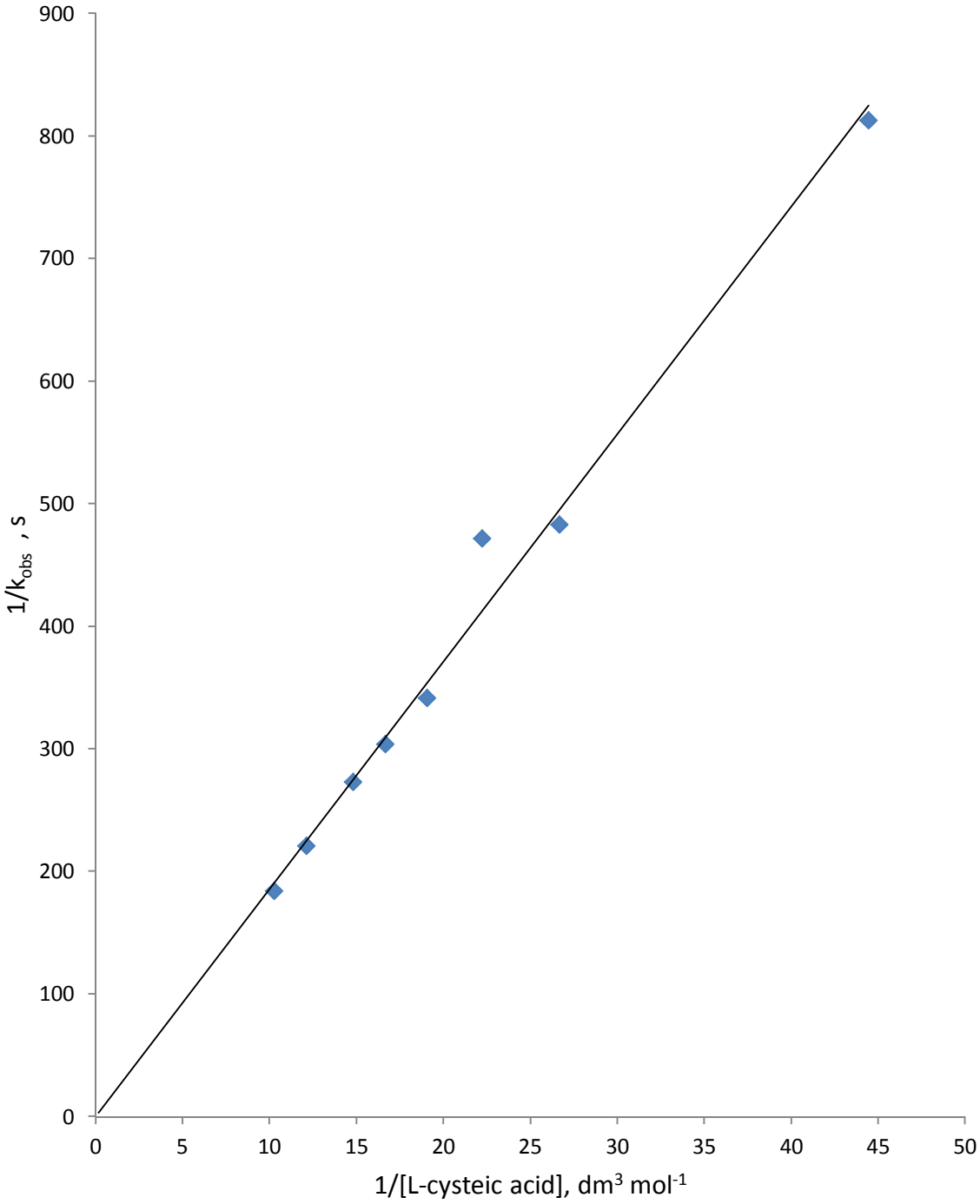


Figure 4.43: Michaelis – Menten plot of $1/k_{obs}$ versus 1/[L– cysteic acid] for the redox reaction of permanganate ion and L– cysteic acid

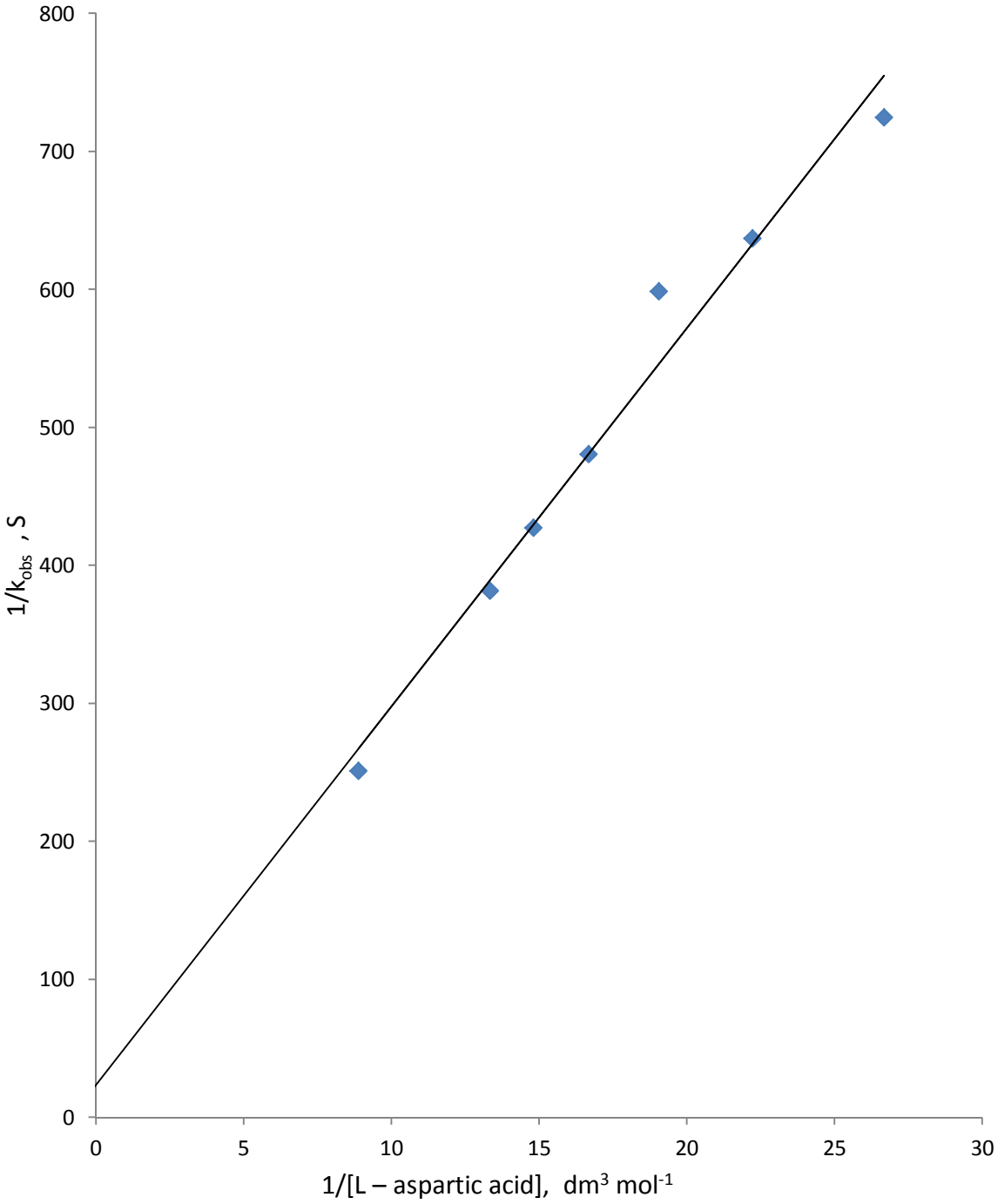


Figure 4.44: Michaelis – Menten plot of $1/k_{obs}$ versus1/[L – aspartic acid]for the redox reaction of permanganate ion and L – aspartic acid

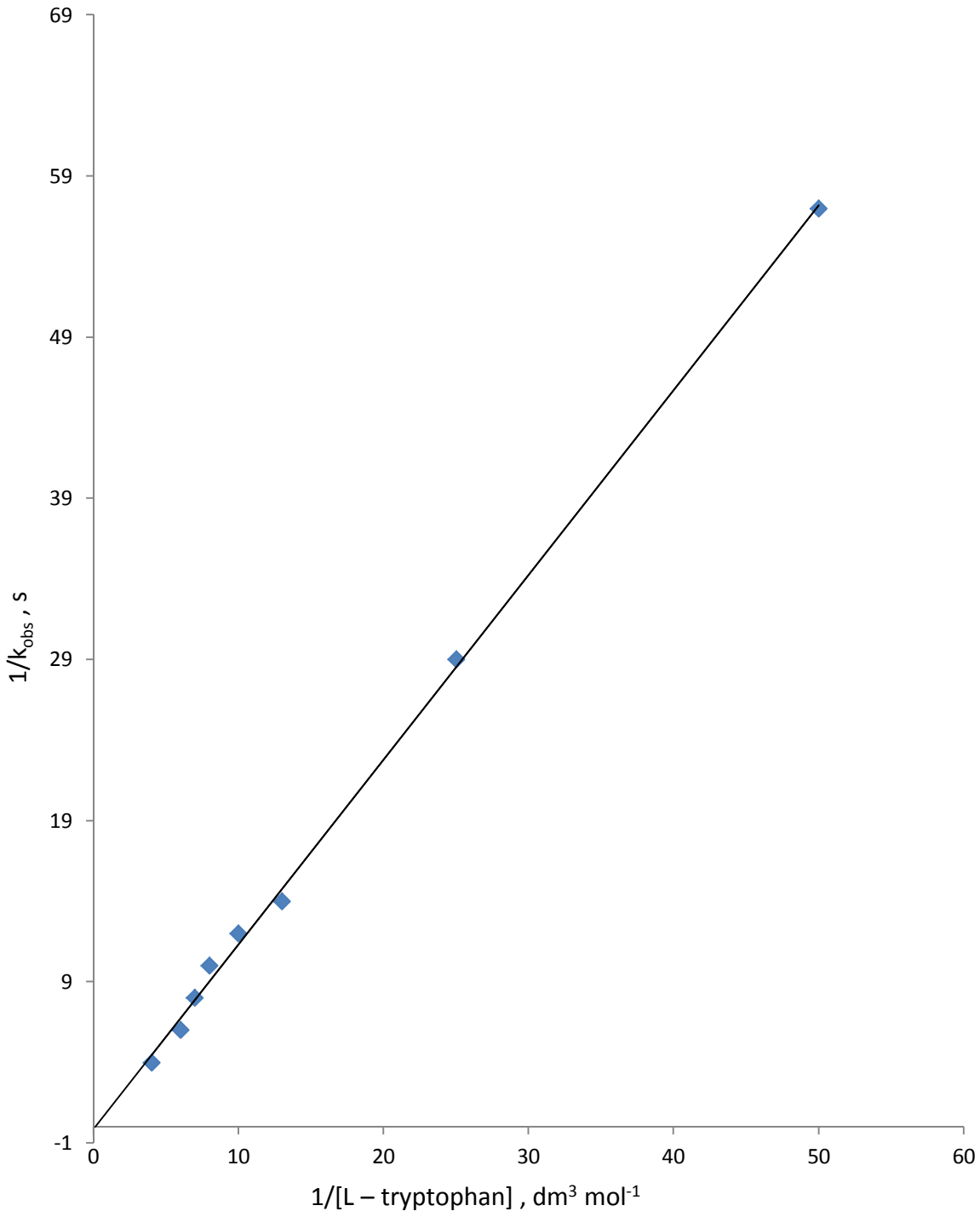


Figure 4.45: Michaelis – Menten plot of $1/k_{obs}$ versus 1/[L– tryptophan] for the redox reaction of permanganate ion and L– tryptophan

4.10 Product analyses

In all cases of the reactions of the reductants (nicotinic acids, L – cysteic acid, L – aspartic acid and L – tryptophan with MnO_4^-), a colourless solution was obtained as product at the end of the reaction, indicating that manganese(VII) was reduced by the reductants mentioned above. The organic product of the reaction in all the systems gave a yellow precipitate with 2,4-dinitrophenylhydrazine, confirming the presence of carbonyl group (aldehydes or ketones). The inorganic products of the reaction of MnO_4^- with all the reductants were qualitatively found to be Mn^{2+}. This was carried out by putting drops of the products of all the systems into a test tube and then dilute with some H_2SO_4 . KIO_4 was then added and warmed gently, purple colour was characteristically observed, signifying that Mn^{2+} has been reoxidized to MnO_4^-. It can be represented thus in an equation below (Glenn *et al*., 1952)

$$2Mn^{2+} + 5IO_4^- + 3H_2O \longrightarrow 2MnO_4^- + 5IO_3^- + 6H^+ \qquad (4.17)$$

Trioxosulphate(IV) was also qualitatively determined as an inorganic product in the reaction of MnO_4^- and L – cysteic acid. This was done by putting 1 cm^3 of the product into a test tube, then barium chloride solution was added. A white precipitate soluble in dilute HCl confirmed trioxosulphate(IV)

$$SO_3^{2-}{}_{(aq)} + BaCl_{2(aq)} \longrightarrow 2Cl^- + BaSO_{3\,(s)} \qquad (4.18)$$

white precipitate.

CHAPTER FIVE

5.0 DISCUSSION

5.1 Permanganate ion – nicotinic acid system

The stoichiometric studies showed that one mole of permanganate ion are consumed by one mole of nicotinic acid. A stoichiometry of 1:1 has also been reported for the oxidation of rosaniline hydrochloride by permanganate ion (Shallangwa *et al.*, 2006),oxidation of malachite green by permanganate ion (Mohammed *et al.*, 2009) and oxidation of methylene blue by permanganate ion (Osunlaja *et al.*, 2012).

Kinetics study showed first order with respect to both the oxidant and reductant. Similar order kinetics has been reported in reactions involving permanganate ion and aliphatic aldehydes (Banerji, 1973), permanganate ion and acetaldehydes (Iyun and Ajibade, 1992), permanganate ion and DL-alanine (Hassan, 1991), permanganate ion and L-asparagines (Zahedi and Bahrami, 2004) and permanganate ion and L-ascorbic acid (Babatunde, 2008).

The results of the acid dependence show that the rate constant increases with increase in $[H^+]$. Plot of $\log k_{obs}$ against $\log[H^+]$ gave a slope of 0.74±0.28, indicating that the reaction is first order with respect to $[H^+]$. Plot of k_2 against $[H^+]$ gave a straight line with an intercept. A graph of this nature indicates that two pathways, one which is acid dependent and the other which is acid independent were followed by the reaction. This suggests that both the protonated and unprotonated species are reactive. Results analogous to this were reported in the reaction between permanganate ion and L- ascorbic acid (Babatunde, 2008), permanganate ion and malachite green (Mohammed *et al.,* 2009), disodium 3,3-dioxobi-indolin-2,2'-ylidene-5,5'-disulphonate and heptaoxodichromate(VI) ion (Edokpayi *et al*., 2010).

The rate of reaction was found to decrease with increase in the ionic strength (Table4.1). The plot of $\log k_2$ against $I^{1/2}$ gave a negative slope of -1.07±0.4 indicating that the reaction showed a negative Bronsted – Debye salt effect (Figure 4.21), which therefore implies that at activated complex there is interaction of both cationic and anionic specie. The deviation of the slope from the whole number is probably due to other interactions that might have occurred in the reaction medium.

The catalysis of the reaction by the added anions and cations is possibly due to the coulombic bridging in which the closeness of approach of the reactant ions in the activated complex is such as to allow added ions to come in between them, thereby affecting the rates of reaction. This is seen when the reactions proceeding through the outer-sphere pathway in which the reactant ions maintain their coordination integrity in the activated complex prior to and during electron transfer (Sharpe, 1982).

The operation of outer-sphere mechanistic pathway in this reaction is further strengthened by the fact that there was lack of spectrophotometric evidence for the formation of intermediate complex as evidenced in the Michaelis Menten plot (Figure 4.42) which gave an intercept of zero.

On the basis of the above findings, the following reaction scheme is proposed for this reaction.

$$NA + H^+ \underset{}{\overset{K}{\rightleftharpoons}} NAH^+ \qquad (5.1)$$

$$NA + MnO_4^- \xrightarrow[slow]{K_1} NAH//\ MnO_4^- \qquad (5.2)$$

$$NAH^+ + MnO_4^- \xrightarrow[slow]{k_2} NAH^+//\ MnO_4^- \qquad (5.3)$$

$$NA//\ MnO_4^- \xrightarrow{k_3} Products \qquad (5.4)$$

$$NAH^+//\ MnO_4^- \xrightarrow{k_4} Products \qquad (5.5)$$

Equations (5.2) and (5.3) are the rate determining steps

$$\text{Rate} = k_1[NA][MnO_4^-] + k_2[NAH^+][MnO_4^-] \quad (5.6)$$

Substituting for $[NAH^+]$ in equation (5.6)

$$\text{Rate} = (k_1 + k_2K[H^+])[MnO_4^-][NA] \quad (5.7)$$

Equation (5.7) is similar to equation (4.9),

where and b = k_2K, a = $k_1$and a = 1.60×10^{-2} $dm^3mol^{-1}s^{-1}$ and b = $1.57dm^6mol^{-2}s^{-1}$.

Equation (5.3) is consistent with the fact that the activated complex involves an anionic and a cationic species, in line with the negative salt effect obtained from the empirical kinetic data. Also equations (5.1, 5.2 and 5.3) depict that, there are two pathways, ie the acid dependent and acid independent pathways, which results in the rate law in equation (5.7).

5.2 Permanganate ion – L-cysteic acid system

The result of stoichiometry study showed that two moles of MnO_4^- reacted quantitatively with five moles of L – cysteic acid. This is in accordance with what has been reported for the redox reaction of MnO_4^- with some aldehydes (Banerji, 1973), acetaldehydes (Iyun and Ajibade, 1992), DL-alanine (Hassan, 1991), and L-phenyl alanine (Insauti *et al.*, 1995).

Kinetic studies indicated first order dependence of the rate on $[MnO_4^-]$ and [L-cysteic acid] respectively. Thus at $[H^+]$ = 0.1 mol dm^{-3} and 27.0±1.0^oC, the rate equation is as shown by equation (4.6). Under experimental condition employed k_2 was found to be (5.49 ± 0.07) x 10^{-2}mol dm^{-3}.

A plot of $\log k_2$ versus $I^{1/2}$ (Figure 4.22) showed that rate constant decreases with increase in ionic strength. This implies that both species at the activated complex are of opposite charges and the product of their charges is -0.60±0.29. The value of the slope -0.60±0.29 is an indication that some other interactions like parallel reactions, ion-ion pair

interactions might have taken place to account for the non-integral value of the slope. Similar results were reported by earlier researchers (Iyun and Tinuoye, 1988; Ayoko *et al.*, 1991b; Onu and Iyun, 2000; Idris *et al.*, 2005).

From the results in (Table 4.2), it is observed that, the rate constants of the reaction increased with increase in acid concentration. The plot of $\log k_{obs}$ versus $\log[H^+]$ gave a slope of 1.02±0.4, indicating that the order with respect to $[H^+]$ is one. The plot of k_2 versus $[H^+]$ was linear with no intercept (Figure 4.16).The acid dependent rate constant k_2 is given by equation(4.11).

The nature of acid dependence from the graph implies that there exist a rapid equilibrium between protonated and unprotonated forms of the reductant prior to the rate determining step and only protonated form is reactive and the reaction followed only one pathway. This is apparent in equation(4.13). Similar results were obtained by Iyun and Onu (1998) for oxidation of rosaniline monochloride by nitrite ion, Idris *et al.,* (2005) for electron transfer reaction of butan-1,3-diol and Cr(VI) in aqueous acidic medium and Edokpayi *et al.,* (2010) in the oxidation of disodium 3,3-dioxobi-indolin-2,2'-ylidene-5,5'-disulphonate by heptaoxodichromate(VI) ion in aqueous acidic medium.

The reaction was catalysed by added cations and anions, (Table 4.7). Catalysis of the rate by added ions is probably the characteristics of reaction that occur through outer-sphere mechanistic pathway.

Spectroscopic evidence and Michaelis Menten's plot of $1/k_{obs}$ versus 1/[L - cysteic acid] (Figure 4.43) suggest that intermediate may be unimportant in the rate determining step.

On the basis of the above findings, the mechanism below is proposed for this reaction.

$HR\square H + H^+ \xrightleftharpoons{K} HR\square H_2^+$ (5.8)

$MnO_4^- + HR\square H_2^+ \xrightarrow[slow]{k_1} R\square + HmnO_3 + H_2O$ (5.9)

$MnO_4^- + H^+ \xrightarrow[fast]{k_2} HmnO_4$ (5.10)

$HmnO_3 + HmnO_4 + 4HR\square H + 4H^+ \xrightarrow{k_3} 4R\square + 2\,Mn^{2+} + 7H_2O$ (5.11)

Equation (5.9) is the rate determining step.

$Rate = k_1[MnO_4^-][HR\square H_2^+]$ (5.12)

From equation (5.8), substitute for $[HR\square H_2^+]$ in equation (5.12)

$Rate = k_1K[H+][MnO_4^-][HR\square H]$ (5.13)

Equation (5.13) is analogous to equation (4.11), the observed rate law,

where $k_2K = c$ and $c = 5.4x10^{-1}dm^6mol^{-2}s^{-1}$.

The rate determining step (equation 5.9) concurred with an empirical results by substantiating the occurrence of the negative salt effect obtained in the empirical results.

Equation (5.14) also displayed high level of consistency with the nature of acid dependence obtained in empirical results. The plot of the second order rate constant as a function of $[H^+]$ gave a linear plot without any intercept, which depict that the mechanism followed one pathway.

5.3 Permanganate ion – L-aspartic acid system

The result of stoichiometry studies showed that for every two moles of MnO_4^- reduced five moles of L – aspartic acid were oxidized according to equation (4.3). This result is consistent with what has been reported by earlier researchers (Barneji, 1973; Hassan, 1991; Iyun and Ajibade, 1992; Insauti *et al.*, 1995).

The observed first order dependence of the rate of reaction on both [MnO_4^-] and [reductant] was earlier reported by the oxidation of glutamic acid (Hussein and Ahmad,1989), mandelic acid (Panari *et al.*, 1998), pantothemic acid (Desai *et al.*, 2002), sugar (Latona, 2004), L-ascorbic acid (Babatunde, 2008) and malachite green (Mohammed *et al.*, 2009) by permanganate ion.

The second order rate constant was determined as a function of [H^+] in the range $5x10^{-2} \leq [H^+] \leq 3x10^{-1}$ mol dm^{-3} and the results presented in Table (4.3). The nature of the acid dependence observed can be fitted into equation (4.10). It shows that parallel reactions of protonated and unprotonated species of L – aspartic acid occurred. The second order [H^+] dependent term was rationalized in term of the pre-equilibrium protonation of L – aspartic acid.

A plot of $logk_2$ versus $I^{1/2}$ (Figure 4.23) showed that rate constant increases with increase in ionic strength within concentration range studied. The positive salt effect observed for the reaction showed the interaction of the like charges in the activated complex (Wilkins, 1974). This agrees with equation (5.16) in the reaction schemes, Babatunde(2008) obtained similar result in the oxidation of L-ascorbic acid by permanganate ion. Least square analysis of Michaelis – Menten plot gave intercept which showed that inner-sphere mechanism is likely involved in the reaction and there was no shift in the λ_{max} of the spectrum of the reaction.

Added anion (NO_3^-) inhibited the rate constant of the reaction whereas added cations enhanced the rate constant. This suggests that substitution of the reactants into their inner co-ordination shell did not preceed electron transfer.

The plausible mechanism for this reaction is

$$H_2P + 2H^+ \underset{}{\overset{K}{\rightleftharpoons}} H_2PH_2^{2+} \quad (5.15)$$

$$MnO_4^- + H_2P \xrightarrow[\text{slow}]{k_1} P + MnO_3^- + H_2O \quad (5.16)$$

$$MnO_4^- + H_2PH_2^{2+} \xrightarrow[\text{slow}]{k_2} P + HMnO_3 + H_2O + H^+ \quad (5.17)$$

$$MnO_3^- + H^+ \xrightarrow[\text{fast}]{k_3} HMnO_3 \quad (5.18)$$

$$2HMnO_3 + 3H_2P + 4H^+ \xrightarrow{k_4} 3P + 2Mn^{2+} + 6H_2O \quad (5.19)$$

Therefore,

$$\text{Rate} = k_1[MnO_4^-][H_2P] + k_2[MnO_4^-][H_2PH_2^{2+}] \quad (5.20)$$

From equation (5.15), substitute for the protonated species $H_2PH_2^{2+}$ in equation (5.20).

$$\text{Rate} = (k_1 + k_2K[H^+]^2)[H_2P][MnO_4^-] \quad (5.21)$$

Equation (5.21) can be compared with equation (4.10): the observed rate law.

where $a = k_1$, $a = 4.0 \times 10^{-3}$ $dm^3mol^{-1}s^{-1}$and $b = k_2K$, $b = 7.58 \times 10^{-1}$ $dm^6mol^{-2}s^{-1}$.

The positive salt effect obtained from experimental result is depicted by equation (5.16). Similar mechanism was proposed when MnO_4^- reacted by L–ascorbic acid (Babatunde, 2008).

5.4 Permangante ion – L – tryptophan system

The stoichiometric of the permanganate ion – L-tryptophan system showed that one mole of permanganate ion was consumed by one mole of L-tryptophan which is consistent with equation(4.4). Similar stoichiometry has also been reported for the oxidation of rosaniline hydrochloride by permanganate ion (Shallangwa *et al.*, 2006), oxidation of

malachite green by permanganate ion (Mohammed *et al.*, 2009) and oxidation of methylene blue by permanganate ion (Osunlaja *et al.*, 2012).

Kinetics studies of the reaction are first order with respect to permanganate ion and first order with respect to L-tryptophan as well. The order of one obtained with respect to L-tryptophan is consistent with the order of one obtained by earlier researchers when amino acids such as DL-alanine (Hassan, 1991), L-asparagines (Zahedi and Bahrami, 2004), glutamic acid (Hussein and Ahmad, 1989), L- arginine (Moghadasi *et al.*, 2001) were oxidized by permanganate ion.

The results of the acid dependence show that the rate constant increases with increase in $[H^+]$. Plot of $\log k_{obs}$ against $\log[H^+]$ gave a slope of 0.70±0.3, indicating that the reaction is approximately first order with respect to $[H^+]$. Plot of $k_2$against $[H^+]$ gave a straight line with an intercept. The acid dependence studies indicated both acid independent and acid dependent pathways with the protonated and unprotonated species being reactive. Results analogous to this were reported in the redox reaction between permanganate ion and L- ascorbic (Babatunde, 2008), permanganate ion and malachite green (Mohammed *et al.,* 2009),disodium3,3-dioxobi-indolin-2,2'-ylidene-5,5'-disulphonate and heptaoxodichromate(VI) ion (Edokpayi *et al*., 2010).

The redox reaction show negative salt effect with the rate decreasing with increase in ionic strength from 0.4 – 1.0 mol dm^{-3} (Table 4.4). The plot of $\log k_2$ versus $I^{1/2}$ (Figure 4.24) gave a straight line with a slope of -0.42±0.22. This observation of negative Debye-Bronsted salt indicates that at the activated complex, there exist cationic and anionic species. The rate constants also decrease with decrease in the dielectric constant of the reaction medium (Table 4.11).

The observed catalytic effect on the second order rate constant as a result of added cations and anions depicts that, the reaction is operating through the outer-sphere mechanism (Penninton and Haim, 1967; Przystas and Sutin, 1973; Adegite *et al.*, 1977). The inhibition of the rate by anion shows that the reactant molecules are not bonded in the activated complex.

Analysis of Michaelis – Menten plot gave no intercept (Figure 4.45). This suggests the absence of intermediate complex formation.

A plausible mechanism consistent with an empirical results is proposed as;

$$LT + H^+ \overset{K}{\rightleftharpoons} LTH^+ \quad (5.22)$$

$$LTH + MnO_4^- \xrightarrow[slow]{k_1} LT//MnO_4^- \quad (5.23)$$

$$LTH^+ + MnO_4^- \xrightarrow[slow]{k_2} LTH^+//MnO_4^- \quad (5.24)$$

$$LT//MnO_4^- \xrightarrow[fast]{k_3} Products \quad (5.25)$$

$$LTH^+//MnO_4^- \xrightarrow{k_4} Products \quad (5.26)$$

Equations (5.23 and 5.24) are the rate determining steps.

$$Rate = k_1[LT][MnO_4^-] + k_2[LTH^+][MnO_4^-] \quad (5.27)$$

Substituting for $[LTH^+]$ in equation (5.27),

$$Rate = (k_1 + k_2K[H^+][LT][MnO_4^-] \quad (5.28)$$

Equation (5.28) is similar to equation (4.10)

where $a = k_1 = 1.70x10^{-1}$ dm^{-3} mol^{-1} s^{-1}, $b = k_1K = 6.85$ dm^6 $mol^{-2}s^{-1}$.

The negative salt effect displayed by the reaction is depicted by equation (5.24), on the ground that positively and negatively charges reacted at the rate determining step. The mechanism of the reaction is the one that involve two pathways which are the acid dependent and acid independent pathways.

5.5 Summary and conclusion

The redox reactions of permanganate ion were studied with nicotinic acid and some amino acids (L-cysteic acid, L-aspartic acid, L-tryptophan). The stoichiometry of 1:1 was observed for MnO_4^- : nicotinic acid and MnO_4^- : L-tryptophan systems while the stoichiometry of 2:5 was observed for MnO_4^- : L-cysteic acid and MnO_4^- : L-aspartic acid systems. The order of the reaction with respect to both oxidant and reductants was first and second order overall in all the systems investigated. The rates of the reactions showed three forms of acid dependence. These are:

(i) First order positive acid dependence with an intercept for MnO_4^-– nicotinic, L-tryptophan reactions.

(ii) First order positive acid dependence without an intercept for MnO_4^- – L-cysteic acid reaction.

(iii) Second order positive acid dependence with an intercept for MnO_4^- – L-aspartic acid reaction.

The reactions therefore conforms to the following rate laws

$$-\frac{d}{dt}[MnO_4^-] = (a + b[H^+])[MnO_4^-][\text{nicotinic acid}]$$

where a = 1.6×10^{-2}dm^{3}mol^{-1}s^{-1} and b = 1.57dm^{6}mol^{-2}s^{-1} at T = 28.0$\pm$ 1.0^{0}C.

$$-\frac{d}{dt} = (c[H^+][MnO_4^-][L-\text{cysteic acid}]$$

where c = 5.4×10^{-1}dm^{6}mol^{-2}s^{-1} at 27.0±1.0^{o}C.

$$-\frac{d}{dt}[MnO_4^-] = (a + b[H^+]^2[MnO_4^-][L-\text{aspartic acid}]$$

where a = 4.0×10^{-3} dm^{-3}mol^{-1}s^{-1} and b = 7.58×10^{-1}dm^{6}mol^{-2}s^{-1} at 29.0±1.0^{o}C

$$-\frac{d}{dt}[MnO_4^-] = (a + b[H^+])[MnO_4^-][L-\text{tryptophan}]$$

where a = $1.7x10^{-1}$ $dm^{-3}mol^{-1}s^{-1}$ and b = $6.85dm^{6}mol^{-2}s^{-1}$ at 28.0±1.0°C

The relationship of k_2 to the rate laws and its respective values for all the systems studied can be represented thus;

Rate $=k_2[MnO_4^-][reductant]$

where 'reductant' = nicotinic acid, L-cysteic acid, L-aspartic acid and L-tryptophan.

The respective values of rate constants with regard to each reductant are given as;

k_2 (nicotinic acid) = $(1.72 \pm 0.015)x10^{-1}dm^3mol^{-1}$ s^{-1},

k_2 (L-cysteic acid) = $(5.49 \pm 0.07)x10^{-1}dm^3mol^{-1}$ s^{-1},

k_2 (L-aspartic acid) = $(3.50 \pm 0.06)x10^{-2}dm^3mol^{-1}$ s^{-1} and

k_2 (L-tryptophan) = $(8.75 \pm 0.14)x10^{-2}dm^3mol^{-1}$ s^{-1}.

The rate of the reaction displayed negative salt effect for the permanganate ion – nicotinic acid, L-cysteic acid and L-tryptophan reactions indicating, the involvement of anionic and cationic species at activated complex, but positive salt effect for permanganate ion – L-aspartic acid reaction, showing that like charges are present at activated complex.

There was catalysis of the reaction's rate by added anion and cations in all the system studied, this indicates the present of outer-sphere electron transfer in all the systems. Free radicals formation was not observed for any of the reactions. The results of spectroscopic investigations and Michaelis – Menten analysis showed no evidence of intermediate complex formation in all the system investigated, except in MnO_4^- – L-aspartic system, in which there was an intercept. From the empirical results obtained, the reactions of permanganate ion with all the reductants investigated probably occur by outer-sphere Smechanistic pathways. Consequently the proposed plausible mechanisms are consistent with all the empirical kinetic data were proposed for all the systems investigated.

5.6 Recommendations

Kinetics and mechanisms of oxidation of amino acids have been well explored and exploited, with different oxidizing agents. Many literatures have also reported on the oxidation of many substrates ranging from organic to inorganic by permanganate ion. It is therefore recommended that:

(a) MnO_4^- should also be used as an oxidant in basic medium since acidic medium has received considerable attention.

(b) Permanganate ion with different buffer in alkaline and acidic medium should be exploited for the oxidation of amino acids.

(c) Computational Chemistry programs should also be employed in the study of the kinetics and mechanism of several reactions in chemistry and compare the result with the spectrophotometric method.

References

Adegite, A., Iyun J.F. and Ojo, J.F. (1977). Kinetics and mechanism of electron transfer reaction between uranium(III) and some ruthenium(III) ammines complexes. *Journal Chemistry Society, Dalton Transaction,* 115.

Ahmed, G.A., Khairu, K.S. and Hassan, R.M. (2003). Kinetics of oxidation of chitosan as polysaccharide by permanganate in aqueous perchloric media. *Journal of Chemical Research,*4 (1): 182-183.

Anders, L. and Karl, F. (1988). The reaction of pyridine carboxylic acids with dicyclohexylcarbodiimide and p-nitrophenol. *Acta Chemica Scandinavica,* (42):408-410.

Ayoko, G.A., Iyun, J.F. and El- Idris I.F. (1991a). Electron transfer at tetrahedral cobalt(II) part I. Kinetics of bromate ion reduction. *Transition Metal Chemistry*, 16: 145-148.

Ayoko, G.A., Iyun, J.F. and El-Idris I.F. (1991b). Electron transfer at tetrahedral cobalt(II). Part II. Kinetics of silver(I) ion catalysed reduction of peroxydisulphate. *Transition Metal Chemistry,* 17:46-49.

Babatunde, O.A. (2008). A study of the kinetics and mechanism of oxidation of L – ascorbic acid by permanganate ion in acidic medium. *World Journal of Chemistry,* 3(1):27-31.

Banerji, K.K. (1973). Kinetics and mechanism of oxidation of aliphatic aldehydes by permanganate. *Indian Journal of Chemistry,* 11:242.

Basolo, F. and Johnson, R.C. (1964). *The Chemistry of Metal Complexes*. Benjamin Inc, New York, PP. 34-60.

Basolo, F. and Pearson, R.G. (1967). *Mechanism of Inorganic Reactions 2nd Edition*. John Wiley, New York, PP. 454-525.

Beattie, J.K. and Basolo, F. (1971). The two-election inner-sphere reduction of chloropentammine platinum(IV) ion by aguochronmium(II) ion. *Inorganic Chemistry,* 10:486.

Bell, C., Abrams, J. and Nutt, D. (2001). Tryptophan depletion and its implication. *Brain Journal of Psychiatry,* 178:399-405.

Burgess, J. (1978). *Metal ion in solution, first edition.* Ellis Horwood Limited. pp 417-433.

Caldin, E.F. (1974). *Fast Reactions in Solution.* Wiley New York, PP. 1-34.

Campion, R.J., Purdie, N. and Sutin, N. (1964). Kinetics of electron transfer reactions. *Inorganic Chemistry,* 3:1091-1094.

Candlin, J.P. and Halpern J. (1965). Volumes of activation of some electron transfer reaction *Inorganic Chemistry,* 4: 1086-1089.

Candlin, J.P. Halpern, J. and Trimm, D.L. (1964). Kinetics of the reduction of some Co(III) complexes by Cr(II), V(II) and Eu(II). *Journal of American Chemical Society,* 86, 1019.

Candlin, J.P. Taylor, K.A. and Thompson, D.T. (1968). *Reactions of Transition Metal Complexes.* Elservier Publ. C. Amsterdan, PP. 157-214.

Capuzzi, D.M., Morgan, J.M., Brusco, O.A. and Intenzzo, C.M. (2000). Niacin dosing: relationship to benefits and adverse effects. *Current Atherosclerosis Report,* 2(1):64-71.

Christenson, R.J. and Espenson, J.H. (1970). Rate of reduction of some Co(III) and Cr(III) complexes by Ytterbium(II). *Journal of Chemical Society, Dalton Transactions,* 12: 756-757.

Connick, E.R. and Poulson, E.R. (1959). Effect of paramagnetic ions on the Nuclear Magnetic Resonance of O_{17} in water and the rate of elimination of water molecules from the first coordination sphere of cations. *Journal of Chemical Physics,* 30: 759.

Cooke, D.O. (1979). *Inorganic Reaction Mechanism.* Allard and son Ltd. Dorking, PP. 1-38.

Cotton, F.A. and Wilkinson, G. (1980). *Advanced Inorganic Chemistry. A Comprehensive text. 4th edition.* John Wiley and Sons, New York, PP. 1183-1215.

Crimi, M. L. and Siegnst, R.L. (2004). Impact of reaction condition on MnO_2. Genesis during permanganate oxidation. *Journal of Environmental Science and Engineering,* 130 (5):562-572.

Cullis, C.F. and Ladbury, J.W. (1955). Kinetics studies of oxidation of aromatic compounds by potassium permanganate part I, II and III. *Journal of Chemical Society Dalton Transactions,* 555, 1407, 2850.

Denis, W. (1911). Oxidation of the amino acids II: alanine and tyrosine. *This Journal,* 9: 73-76.

Desai, S.M., Halligudi, N.N., Mavalangi, S.K. and Nandibewoor, S.T. (2002).Kinetics of oxidation of pantothemic acid by permanganate in aqueous alkaline medium. *Journal of Physical Organic Chemistry,* 216 (6):803.

Edopkayi, J.N., Iyun, J.F. and Idris, S.O. (2010). The Kinetics of the oxidation of disodium 3,3-dioxobi-indolin-2,2'-ylidene-5,5'-disulphonate by heptaoxodichromate(VI) ion in aqueous acidic medium. *Archives of Applied Science Research,* 2(5):126-134.

Edwards, J.O. (1964). *Inorganic reaction mechanisms.* W.A. Benjamin Inc. New York, PP.1-124.

Eigen, M. and Maeyer, D.L. (1963). *Techniques of Organic Chemistry (Friess, S.L, Lewis E.S and Weissberger A, Eds)* Interscience New York, PP. 895.

Espenson, J.H. (1965). Kinetics of the reaction of vanadium(III) and chromium(II) ions in acid solution. Evidence for a binuclear reaction intermediate. *Inorganic Chemistry,* 4(7):1025-1029.

Frank, L.S. and Leslie, B.C. (1997). Reductive dechlorination of a 2- chloronicotinic acid under Finkelstein conditions. *Journal of Arkansas Academy of Science, 51:212.*

Gibson, S.N. (2010). Oxidation of pharmaceuticals and personal care products by permanganate: *a thesis presented to the academic faculty, for the award of Master of Science in Environment Engineering in the School of Civil and Environment Engineering Georgia Institute of Technology, U.S.A.*

Glenn, R., Hayes, A.M and Dons, S.M (1952) Kinetics of periodate oxidation of manganese to permanganate. *Journal of American Chemical Society,* 74(1):15-20.

Green, M. and Sykes, A.G. (1970). Evidence of one and two electron paths in the reaction of vanadium(II) with Mercury(II). *Chemical Communications,* 241.

Greenwood, N.N. and Earnshaw, A. (1997). *Chemistry of the Elements 2nd edition* Oxford: Butherworth Heinemann. Pp 182-189.

Hassan, R.M. (1991). Kinetics and mechanism of oxidation of DL-alanine by permanganate ion in acidic perchlorate media. *Canadian Journal of Chemistry,* 69:2018-2023.

He, D., Guan, X.H., Ma, Yum. (2009). Influence of different nominal molecular weight fractions of humic acid on phenol oxidation by permanganate. *Environmental Science and Tech*nology, 43:8332-8337.

Hirmath, G.A., Timmanagoudar, P.L. and Nandibewoor, S.T. (1996). Kinetics of oxidation of thalium(I) by permanganate in aqueous Hydrochloric acid medium using the stopped flow techniques. *Transition Metal Chemistry,* 21:560.

Holleman, A.F. and Wiberg, E. (2001). *"Inorganic Chemistry"* Academic. Press San Diego, PP. 67-69.

Huang, K.C., Hoag, G.E., Chheda, P., Woody, B.A. and Dobbs, G.M. (2001). Oxidation of chlorinated ethene by potassium permanganate. *Journal of Hazardous Materials,* 87 (1):155-169.

Hubbard, C.D., Gerhard, A. and Van Eldik, R. (1991). Oxidation of dihydroxyl aromatic substrate by hexachloroiridate(iv): Mechanistic information from volume of activation. *Inorganic Chemistry,* 80:5023-5030.

Hussein, M.Y. and Ahmad F. (1989). A comparative kinetic and mechanistic study of glutamic acid oxidation by acid permanganate in the absence and presence of sodium dodecyl sulphate. *Transition Metal Chem*istry, 14:169-174.

Huchital, D.H and Wilkins, R.G.(1967). Intermediates formed in the reaction of ethylene diammine tetraacetate cobaltate(11) with ferricyanide ions. *Inorganic Chemistry,* 6(5):1022-1027.

Idris, S.O., Iyun, J.F. and Agbaji, E.B. (2005). Electron transfer reaction of butan-1,3-diol and Cr(VI) in aqueous acidic medium. *Nigerian Journal of Chemical Research,* 10:16-22.

Ikeda, M., Tsuji, H., Nakamura, S., Ichiyama, A., Nishizuka, Y. and Hayaishi, O. (1965). A role of picolinic carboxylase in the biosynthesis of nicotinamide adenine dinucleotide from tryptophan in mammals. *Biological Chemistry,* 240(3):1395-1401.

Insauti, M.J., Mata-Perez, F. and Alvare- Macho, (1995). Kinetic study of oxidation of L-plenyl alanine by potassium permanganate in acid medium. *International Journal of Chemical Kinetics,* 27,507.

Isied, S.S. and Taube, H. (1973). Rates of intramolecular electron transfers. *Journal of American Chemical Society,* 95:8198.

Iyun, J.F and Ajibade, F. (1992). The kinetics and mechanism of oxidation of acetaldehyde, by dichromate and permanganate ions in agueous acidic solution. *Journal of Chemical Society of Nigeria,* 17,35.

Iyun, J.F, and Adeyanju, A.O. (2004). Kinetics and mechanism of the oxidation of DL-methionine by chromium(VI) in aqueous acidic media. *Chem Class Journal,* 185-188.

Iyun, J.F. (1982). Kinetics and mechanism of the oxidation reduction of some metal ion complexes in acid solution. Ph.D thesis. Ahmadu Bello University, Zaria-Nigeria.

Iyun, J.F. and Onu, A.D. (1998). Kinetics and mechanism for oxidation of rosalinine monochloride by nitrite ion in aquous media. *Nigerian Journal of Chemical Research*, 3:24-27.

Iyun, J.F. and Tinuoye, E.O. (1988). Chromium(VI) oxidation of L-cysteine. *Chem Class Journal,* 56-59.

Jiang, J., Pang, S.Y. and Ma, J. (2009). Oxidation of triclosan by permanganate(VII). Importance of ligands and *in situ* formed manganese Oxides. *Environmental Science and Technology,* 42(21):8326-8331.

Kolb, K.E. (1986). Oxidation of cyclohexane, cyclohexene and cyclohexanol by permanganate in alkaline medium *Journal of Chemistry Education*, 63:977.

Ladbury, J.W. and Cullis, C.F. (1959).Oxidation by permanganate: The development of the reaction with time. *Journal of Chemical Society of India,* 1010.

Laguna, J. and Carpenter, K.J. (1951). Raw versus processed corn in niacin deficient diet. *Journal of Nutrition,* 45(1):21-28.

Latimer, M.W. (1952). *The oxidation states of elements and their potentials in aqueous solution.* Prentice Hall, Eagle Chiffs, New Jersey, PP. 78.

Latona, D.F. (2004). Kinetics of oxidation of sugar in alkaline permanganate and chromic acid media. *Journal of Chemical Society of Nigeria,* 29(1):5-7.

Lehninger, E., Albert, L., David, L. and Michael, L. (2000). *Principles of Biochemistry (3rd edition)*. New York, W.H. Freeman, pp 153-156.

Leuchtenberger, W., Huthmacher, K. and Drauz, K. (2005). Biotechnological production of amino acids and derivatives: current status and prospects". *Appl*ied *Micrbio*logy and *Biotechtechnology,* 69(1):1-8.

Lohdip, Y.N. and Iyun, J.F. (1993). Kinetics studies of oxidation of acetaldehyde with bromate in aqueous perchloric acid. *Journal of Chemical Society of Nigeria,* 18, 61-64.

Marcus R.A. (1956). Theory of oxidation reduction reaction involving electron transfer (I) *Journal of Chemical Physics,* 24:966-978.

Marcus, R.A., Zwolinski, J.B. and Eyring, H. (1954).The electron tunneling hypothesis for exchange reactions. *Journal of Chemical Physics,* 58:432 .

Mc Auley, A. and Hill, J. (1969). Kinetics and mechanism of metal complex formation in solution. *Quarterly Review, 23* (1) 18-36.

Meyer, J.T. and Taube, H. (1987). Electron transfer reactions. In Wilkinson G.(Ed) *Comprehensive Coordination Chemistry,* 1:331-380

Michael, C., Lehninger, L. and Nelson, D.R. (2000). *Lehninger principles of Biochemistry.* New York: Worth Publishers, PP. 153-156.

Mittal, M.K., Florin, T., Perrone, J., Delgado, J.H. and Osterhoudt, K.C. (2007). Toxicity from the use of niacin to beat urine drugs screening. *Annals of Emergency Medicine* 50 (5):587-590.

Moghadasi, M., Rashidid, N. and Iloukhani, H. (2001). Oxidation of L – arginine by manganese(VII) in concentrated sulfuric acid medium. *Physics and Chemistry of Liquids,* 39: 267-275.

Mohammed, Y., Iyun, J.F. and Idris, S.O. (2009). Kinetic approach to the mechanism of the redox reaction of malachite green and permanganate ion in aqueous acidic medium. *African Journal of Pure and Applied Chemistry* 3(12) :269-274.

Onu, A.D. and Iyun, J.F. (2000). Redox kinetics of monomethyl fuchsin by dithionite ion in aqueous hydrochloric acid. *Nigerian Journal of Chemical Research* 5:33-36.

Orhanovic, M. and Earley, J.E. (1975). Kinetics of reduction of pentaamine chlorocobalt(II) and cis- and trans-bis (1,2-ethanediammine) dichlorocobalt(I) by titanium(III). *Inorganic Chemistry,* 14: 1478.

Osunlaja. A.A., Idris, S.O and Iyun J.F (2012) Kinetics and mechanism of methylene blue-permanganate ion reaction in acidic medium. *Archives of Applied Science Research,* 4(2) :772-780.

Pallaghy, P.K., Melinikova, A.P., Jimenez, E.C., Olivera, B.M. and Norton, R.S. (1999). Solution structure of contryphan "R" a naturally occurring disulfide bridged octapeptide containing D-tryptophan. *Journal of Biochemistry*, 38 (35):1155-1159.

Panari, R.G., Chougale, R.B. and Nandibewoor, S.T. (1998). Kinetics of Oxidation of mandelic acid (MA) by permanganate in aqueous alkaline medium. *Journal of Physical Organic Chemistry,*11 (7):448-454.

Parker, R., Brunton, L., Gilman, S., John, S., and Gilman, A, (2006). *Goodman and Gilman's the Pharmacological Basis of Therapeutics.* New York: McGraw-Hill, PP. 215- 218.

Pearson, G.R. and Buch, T. (1962). Electron paramagnetic relaxation in ionic solutions. *Journal of Chemical Physics* 36: 1277.

Penninton, O.E. and Heim, A. (1967). Kinetics and mechanism of chromium(II) catalysed – substitution of iodine ion in iodo – pentaaquo chromium(III) ion by water, fluoride chloride and bromated ion. *Inorganic Chemistry,* 6:2138.

Pitsavas, S., Andreou, C., Bascialla, F., Vasilis, P.B. and Karavatos, A. (2004). Pellagra encephalopathy following B-complex vitamin treatment without niacin. *International Journal of Psychology and Medicine,* 31(1):91-96.

Platzman, R.L. and Franck, J. (1954). Hydration configuration in electron transfer processes involving ions in aqueous solution. *Chemical Abstract,* 48, 13364.

Prakash, R., Gandora, S., Singh, L.K., Das, B. and Lakra, A. (2008). Rapid resolution of delusional parasitosis in pellagra with niacin augmentation therapy. *General Hospital Psychology,* 30(6):581-584.

Przytas, T.J. and Sutin, N. (1973). Kinetic studies of anion assisted outer sphere electron – transfer reaction. *Journal of American Chemical Society,* 95:5545 – 5555.

Rajanna, K.C., Lakshmi, P.J. and Saiprakash, P.K. (1996). Mechanism of oxidation of irons (II) chelates by heptavalent manganese in aqueous sulfuric acid and micellar media: a kinetic approach. *Transition Metal Chemistry,* 21:135.

Rao, K.V., Roa, M.T. and Adinarayana (2004). Kinetics of oxidation of some monosaccharide by permanganate in aqueous alkaline medium. *International Journal of Chemical Kinetics,* 27(6):55-60.

Rao, V.S., Sethuran, B. and Rao, T.N. (1979). Kinetics of oxidation of some aminoacids by $KMnO_4$ in a moderately concentrated H_2S0_4 medium, in the presence and absence of Ag^+. *International Journal of Chemical Kinetics,* 11, 165.

Rawalay, S.S. and Shechter, H. (1967). Oxidation of primary, Secondary and tertiary amines with neutral permanganate: Simple method for degrading amines to aldehydes and ketones. *Journal of Organic Chemistry.* 32 (10):3129-3131.

Shallangwa, G.A., Iyun, J.F. and Harrison, G.F.S. (2006). Mechanism of oxidation of rosaniline hydrochloride part II. Kinetic of redox reaction with heptavalent manganese in acidic medium. *Chem Class Journal,* 3: 91-95.

Sharma, K., Ashok, P., Punit, K. and Gupta, K.S. (2008). Comparative rate study on the oxidation of nicotinamide and isonicotinamide by permanganate in acidic medium. *Indian Chemical Society.*85 (9):920-925.

Sharpe, A.G. (1982). *Inorganic Chemistry*. First edition Longman, London, PP. 518-534.

Shea, H. and Haim, A. (1973). Adjacent attack in redox reaction between penta-amine cobalt(iv). *Inorganic Chemistry,*12: 3013.

Simmons, W.J. and Meisenberg, G. (2006). *Principle of medical biochemistry*. Mosby Elsevier, PP. 19.

Song, C., Chen, L. and Shan, J. (2008). Kinetics and mechanism of oxidation of leucine and alanine by Ag (III) complex in alkaline medium. *Research Letter in Inorganic Chemistry Article* 1D, 786857. 4.

Sridevi, G. and Vani, P. (2010). Kinetics and mechanism of oxidation of L-arginine by sodium ion periodate in alkaline medium. *Research Journal of Pharmaceutical, Biology and Chemical Science,* 1 (4):977-986.

Stewart, R. (1965). *Oxidation by Permanganate. In Oxidation in Organic Chemistry.* Wiberg, K.B. Academic Press New Haven, CT Vol. 5, PP. 168.

Stewart, R. and Mocek M.M. (1963). The mechanisms of permanganate oxidation of fluoral hydrate. *Canadian Journal of Chemistry*. 41, 1160.

Stryer, L., Berg, J.M., Tymoczko, J.L. (2002). *Biochemistry*. San Franscisco: W.H. Freeman, PP. 693-698.

Sutin, N, (1968). Free energies barriers and reactivity patterns in oxidation – reduction. *Accounts of Chemical Research,*1 (8): 225-231.

Sutin, N. (1966). Electron exchange reactions in solution. Energy communication BNL-9191. *Chemical Abstract,* 62:14.

Sykes, A.G. (1967). Further advances in the study of mechanism of redox reactions. *Adv*anced *Inorganic Chemistry and Radiochemistry,* 10:153.

Taube, H. (1959). Bridging and non-bridging ligand effect on redox reaction of metal ions. *Canadian Journal of Chemistry,*37: 129.

Taube, H. Meyer, H. and Rich, R.L. (1953). Observation on the mechanism of electron transfer in solution. *Journal of American Chemical Society,* 75:4118.

Vogel, A.I. (1961). *A Textbook of Qualitative Inorganic Analysis: Including Instrumental Analysis*. 3rd edition, Longman Green, London – Revised by Bassel, J., PP. 27, 284, 349-350, 383-385.

Waldemer, R.H. and Tratnyek, P.G. (2006). Kinetics of contaminant degradation by permanganate. *Environmental Science and Technology,* 40 (3):1055-106.

Wang, R.T. and Espenson, J.H. (1971). Kinetics and mechanism of the reduction of cobalt(III) complexes by uranium(III) ions. *Journal of American Chemical Society,* 93 (2): 380-386.

Waters, W.A. (1958). Mechanism of oxidation by compounds of chromium and manganese. *Quarterly Reviews,* 12, 277.

Weast, R.C. (1981), CRC *Handbook of Chemistry and Physics (62nd edition)*, Boca Raton, FL: CRC Press, PP. 259.

Wei, M.M. and Stewart, R. (1966). The mechanism of permanganate(VII) oxidation substituted benzyl amines. *Journal of American Chemical Society,* 88:1974.

Weiss, J. (1954). The theory of electron transfer process in aqueous solution *Procedure for Royal Society London,* A 222. PP. 128-134.

Wilkins, G.R. (1974). *The Study of Kinetics and Mechanism of Reactions of Transition Metal Complexes*. Allyn and Bacon Inc. Boston, PP. 56- 62.

Wilkinson, F.(1980). *Chemical Kinetics and Mechanism.* Van Nostrand Reinold Co., PP. 66.

Zahedi, M. and Bahrami, H. (2004). Kinetics and mechanism of the autocatalytic oxidation of L-asparagines in a moderately concentrated sulfuric acid medium. *Kinetics and Catalysis,* 45 (3):351-358.